Performance Evaluation of Spectrum Sensing and RF Energy Harvesting for Cognitive Radios based on SDR

A Thesis

Submitted in the fulfillment of the requirement for the award of degree

of

DOCTOR OF PHILOSOPHY

Submitted by

Supreet Singh

Registration No: 951206004

Under the Supervision of

Dr. Surbhi Sharma

Assistant Professor, ECED

Department of Electronics & Communication Engineering

Thapar University,

Patiala-147004, Punjab, India

Certificate

This is to certify that the thesis entitled **"Performance Evaluation of Spectrum Sensing and RF Energy Harvesting for Cognitive Radios based on SDR"** being submitted by **S. Supreet Singh**, Registration No. 951206004 to the Department of Electronics and Communication Engineering, Thapar University, Patiala, Punjab for the award of the degree of Doctor of Philosophy in Electronics and Communication Engineering, is a bonafide research work carried out by him under the supervision and guidance of the undersigned. His thesis has reached the standard of fulfilling the requirements for the regulations related to the degree. The contents in this thesis have not been in part or full submitted to any other university for award of any degree.

Dr. Surbhi Sharma,
Assistant Professor,
ECED, Thapar University,
Patiala, Punjab

Abstract

Cognitive Radio (CR) presents a lot of challenges to develop the techniques and methodologies to dynamically utilize the unused or underused spectrum. Spectrum sensing is identified as a very important task upon which the entire operation of cognitive radio depends.The issue of efficient utilization of radio resources can be implemented unitedly through dynamic waveform design and an efficient spectrum sensing. In this research work, waveform design using Spectrally Modulated Spectrally Encoded (SMSE) framework is conjoined with the Cyclostationary based Sensing technique (CSS) for CR. We take a simple system model in which one Primary transmitter communicates with one Primary Receiver and one Secondary transmitter with one Secondary Receiver in an interweave manner. In order to identify the free spectrum, an analytical expression of waveform design variables in terms of sensing parameters has been derived. Further, to find the channel occupancy/spectrum holes, a new joint CSS and SMSE based test metric has been proposed. The joint test stat offers a better and clear decision by providing a large gap between test stat and the required threshold setting. In particular, we combine the flexibility (dynamic channel allocation and dynamic waveform design) provided by SMSE framework and sensitivity (ability to deal with the weak signals) provided by CSS to improve the accuracy of the final decision of spectrum sensing. To evaluate the receiver performance, receiver operating characteristic (ROC) curves have been plotted which show that the proposed joint scheme achieves a significant performance improvement at lower SNR values when compared with traditionally available detectors. The spectrum sensing and proposed scheme is then extended in a multiple antenna scenario with maximal ratio combining used at the secondary transceiver.

From the deployment point of view and to increase the spatial distance of SU communication, co-operative two way relay communication is a powerful tool for CR. Due to certain observations, the previously proposed system model is modified to include the cognitive relay based SU communication. However,

in many practical scenarios, the relay may consist of a battery powered device operating under energy constraints. Thus, for prolonging the lifetime of a relay device in wireless network, energy harvesting (EH) from RF signal has received much greater attention recently. Therefore, the performance of energy harvesting (EH) relay based Interweave/Underlay Cognitive Radio Network is investigated. We employ Amplify and forward (AF) relay technique along with Time-switching relaying protocol (TSR) for energy harvesting at the cognitive relay. Based on sensing accuracy, we derive an expression for optimization of charging duration TSR parameter and sensing duration for maximizing throughput of interweave Cognitive Radio. Based on sensing efficiency, throughput and outage probability for underlay CR is analyzed considering the interference temperature constraints and optimal power distribution parameter at secondary user (SU) terminals. Variations in the sum-rate and detection probability are considered in terms of CDF of the terminal SNRs. We prove that erogodic sum-rate is maximized in underlay CR case, when interference power distribution parameter is half across the SU terminals. The optimized values of switching-time ratios have been derived analytically for both Interweave and Underlay CR. The results thus obtained are compared by taking symmetrical and asymmetric channels between SU terminals. Analytical results are also validated through monte-carlo simulations to confirm the accuracy of the derived expressions.

Acknowledgement

I would like to offer my heartiest salutation to the Almighty Dhan Sri Guru Nanak Dev ji for unbroken health, motivation and courage bestowed upon me in all the adversities at every step and at every moment throughout the entire span of my studies and in every aspect of my life. My deep sense of appreciation to my parents Sardar Gurbachan Singh and Sardarni Jatinder Kaur for their continuous support, affection and encouragement. The completion of any academic work would have been without the guidance of a guide. I acknowledge and extend my gratitude to my guide Dr. Surbhi Sharma, Assistant Professor, Department of Electronics and Communication Engineering, Thapar University, Patiala, whose continuous encouragement, constructive discussions and encouraging gesture at every step of my work enabled me to complete my research work. Despite her various academic, official and home assignments, she spread her precious time. I thank Dr. Rajesh Khanna, Professor, Department of ECE, thapar University for his valuable comments at every step and improving the research work. I also thank Dr. Kulbir Singh for his able help rendered.

I extend my deep thanks to my mentor Dr. Shankar Prakriya, Professor, Department of Electrical Engineering, IIT Delhi who boosted my confidence and morale for a fruitful research and without whose permission this work would never have been completed. I also thank Modem Sudhakar, Komal Janghel, both Research Scholars at IIT Delhi for their help. I would also like to thank other research members in DSP LAB of Bharti School of Telecommunication, IIT Delhi for their fruitful discussions.

I would like to thank Dr. Gurcharan Singh Lamba, Principal, Baba Banda Singh Bahadur Engineering College for his able motivational attitude. I thank Dr. Sukhwinder Singh, Head Department of Mathematics, Sri Guru Granth Sahib World University, Fatehgarh Sahib for his able help and support. I like to thank Dr. Niraj Bala, Head, R & D Baba Banda Singh Bahadur Engineering College, Fatehgarh Sahib. Out of deep sense of gratefulness, I express my sin-

cere thanks to Dr. O.P. Pandey, Dean (RSP), Dr. Alpana Agarwal, Head ECE and members of doctorate committee for continuous appreciation and support. comments have really helped me in bringing this thesis to the present shape. I am also thankful to all my colleagues, dears and nears and all others who have directly or indirectly helped me in this work. I am thankful to the various International Journals (published by IEEE, Elsevier, Taylor & Francis, Springer etc.) who examined my research papers. Their suggestions and comments have really helped me in bringing this thesis to the present shape. Finally, words are not adequate to express my gratitude to my wife Navjot Kaur and children "Manfateh Singh", "Hargunpreet Singh" and my brother Jaspreet Singh for their patience, support and active assistance in many ways.

Supreet Singh

Contents

List of Tables

List of Figures

List of Symbols

P_{fa}	Probability of false alarm
P_d	Probability of Correct detection
P_{md}	Probability of missed detection
λ	System Threshold
f_s	Sampling frequency
β	Fraction of the time for Energy Harvesting (TSR parameter)
τ	Fraction of the time frame for Sensing
ζ	Efficiency of Energy Harvesting Circuit
P_a	Transmission Power of SU terminal, T_a
P_b	Transmission Power of SU terminal, T_b
γ_a	End-to-End SNR at SU terminal, T_a
γ_b	End-to-End SNR at SU terminal, T_a
γ_{th}	SNR Threshold
ln(.)	Natural Logarithm
I_p	Interference Threshold limit
α	Interference Power Distribution Parameter (IPDP)
$\wedge$	Test Metric
N_f	Number of frequency components
α_0	Cyclic frequency
τ_0	TIme-lag for cyclic autocorrelation
$\Re.$	Real part of some complex quantity
∇f	Frequency Resolution

Chapter 1

Introduction

1.1 Basics of Cognitive Radios

Cognitive Radio (CR) has emerged as a promising technology to address the problem of spectrum shortage and improving the spectrum efficiency and its utilization. Cognitive radio was originally proposed by J. Mitola [4] to promote the efficient use of the spectrum by exploring and exploiting white spaces (underused and unused) in the spectrum. Actually the Federal Communications Commission (FCC) analyzed the spectrum and under-took the various measurements for spectrum analysis and investigated that frequency bands are under-utilized which means that either the portions of spectum are unused or less used for significant periods of time [5]. The report further analyzed that the spectrum scarcity is not due to spectrum shortage but due to inefficient spectrum utilization and explained that the licensed spectrum is not utilized to its full potential and 80%- 85% of the spectrum being under utilized. The usage also varies over geographical area and over different spectral regions. FCC proposed to open up the licensed frequency band to unlicensed users to efficiently utilize the resources. In Cognitive Radios, in the context of the spectrum usage, the network is divided into two groups - primary network or licensed network and the secondary network or CR network. The primary network is the existing licensed network and the Primary users (PUs) are defined as the users which are licensed to operate in a certain (licensed) spectrum band. Due to their license, PUs are given the priority and their operations should not be affected.

The Secondary network (or CR network) does not have an operational license. The secondary users (SU) are defined as the users which do not have a license to operate in a desired frequency band but they can engage the spectrum in the absence of primary users. In other words, secondary users operate in the vacant frequency band in the licensed spectrum; should vacate that spectrum band when licensed users are detected in the spectrum channel and move to the another available vacant spectrum immediately. With the Secondary users, the concept of spectrum hole is also introduced. The spectrum hole is defined as the vacant portion of the primary spectrum channel/band.

To achieve the goal of Cognitive Radios, dynamic spectrum allocation and access has been proposed [6] and several paradigms have been put forward. In other words, to improve the spectral efficiency, dynamic spectrum allocation operates via spectrum sensing, dynamic spectrum access by exploring the time and space limited statistics of various users. Efficient and dynamic spectrum management techniques are used to attain visualized goal of CR networks as a uninterrupted roaming, providing higher bandwidth and new wireless services. The following spectrum management functions are proposed in literature [7].

- Spectrum Sensing
- Spectrum Decision
- Spectrum Sharing
- Spectrum Mobility

Each user in the network must: perform the spectrum sensing to determine the different vacant portions of the available spectrum (If licensed users are present it should determine the underused spectrum bands), selecting the best from among the available channel for transmission (*spectrum decision*), coordinating the access with other communicating users to avoid unnecessary interference (*spectrum sharing*), abandon the transmission in that frequency channel and move to the other vacant channel when a licensed user is detected (*spectrum*

mobility). The interdependence of all these functions on each other is shown in the figure 1.1.

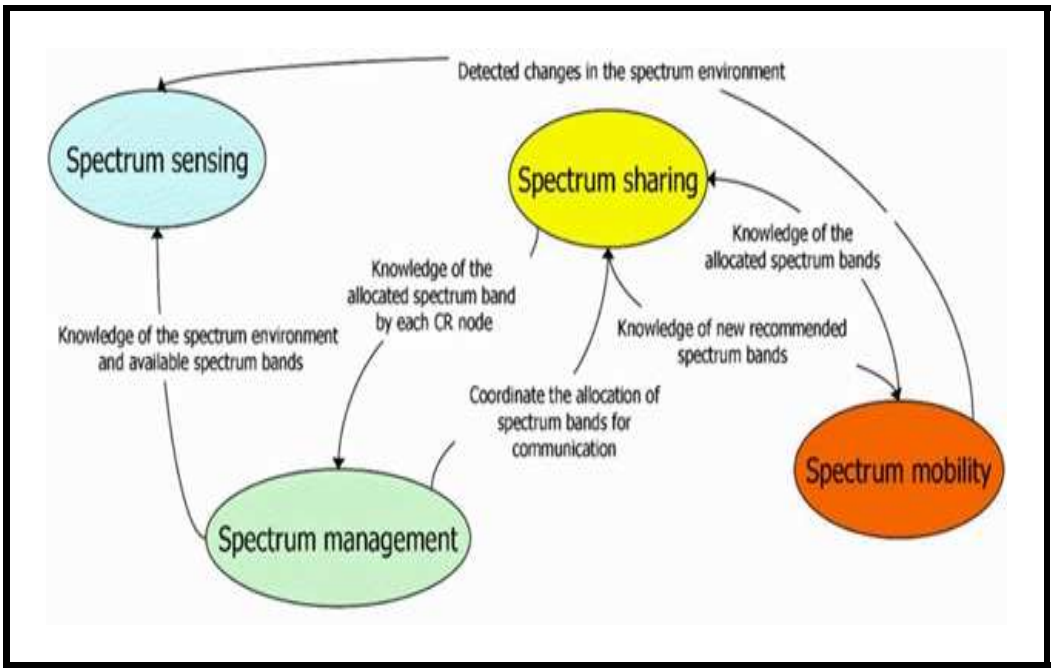

Figure 1.1: Interdependencies of different CR functionalities

1.1.1 Frequency Bands for CR Networks

Specifically, as per IEEE 802.22 recommendations, cognitive radios with wireless base stations (such as point to multi-point communication) are proposed to use the VHF/UHF bands of television broadcast frequency range. The variations in the spectrum occupancy has been observed in HF band. There has been a lot of effort for spectrum occupancy measurements [8][9][10]. The different frequency bands may be used over the geographical area which may also vary according to the country's own regulatory policy. In particular, TV channel from 2 to 51, (54 MHz to 698 MHz) each of 6MHz bandwidth has been found to be most suitable. Some regulatory committees have found 54 MHz to 862 MHz frequency bands whereas the extreme range as per international standard is from 47 MHz to 910 MHz. This ranges from HF band to UHF bands. The UHF TV band is widely considered as a good candidate for CR based Networks. Irrespective of the frequency or geographical area, the CR devices should not

cause any hinderance or interference to existing primary networks and licensed users. Moreover, CR's will benefit in providing internet and education access to unprivileged areas.

1.2 Different Paradigms of CR Networks

Cognitive Intelligence is emerging as a predicting technology to utilize the wireless spectrum more efficiently. Different paradigms have been put forward to implement the concept of Cognitive Radio. [11]

1.2.1 Interweave CR

The first paradigm is InterWeave(IW) CR, also called opportunistic spectrum access. In this, unlicensed user performs spectrum sensing first to determine the spectrum holes and transmits only when PU is absent on a particular spectral band. In other words, IW exploits the unused specral regions as shown in figure 1.2. Secondary user first performs the spectrum sensing to decide which parts of the spectrum are unused and vacant.

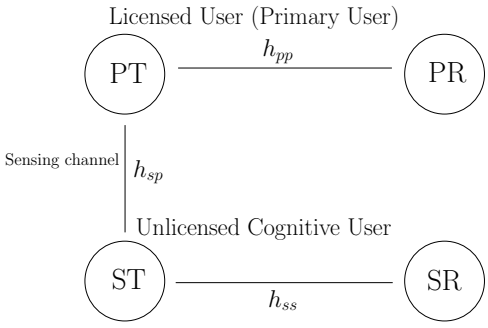

(a) Interweave CR paradigm

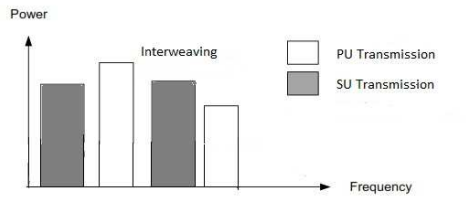

(b) Unused frequencies used in IW CR after spectrum sensing

Figure 1.2: Interweave CR

1.2.2 Underlay CR

Underlay CR exploits the underused spectrum regions in a way that PU operation or communication is not disturbed or interfered. Underlay CR is also

termed as spectrum sharing technique because according to this the secondary users share the same spectrum and coexist with the primary users, using the same frequency band at the same time under the condition that it will not cause any harmful interference to PU's operation. In other words, underlay CR approach can use more spectrum at low power than interweave but below the noise floor of primary users [12] as shown in figure 1.3. The interference alignment is proposed to achieve higher multiplexing gain for performance improvement in [13]. In case of Underlay CR, there is no need of spectrum sensing and secondary users can share the spectrum with primary users without performing spectrum sensing. Sensing-based spectrum sharing is proposed in [14] which operates in a hybrid manner depending upon the sensing result, that is, if channel is occupied, CR operates in underlay manner and if channel is idle, CR operates in an interweave manner. This approach results in increasing the transmission opportunities of the secondary users.

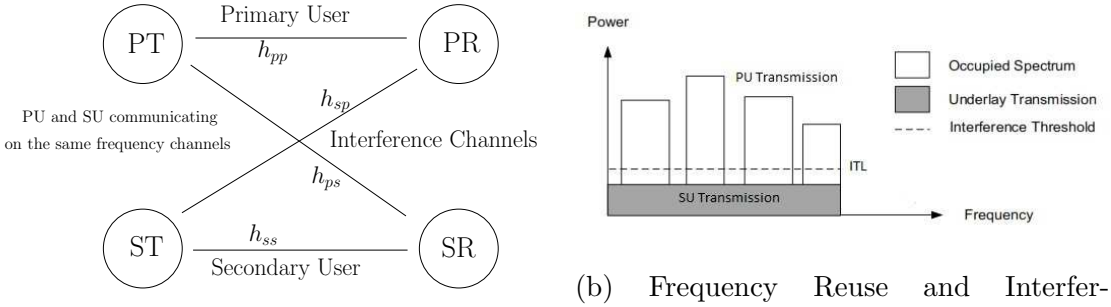

(a) Channels in Underlay CR

(b) Frequency Reuse and InterferenceThreshold in UL CR

Figure 1.3: Underlay CR Paradigm

1.2.3 Overlay CR

In overlay CR Networks, SU cooperates with PU as potential relays and aims to ask for a right to access the licensed spectrum to transmit their own information. Overlay CR Network are also termed as cooperative CR networks (CCRN). The most challenging problem for CR designer is the spectral awareness. In a broader sense, CR with correct spectral awareness can achieve greater

capacity and exploit more spectral opportunities [15]. An important requirement of Cognitive Radios is that they must rapidly occupy the vacant spectrum channels (i.e., portions of the licensed spectrum which either unused or underused) without creating harmful interference to PUs. This job of spectral awareness is enabled by spectrum sensing by detecting the spectral opportunities and existence of PUs in a given frequency band or geographical area [16]. In other words, a CR device must be "able to detect the changes in wireless network with which it is connected". It also needs to change its different transmission parameters according to the new opportunities that are detected. Hence, spectrum sensing in CR aims to find the holes in the PU transmission bands which are the best opportunities to be used by the SU [17]. In a hybrid CR, before starting transmission by CR user, spectrum sensing has to be performed so that if some spectrum channel is unused in space and time, SU can operate with full power in that spectrum hole in an interweave manner, thereby significantly enhancing the performance of the system. But if some PU is already camping on that spectrum slice, SU can still share the channel in an underlay/overlay manner under power limits and interference constraints [18]. Up-to-date discussion on research work for spectrum sensing is provided in [19] and the authors identify some open key research challenges related to practical sensing framework. Various spectrum sensing techniques have been proposed which are discussed in the next section.

1.2.4 Hybrid CR

Hybrid CR generally combines the advantages of Interweave and Underlay CR systems. Both spectrum sensing employed in interweave CR and power control mechanism used in underlay CR at secondary transmitter is implemented in hybrid CR [20]. In the literature [21][22], underlay and overlay methods of spectrum sharing are also combined to optimize the sensing time and maximize the throughput of the secondary system.

1.3 Different Spectrum sensing techniques

Spectrum sensing has been described as the most important function and the key step of the cognition cycle for designing the cognitive radio system. Identifying the white or grey spaces through direct detection or sensing of the licensed bands and monitoring the dynamic availability of these bands is the most challenging issue of the CR [23]. Identification process, in itself involves the detection (spectrum sensing) and spectrum decision (spectrum assignment). Spectrum sensing must be performed by secondary users (SU), unlicensed users to detect the vacant spectrum or spectrum holes before exploiting the primary users (PU) resources. Spectrum sensing methods traditionally available relate the sensing in three dimensions: frequency, time and space. A numbers of parameters are there to sense and characterize the spectrum. These parameters include power consumption, how much spectrum is vacant, noise level, interference level etc. Spectrum sensing is done particularly in two areas viz. frequency and time. But it is not mandatory that spectrum sensing is done only in these two areas. There are number of areas like code domain and the area of the phase where coding and angles come into existence. Based on this, several spectrum sensing methods have been studied including matched filter detection (MFD), Energy based detection (ED) and cyclostationary based feature detection. These are discussed in the next section.

1.3.1 Energy Detection

Energy detection (ED) method is the simplest of the sensing techniques but its performance suffers from the noise uncertainity. It is also shown [24] that at low levels of SNRs, ED does not perform well. ED based method cannot be used below certain SNR and in fact, "there exists an SNR wall beyond which ED is theoretically impossible"[24]. Still energy based detection is the most popular spectrum sensing technique because of its simplicity in hardware implementation and low signal processing cost. In 1967, Urkowitz [25] first proposed the energy detector by taking an unknown deterministic signal over a AWGN noise

channel. The work was extened over different fading channels by Kostylev [26]. Then, Digham et al. [27] derived closed-form mathematical expressions for the probability of detection over Nakagami and rayleigh flat-fading channels for ED based sensing. An energy detector decides on the presence of the PU by measuring the energy received on a licensed primary frequency channel and comparing it with a system threshold.

$$X = \left(\sum_{i}^{N} |x_i|^2 \right) \lessgtr \lambda, \tag{1.1}$$

where λ is threshold of decision for the PU signal. Energy based spectrum sensing method is relatively very easy and simple to implement but its performance degrades rapidly under low SNR environment.

1.3.2 Cyclostationary spectrum sensing

Cyclo-stationary feature detection [28] based spectrum sensing is able to perform well under the effect of low SNR however its implementation needs high computation complexity. The main reason for choosing Cyclostationary spectrum sensing method among others is that it works on the built in periodicity of the modulating signal which is incorporated in the communication signal during basic transmission operations like sampling, coding and modulation. These basic operations are always performed on digital communication signals and hence their statistical properties vary periodically in time except for noise. The noise is aperiodic and acyclic in nature. The cyclic spectrum of the communication signals show the peaks at certain defined repeated locations, called cyclic frequencies. The location of these cyclic frequencies is defined by the signal parameters, such as carrier frequency, bandwidth and symbol rate etc.[29]. Cyclostationary detection method is based on the periodicity or autocorrelation of the signal that varies periodically over the time. Because noise is wide-sense stationary and shows no periodicity, cyclostationary feature method has high noise rejection capability and hence ability to distinguishes between the primary user and the noise at even very low SNR regions. Two

parameters namely Cyclic autocorrelation function (CAF) and Spectral Correlation Density function (SCD) are used in this spectrum sensing technique for detecting the primary user signal [30]. The conditions for the process to be cyclo-stationary are as follows:

$$E\{x(t+T_0)\} = E\{x(t)\}$$
$$R_x = E\{x(t+\tau_0) * x(t)\}. \tag{1.2}$$

That is, both mean and auto-correlation function needs to be periodic with some period, T_0. The traditional cyclostationarity detectors for cognitive radio networks search for a cyclic frequency at a particular time lag τ_0 in the cyclic autocorrelation function (CAF) of the PU signal. The Hypothesis model framed for this technique is

$$H0: \quad R_x^{\frac{n}{T_0}}(\tau_0) = 0$$
$$H1: \quad R_x^{\frac{n}{T_0}}(\tau_0) \neq 0\ . \tag{1.3}$$

Under the alternative hypothesis, CAF is nonzero which means occupied spectrum whereas under the null hypothesis it is zero, showing the vacant spectrum band. Signal characteristics under the null hypothesis need not to be exploited except for noting that its CAF would be zero because it shows the presence of noise only. But its implementation requires computation of the covariance matrix of estimated CAFs real and imaginary parts. Another feature of Cyclostationary spectrum sensing technique is that it can also be used to detect the modulation technique used by the primary user. Cyclostationary detection can also classify signals exhibiting cyclo-stationarity at different cycle frequencies and at different time lags. One of the added advantage of cyclostationary detection over energy detection is that it can be used to recognize the different air interfaces, a job which energy detector cannot perform. Some of the disadvantages of Cyclostationary method include longer observation time, computational complexity and non-linearity etc.

1.3.3 Matched filtering based sensing (MFD)

Matched filtering based detection requires prior knowledge of PU signal characteristics to process. MFD achieves a reliable detection probability in a shorter sensing time for a given probability of false alarm but it needs the prior knowledge of primary user signal features such as bandwidth, modulation type and operating frequency etc and also accurate synchronization. Implementation of matched filter detection is possible only when the primary user have pilots, preambles, synchronization words that can be used for coherent detection. In digital signal processing, matched filter is represented by a linear filter which is designed for a given input signal in order to maximize the output SNR. This filter correlates the primary user signal with time shifted version of the prior known signal and compares the final output with the predetermined threshold [31]. In other words, the convolution operation of the primary user signal $x(n)$ is performed with the time shifted version of the prior known signal $z(n)$. The output of the filter is compared with the threshold. Hence, for the Matched Filter Detection, the decision statistic is given by

$$T_{MFD} = \sum_{0}^{N-1} x(n)z(n) \ . \tag{1.4}$$

where x(n) is the input signal of interest and z(n) is the deterministic signal (or prior known signal) with energy

$$E = \left(\sum_{i}^{N} |z(n)|^2 \right) \ . \tag{1.5}$$

Considering AWGN channel, the basic hypothesis model for this technique can defined as follows:

$$\begin{aligned} H0: &\quad x(n) \simeq N(0, \sigma_w^2) \\ H1: &\quad x(n) \simeq N(E, \sigma_w^2) \ . \end{aligned} \tag{1.6}$$

NULL Hypothesis H0, indicates the absence of the primary user and alternative hypothesis H1, indicates the presence of the primary user in the certain pre-known spectrum of interest. The comparison of various sensing methods

accuracy and complexity is shown in figure 1.4.

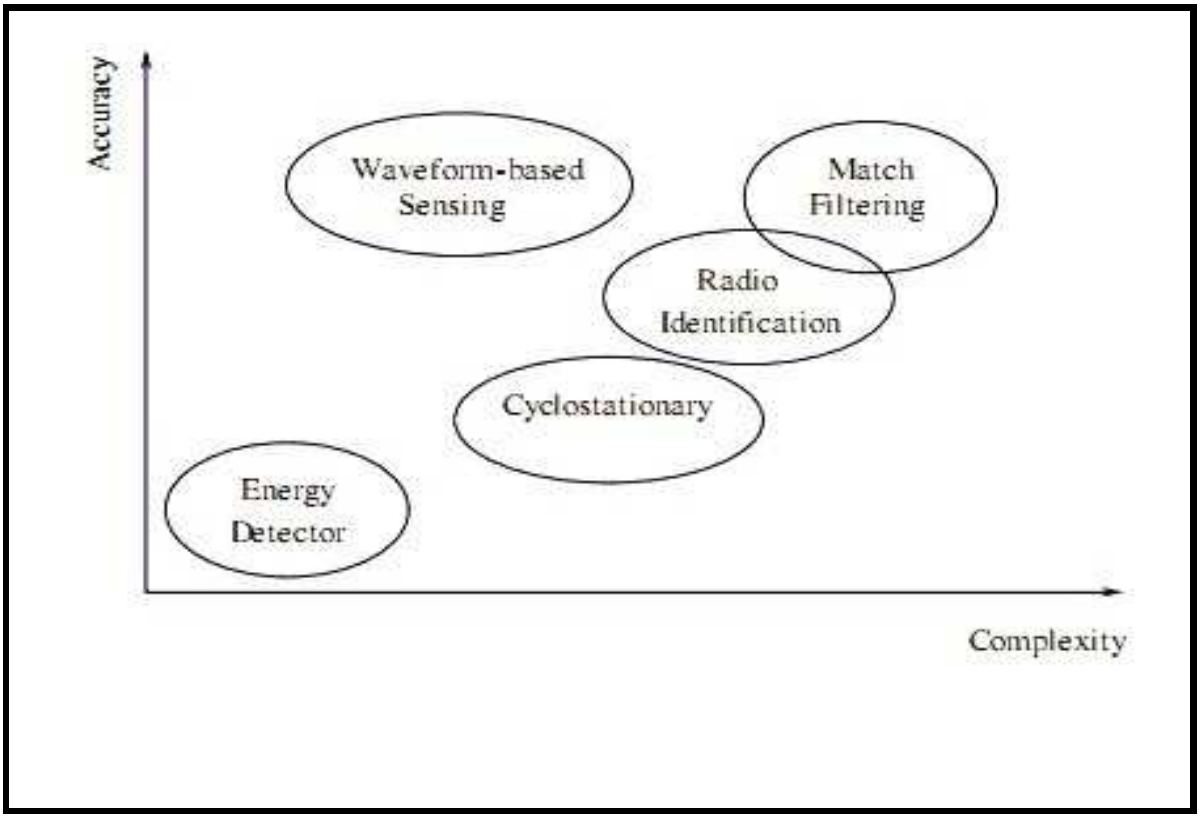

Figure 1.4: Main sensing methods in terms of their sensing accuracies and complexity [1]

1.3.4 Performance Parameters of Spectrum Sensing

Spectrum sensing is the most important part of any CR as all the other functionality like channel selection, spectrum sharing, dynamic spectrum allocation (DSA) and mobility etc depend on the information fetched by the spectrum sensing. Reliable spectrum sensing is the one of the most important tasks in cognitive radios. Due to noise and channel imperfections, the spectrum sensing can never be perfect and sensing errors always exist [32]. Mainly three parameters are defined for spectrum sensing in cognitive radios. These are discussed as follows:

- P_d - Probability of detecting the signal when the PU signal is actually

present.

- P_{fa} - Probability of false alarm, that is, deciding the PU signal present when it is indeed not present.

- $P_{md} = 1 - P_d$ - Probability of missed detection, that is, not detecting the signal when it is actually present.

A high value of false alarm P_{fa} means that the detector is detecting the unoccupied spectrum as occupied, which results in increase in the number of missed opportunities which ultimately results in low spectrum utilization. While a higher missed detection P_{md} means the vice-verse which means that it is detecting the occupied spectrum as unoccupied which results unnecessary collisions with the primary user and hence causing interference.

1.4 Software Defined Radios based CR

Several definitions have been put forward to define the term SDR. In European Telecommunications Standard Institute (ETSI) [33], SDR is defined as radio in which the radio frequency (RF) operating parameters including frequency range, modulation type, or output power can be set or altered by software, and/or the technique by which this is achieved. The Wireless Innovation Forum (formerly known as SDR Forum) Software Defined Radio is defined as [34]: "Radio in which some or all of the physical layer functions are software defined". Most radios are software controlled instead of software defined. As an example, our modern cellular phone can support different cellular standards such as GSM (2G, 3G or 4G) and WCDMA (3G or 4G) etc. The selection of the network is controlled internally by software but not by the user. Since the user is not required to switch on to a separate module or so, this operation of the cellular phone is defined as a software-controlled radio [2]. Such a radio uses a microcontroller for handling the functionality of the radio and a block diagram is shown in figure 1.5.

Software-defined radio is an intelligent and self aware radio that can adapt

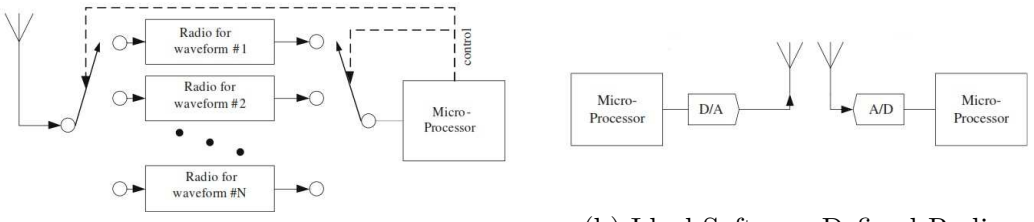

(a) Basic Software Controlled radio

(b) Ideal Software Defined Radio

Figure 1.5: Software Controlled Radio and Software Defined Radio [2]

itself to the wireless environment. The signal constellation or coded data is mapped to the desired waveform characteristic in the microprocessor. The device can reprogram itself to the extent that it was not originally intended to. The transmitted or received signal at the antenna is directly send to digital to analog converter and processed in real time. The microprocessor is replaced by generic digital signal processing operations. The ideal SDR hardware can support any waveform at any carrier frequency and any bandwidth [35]. The main idea is to enable the transeivers to operate in different air interfaces with different specifications using single hardware platform. This flexibility is provided through the reconfiguration or reprogramming. SDR handset with dynamic reconfigurability in multi-standard air interface is required to implement the global roaming capabilities and integrated services. The RF hardware used for SDR should be capable to sense any part of the radio spectrum and this is possible with RF hardware technologies such as wideband power amplifiers, wideband antenna or software defined filter banks etc. SDR also needs to operate at different bandwidths and at wide range of different frequency bands. However, to be able to sense and process the signal at very low power levels, the RF front-end of the SDR needs to have high sensitivity.

1.4.1 Difference between Hardware defined and Software defined radios

In general, the front end RF unit of SDR filters the channel of interest from a wide frequency spectrum band. Then, it converts these frequency channels to baseband for sensing. The signal is demodulated and decoded to the resulting information. In the traditional hardware defined radio, the functions such as modulation, demodulation, extracting the channels of interest from a spectral band, downconverting, baseband processing, encoding/decoding, security etc. are all supported through a fixed-function hardware architecture. The hardware components including RF/digital discrete components allow the flexibility with a software control for choosing the channel or setting any transmit power level. The device may need to support any air-interface standard which consists of RF integrated circuits to support the target air-interface standard but the basic radio functionality is relatively fixed.

In a software defined radio, significant flexibility is allowed in the radio functionality through software reconfigurability which provides multiple benefits for wireless manufacturers along with the service providers through end-users. Some of these benefits of SDR are as under:

- Software development based on flexible waveform components can substitute a ASIC development cycle thereby reducing the associated costs with product development. Because now a single development project can potentially support multiple market segments.

- Can achieve the mobility and smooth roaming across the different network boundaries and to interoperate on different independent networks with varying specifications.

- Reducing installation and support costs, since a common set of inventory like DSPs, FPGAs etc. can be utilized for multiple markets. Also, "bug fixes" can be easily done through software redesign instead of hardware redesign.

- Improving time to market in supporting new revenue generating services or features. These features can be upgraded and provided through a simple software download.

1.5 Dynamic Waveform design and SDR based implementation for CR networks

With the increasing demand of wireless services, number of wireless protocols and new generation of mobile communication networks featuring new services, the dynamic multi-access has become of paramount importance. Flexibility becomes a important aspect for the transceiver. The generalized hardware platform that can provide flexibility and support multiple protocols, controlled and defined by intelligent software is the future.

The framework for CR based dynamic waveform design has already been proposed in [12] that provides the generalized analytical platform for designing multi-carrier, multi-user waveforms like MC-CDMA, CI/OFDM for SDR based CR. The coding, dynamic waveform design along with the sensing parameters is another dimension that can be explored. The two waveforms Dyanmic OFDM and MC-CDMA[36] are the good candidate waveoforms for secondary users. Dynamic waveform design based on Software Defined Radio (SDR) and spectrum sensing technique along with the decision metric can be used together for better utilization of radio resources. The authors in [37] studied the spectrum sensing taking two cases as known noise variances and unknown noise variance case for OFDM signals. To improve the performance of secondary users and spatial distance of communication, a lot of researchers have focussed on the combination of CR with relaying. Cognitive relay networks offer an added advantage.

1.6 Relay based Cognitive Radio Communication

In simple words, relay is just an intermediate node that receives the signal from the source/transmitter and facilitates the transmission to some distant destination or reciever. CR user is allowed to access the licensed spectrum of PUs when the wireless channel is idle or with power and interference constraints as long as it does not cause performance degradation to PU network. In such a spectrum sharing scenario, co-operative two way relay communication is a powerful tool to combat the channel fading and to improve the transmission performance as well as spatial transmission distance of the wireless network. A simple cognitive relay network is shown in figure 1.6.

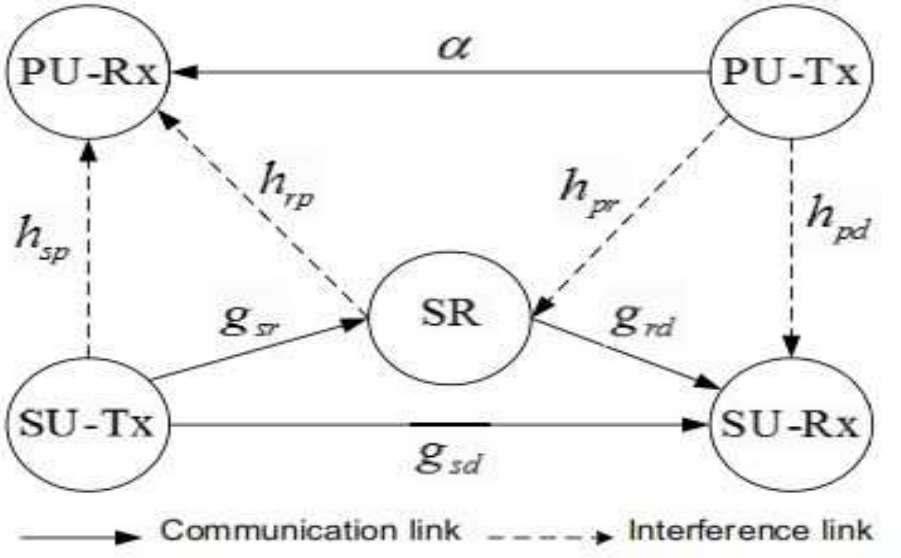

Figure 1.6: A simple cognitive relay network with Interference [3]

However, in many practical scenarios the relay may consist of a battery powered device operating under energy constraints. In [38] the authors have derived exact closed-form expression for the outage probability of the cognitive two-way relay network over Rayleigh fading channels considering the interference both from SU to PU and PU to SU. Two-way Relay can forward the data in different ways as described below.

1.6.1 Decode and forward relay

In decode and forward type relay (DF), relay receives the signal from the source; decodes and re-encodes it before sending it to the destination. The basic advantage of using DF relay is that the relay can decode-encode the signal in such a way that it can cancel the interference or overcome the fading effects. But the decision made at the relay affects the overall performance of the system. The system works in two time slots - decoding and forwarding. Additionally, destination node needs to know the characteristics of the source-relay and relay-destination channel for efficient functioning.

1.6.2 Amplify and forward relay

In this type of relay network, relay simply amplifies and forwards the information from source to destination considering the transmit power limits. Amplify and forward relay is particularly useful when relay power is limited because power can be individually constrained in these types of relays. Cognitive relay networks mostly prefer this type of relay due to its simple functionality that can apply the interference power constraints on relays.

For prolonging the lifetime of a relay device in wireless network, energy harvesting (EH) from Radio frequency (RF) signal has received much greater attention recently [39, 40, 41, 42]. The underlaying advantage of EH lies in the fact that RF signals can carry both information and energy at the same time which was originally proposed in [43]. The harvesting-throughput trade-off was studied in [42], where the authors optimize simple harvesting ratio considering the interference constraints of the primary user. Combined with the energy harvesting, two different types of practical relaying protocols have been proposed in [44], namely, multiple access broadcast (MABC) and time division broadcast (TDBC). Both delay-limited transmission and delay tolerant transmission modes of transmission has been studied for these two protocols for two-way relay networks.

1.6.3 Symmetric and Asymmetrical Wireless Relay channels

Ideally, symmetric wireless channel refers to the channels that behave in the same manner in both directions. In other words, the data transmission and reception speeds are same. In relay based communication, two different channels always come into picture. One is from transmitter to relay g_{sr} and the second is from relay to destination g_{rd} as shown in figure 1.6. If both channels are same, that is, the behavior of channels at both sides of relay is same, then we say that the channel is symmetric [45]. We can apply standard rayleigh fading distribution for both channels and can find end-to-end parameters which are more of interest in this case. In certain applications such as two-way video conferencing the symmetric channel is the requirement.

In asymmetric channels, the channel behavior is different as seen from transmitter side and receiver side. The wireless channel cannot be taken as reciprocal in this case. This type of wireless channel is more practical because most of the time download and upload speed requirements are not same. Generally, download speeds are greater than upload speeds. Asymmetrical data flow makes more efficient use of the available resources and infrastructure in most of the applications. In relay based cooperative communication, the channel is said to be asymmetrical if wireless channel on both sides of the relay behaves differently. Asymmetry can be induced if distance of wireless nodes on either side of the relay is not same.

1.7 Energy Harvesting based Cognitive Relay Networks

The authors in [46] proposed two protocols for wireless energy harvesting and information processing, namely Time-switching relaying protocol (TSR) and Power splitting relaying protocol (PSR) and studied the throughput of AF relaying energy harvesting for both TSR and PSR.

1.7.1 TSR Protocol

In TSR protocol, the time frame is divided into three time slots. In the first time slot (small fraction of the time frame), relay harvests energy from the RF signal. In the second time slot, the nodes transmit information to the relay and in the third, relay transmits the data bidirectionally using the energy harvested in the first time slot. The simple TSR protocol is shown in figure 1.7.

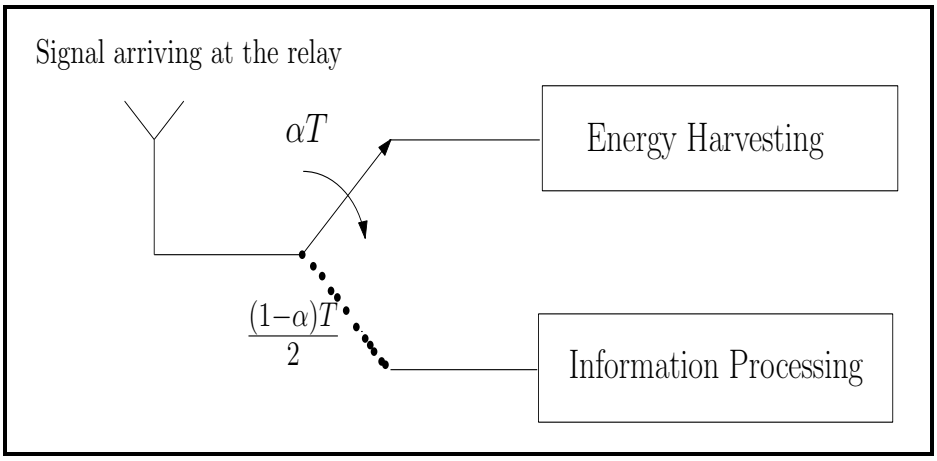

Figure 1.7: Time Switching Relaying Protocol

1.7.2 PSR Protocol

In PSR protocol, a small portion of the received wireless signal power is used for energy harvesting and the remaining for information processing as shown in the figure 1.8. Very recently, the authors in [47] discussed to optimize the sensing time that could maximize the energy efficiency for SU. The authors proposed an algorithm with low computational complexity to determine the joint optimal transmission power and sensing time. The optimization of the sensing interval considering imperfect spectrum sensing to minimize the interference to PU along with energy consumption for spectrum sensing is considered in [48]. The impact of residual transmit radio-frequency impairments (RTRIs) on a dual-hop energy-harvesting system in which a source and a destination both having multiple antennas and communicate to each other with the help of single-antenna amplify-and forward relays is studied in [49]. The source and

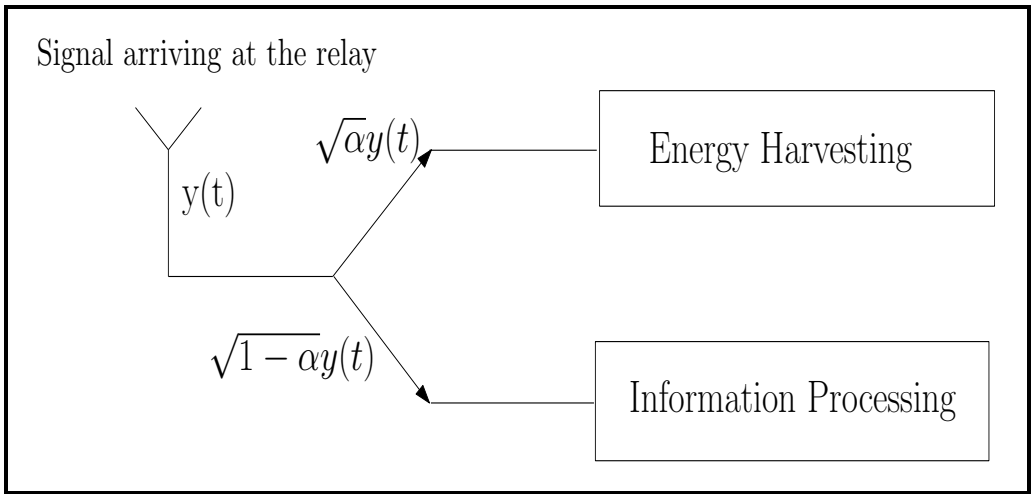

Figure 1.8: Power Splitting Relaying Protocol

destination employ maximum ratio transmission (MRT) and maximal ratio combining (MRC) respectively, to exploit the benefits of using multiple antennas. Considering the interference constraints, the joint optimization of sensing time and transmission time along with sensing errors resulting in opportunity loss to SU has been considered in [50]. The work on energy harvesting-aided spectrum sensing in heterogeneous cognitive networks is done in [51] where the authors propose a spectrum sensor scheduling algorithm to allocate channels while considering energy harvested dynamics and protection of PU transmissions. To the best of the author's knowledge, the performance of EH relay based two-way interweave/underlay CR network considering the sensing accuracy and efficiency has not been studied yet.

1.8 Organization of the thesis

The thesis has been organized into six chapters. The contents of each chapter are briefly described as under:-

Chapter One presents introduction of the cognitive radios, different paradigms and spectrum sharing along with the protocols for RF energy harvesting. The organization of the thesis is also explained towards the end of the chapter.

Chapter two covers the comprehensive literature survey of the spectrum sens-

ing in CR and RF energy harvesting. Based on the literature survey, the objectives of the research work are listed towards the end of the chapter. The main constribution of the research work carried out of the above objectives have been itemized.

Chapter three describes with system model taken to study the CR and SMSE framework for investigating the CR. Analytical expressions have been derived to implement cyclostationary spectrum sensing with SMSE framework. The new decision metric is defined and simulation results have been plotted taking two modulation scenarios.

Chapter four investigates the performance of spectrum sensing in multiple antenna scenario. From deployment centric veiwpoint, relay based RF energy harvesting CR network has been studied. A new system model has been proposed. Without considering sensing the expressions for end-to-end SNRs and terminal outages aloong with the throughput for an underlay CR are derived

Chapter five analyzes the performance of RF energy harvesting in a hybrid Interweave/Underlay CR. The algorithm for optimization of sensing duration and charging ratio parameter to maximize the throughput of the CR system is defined. We derived the optimized values of TSR time-switching charging ratio parameter and sensing duration for Interweave CR. We also optimize the interference-power distribution and time-switching ratio parameters for Underlay CR. The expressions for throughput, terminal outages and sum-rate for an underlay CR are also derived and results analyzed by comparing with symmetrical and asymmtrical channels.

Chapter six concludes the research work and presents future scope for further extensions of the work.

Chapter 2

Literature Survey

2.1 Introduction

In this chapter we present a comprehensive literature review of performance issues related to spectrum sensing. Spectrum Sensing is the most important functionality of CR as the entire channel allocation, spectrum management and further communcation depends on spectum sensing in interweave CR. In section 2.2, previous research related to different techniques of spectrum sensing has been discussed. Literature Reveiw on SDR implementation and Dynamic Waveform Design framework is presented in section 2.3. The section 2.4, extends the literature survey of spectrum sensing in multiple antenna scenario. In section 2.5, previous work based on RF energy harvesting techniques in cognitive radios has been presented.

2.2 Spectrum sensing in Cognitive Radios

In 2008, Mohanty [7] discussed the open research issues and developments in spectrum management in CR Networks. The paper focussed on various spectrum management functions. The various applications of CR networks may demand different QoS requirements, the implementation of new network paradigm impose new research challenges due to the dynamic nature of the available spectrum. The authors discussed that with the implementation of dynamic spectrum access techniques and heterogeneous wireless architectures, cognitive radios could provide high bandwidth and uninterrupted roaming. The com-

prehensive survey in spectrum sensing was provided in [1] where the authors presented various spectrum sensing methodologies. The authors also introduced multi-dimensional spectrum sensing concept and studied statistical modeling of the behaviour of primary user taking different network traffic models. Sensing features and specifications of some current wireless standards are also given. In the same year, the specifications of IEEE 802.22 standard were published. The article [52] discussed an overview of the specifications of IEEE 802.22 standard for cognitive wireless regional area networks (WRANs) that was under development in the IEEE 802 Standards Committee. The authors discussed that broadband wireless access cannot be provided to less densely populated areas by wireline or other wireless means because it its economically not viable. Cognitive Radio techniques could allow the same in the traditional VHF/UHF television broadcast bands on a non-interfering basis. This could also provide societal and economic advantages while increasing the utilization efficiency of that spectrum band.

However, the authors in [53] provided the overview of research work and advances in spectrum sensing and sharing techniques for cognitive radios over last one decade. As the licensed communication is given the priority and should be protected through different access strategies. This requirement presents challenges to the implementation of CR for increasing the spectrum utilization efficiency. The secondary users should be able to estimate the activities of the PUs through spectrum sensing techniques. Cooperative spectrum sensing has been proposed by the authors to deal with the limitations of the spectrum sensing techniques by a single SU.

Up to date survey of spectrum sensing has been provided in the recent paper by A. Ali [19]. The authors bring forward the recent advancements in the spectrum sensing and study the comprehensive framework for the interweave cognitive radio. Since secondary users cannot access the spectrum channel concurrently with primary users in interweave communications, the spectrum sensing parameters supply the necessary information. The different aspects

such as complexity, power consumption, throughput etc have been considered from the implementation point of view. The recent efforts in standardizing the cognitive radio specifications has been addressed. The CR network model along with the cooperation with Internet of Things has been showcased as potential part of the next generation cognitive radio networks. The up-to-date knowledge and research effort in cooperative spectrum sensing is also discussed for each of the cooperative communication element including knowledge base, control channel, data fusion and hypothesis testing.

2.2.1 Literature review on Energy Detection based spectrum sensing

In [27], performance of energy detection is studied for both AWGN and fading channels for an unknown transmit signal. By implementing the square-law combining and selection diversity, alternative closed-form mathematical expressions for the detection probability is presented. With reference to cognitive radio technologies and ultra-wideband, the performance of this energy detector is analyzed. The energy detector does not work below certain SNR levels and was proved in [24] where the authors considered the detection of signals in uncertain low SNR environments. The authors propose "SNR wall" concept which determines the minimum signal to noise ratio below which reliable detection is impossible through energy detection irrespective of the long channel observation time. Small modeling uncertainties and robustness can a fundamental performance metric and should not be ignored in any practical system. But the impact of these uncertainties can be measured by the "SNR wall" position. A mathematical modelling is presented for the uncertainty in the channel noise. The tradeoff between the sensing capabilities and primary users capacity has been captured by computing the SNR wall in the context of interweave CR.
This work was extended in [54] where the authors suggested cross-correlation to obtain higher sensitivity of energy detector. The authors measure the "SNR wall" mathematically and show that it is proportional to value/amount of noise

uncertainity. The mathematical equations are derived to express the detection performance in terms of relevant system parameters for a cross-correlation system. To get the desired performance of detection measurement time is required to be estimated. Faster detection is possible with cross coorelation as compared to standard energy detector. By using some approximations and IEEE 802.22 requirement parameters, the authors show that without having any knowledge of the signals to be detected, the proposed cross-coreelation system is able to satisfy the sensing specifications. The comparison between sensing accuracy and sensing complexity in terms of receiver operating characteristic (ROC) curve is studied in [55]. The authors analyze energy and maximum minimum eigen value (MME) detectors to study the effect of the signal bandwidth with the observation bandwidth. The authors prove that the detection probability increases monotonically with the increase in the signal bandwidth in the case of energy detector but an optimal ratio of these parameters has to be computed for MME detector based on the system dimensionality. A combined two-stage detector is proposed as a solution and the performance is evaluated based on measurements and simulations. Better sensing accuracy is achieved by proposed combined detector than the two individual detectors. However, the proposed detector is self adaptable whereas the implementation and computational complexity in between the two individual detector's complexities.

The authors in [56] propose a new spectrum sensing algorithm based on the dynamic state−space model which characterize occupancy statistics of PU as two hidden states. Jointly the channel statistics and PU occupancy states are considered to perform spectrum sensing with this new approach. Due to non-stationary distributions, the generalized likelihood ratio test (GLRT) becomes impractical. The authors show that simple bayesian decision method is also impractical for this problem because of non-existence of likelihoods. An iterative algorithm is proposed to overcome this problem in which the primary user occupancy states and the dynamic multipath channel are estimated recursively. The noise uncertainty parameter is also addressed in the proposed algorithm

conveniently. The authors in [57] propose a low-complexity energy detection spectrum sensing scheme based on GLRT algorithm. To deal with timimg misalignment arising due to random arrivals of primary-user signals, Bayesian and generalized likelihood ratio test detectors have been studied before in the literature. However, due to implementation complexity and imperfect knowledge about the distribution of unknown parameters, bayesian becomes impractical. The authors mathematically derive the detection probability for the timing misalignment in maximum-likelihood estimation. The proposed GLRT detector is shown to have performance improvement and low-complexity.

E. Axell et al. in [15] considers the OFDM signals and then employs the concept of sensing in AWGN channel. The detector that has been employed in this paper is optimal and correlates the OFDM signals using cyclic prefix. The optimal detector is Neyman-Pearson and has been employed considering deterministic noise. The comparison of the optimal detector has been carried out with that of the simple energy detector. GLRT (generalized likelihood radio test) approach has been exploited, if the signal's awareness is not known. Then afterward the GLRT detector has been compared to the detector that has been employed to access the performance of the OFDM signals. The GLRT method is precise one in comparison to others, if the awareness of the noise is unknown. In this paper, the Neyman-Pearson detector is first derived for OFDM signals. The model that has been employed is a complex, discrete-time baseband model. One second-order statistics detection has also been evaluated. The detector that is based on the statistics of the second-order is complicated. Monte-Carlo simulation has been carried out to accomplish the results. The authors in [58] studied cooperative spectrum sensing considering two sensing schemes. In first scheme, all the information by secondary users is exchanged locally. In the second scheme, there is one central controller to which all the information by secondary users is relayed. Second scheme is the optimized scheme because the relay performs the dual operation depending upon the SNR. Results recommend that the proposed scheme performs well in comparison to the existing

techniques. The authors in [59] considered the cooperation based spectrum sensing. In this scheme, cognitive radios use energy detection and cooperate with each other to detect the vacant spectrum. The threshold is optimized based on the voting rule. To satisfy the limiting errors, a new spectrum sensing algorithm is proposed which needs less number of cooperating cognitive nodes. Extension of this work is done in [60] where authors study a novel multirate sub-Nyquist sensing (MS^3) over fading channels. To mitigate the distortion effects of sub-Nyquist sampling, different sampling rates are applied in such a way that sample numbers are prime. The sensing performance is analyzed over Rayleigh fading and log normal fading channels. The authors prove that the aliasing effects can be mitigated using different sub-Nyquist sampling rates.
S. Nallagonda et al. in [61] studied the energy detection method in different fading channels for cognitive radios. The performance has been analyzed under different fading channels like AWGN, log-normal shadowing, Nakagami, Rayleigh, Wiebull etc. To investigate the performance, different probabilities of sensing have been evaluated and receiver operating curves (ROC) has been plotted. The parameters that have been evaluated to see the performance are false alarm and missed detection. The only scenario in which the spectrum can be exploited by CR is that it should not cause any intrusion to the primary user. In some scenarios the intrusions affected by the fading, shadowing may be high and CR cannot spot the primary user. Simulation has been done in various scenarios. The matrices of the numerous parameters viz. missed detection, false alarm probabilities have been evaluated. The authors in [62] consider energy efficiency and spectrum efficiency together and define a joint function to study their effect in cooperative spectrum sensing. The threshold optimzation is derived analytically using the joint proposed utility function in a simple sensing scenario. The authors also study the traditional sensing frame structures and propose a novel frame structure based on the fact that the older structures downgrade the sensing performance. The new proposed structure is one which takes into account reporting time of the sensing along with the other

parameters of sensing which was the drawback in the older frame structures. For flat and frequency selective fading channels, a new multi-minislot scheme is proposed which operates on the basis of achieving the time diversity gain. The sensing results which are reported at different time−points achieve a more diversity gain for cognitive user. The analytical derivations for optimized decision and optimized threshold are also presented. Simulation results show that using an optimized number of cooperating SUs, the improvement in sensing energy efficiency through the use of proposed multi-minislot scheme can be achieved.

2.2.2 Literature review on Cyclostationary based Spectrum Sensing

In [63], Gardner presented a comprehensive survey for half century of research in cyclostationarity providing an extensive bibliography at the end. Literature in all languages, in which a substantial amount of research has been published, is included. Both stochastic and nonstochastic approaches along with the seminal contributions for licensed signal analysis are identified. In the first approach, which is a traditional method, signals are realized as stochastic processes. However in the second method, time series and time functions for statistical analysis are used to model the signals. These functions define infinite time series averaging in place of ensemble averages. A lot of applications of cyclostationarity related to signal processing and communications are discussed. To realize the cyclostationarity property strip spectral coorelation algorithm (SSCA), FFT-accumulation algorithm (FAM) along with the direct estimation of cyclic periodogram and SCD method have been studied in [64]. Time varying quadratic system is used to characterize the theoretical framework along with the kernel function. The comparative analysis for the proposed and considered algorithms show that SSCA takes less detection time at low signal-to-noise regions.

In 2009, Simon Haykins [65] provided the experimental results and discussed the effectiveness of using cyclostationarity in signal detection and classification for CR. To improve the spectrum utilization, cognitive radios need to focus on the reliability of spectrum sensing and its computational complexity. The

authors claim that CR should have high sensitivity and should be able to detect the different interfering signals and estimate the under-used and unused bands rapidly. The authors proposed a new spectral estimation technique using multitaper method (MTM) for increasing the effectiveness, reliability and accuracy of the spectrum sensing. A tutorial on MTM is provided and is extended to perform space time analysis. The experimental results are discussed using ATSC digital television specifications under the effects of Rayleigh fading. This experimentation is further extended and a blind cyclic autocorrelation function (SP-CAF) based detector is implemented and tested using GNU Radio and universal software radio peripheral (USRP N210) platform in [66]. The comparison between traditional energy detector and proposed blind SP-CAF based detector is studied in real time scenario and taking different application specific conditions and parameters. The authors show that the proposed cyclostationary feature detector performs better than the traditional energy detector with a surety of acceptable low detection time and reasonable complexity. It is demonstrated through different experimental results that the proposed blind sensing detector can achieve higher probability of detection at a low false alarm probability under real channel conditions. It is shown that the proposed technique requires less samples and is more efficient than traditional ED. A simple multi-cycle based cyclostationary sensing algorithm for OFDM based cognitive radio networks is proposed in [67]. A three step algorithm is proposed along with the test statistics formulated as a ratio of two quadratic cyclic autocorrelation functions. The proposed multi-cycle algorithm yields better probability of detection when compared with the existing detection algorithms.

L. Yang in [68] proposed a combination of cyclostationary and energy detector also called cyclo-energy detector for the performing spectrum sensing which could sense the spectrum while transmitting. The main test statistic is based on analyzing the cyclostationary property of the PU signal. The proposed detector can work simultaneously with secondary user and sensing can be performed during SU transmissions. This is based on the fact that PU signal received

power can be detected using the analysis of cyclostationary properties of SU signals. In other words, it can sense the spectrum when the channel is being used by the SU. G. Huang in [69] proposes a simplified the spectrum sensing method. In this method, there is no need to estimate the complex and large covariance matrix to estimate which is required in some previous works. The single and multiple time lags are considered for finding the cyclic frequency in a CAF of a licensed user signal. Multiple antenna scenario is also considered. The effectiveness of the proposed detector is shown by simulation and the performance is analyzed by comparing with the existing algorithms for a fixed probability of false alarm. Another similar approach is used in [70] where the authors propose a spectrum sensing method based on signal cyclostationarity. The authors argued that the signal characteristics such as modulation, coding, carrier frequency and data rate is generally not known to cognitive users with certainity. This introduces some problem in searching for vacant spectrum channels in cognitive radios. Detecting the PUs signal presence/activities is very difficult at low SNR regions. The proposed sensing method is fully blind and much simpler as compared to conventional cyclostationary spectral correlation detection.

In [71], cyclic frequency mismatch due to clock error or oscillator error and its impact on cyclostationary spectrum sensing is analyzed. The authors study the origin of mismatch and the impact of it on sensing performance. It is shown that the cyclostationary detection is actually very sensitive to the mismatch. This work is extended and new technique to mitigate the effect of cyclic frequency mismatch using Slepian basis expansion is proposed in contrast to the widely used Fourier basis expansion. It is shown that the deviation and variation in the cyclic frequency is captured using the proposed methodology. In this way, sensing performance is improved even if there is a cyclic frequency mismatch. It is concluded that the traditionally used Fourier transform approach is the best if there is no cyclic frequency mismatch whereas the proposed Slepian based methodology provides significant performance improvement when com-

pared with the conventional block-based and basis-based Fourier approaches in the presence of cyclic frequency mismatch.

The authors in [72] propose a new spectrum sensing method which is based on the last status change point of the Primary Users. Maximum likelihood estimation (MLE) with dynamic programming is used to estimate the last status change point (LSCP). With Dynamic programming the computation becomes fast and the efficiency of the proposed method increases. The sensing method is based on the assumption that multiple PUs may change their status during sensing period. The performance enhancement is achieved in terms of detection probability and a new cumulative sum based scheme is also proposed. It is shown through simulations that better detection probability is achieved with the proposed method when compared with spectrum sensing methods under consideration. The author in [73] studied the spectrum sensing in context to cognitive mesh networks. The authors propose spectrum sensing scheduling algorithm and allocation method to allow mesh routers to learn by itself using reinforcement learning. A spectrum sensing, decisioning and allocation based on reinforcement learning is proposed to increase efficiency and adaptivity. The simulation results show the increased throughput of the CR based mesh networks.

Since optimal detector may need to know the CSI or characteristics of the waveform to be detected, the sub-optimal detector may use pilot symbols or some training sequences which are used for synchronization and channel estimation purposes. Therefore, Locally optimum detection (LOD) discussed in [74] behaves optimally under low SNR regions. The authors propose a combination of two detectors which is termed as weighted semi-blind locally optimum detector (WSBLOD). The simple combination of these two detectors does not give an optimal performance. The proposed detector is designed by optimising the weights for the test statistic to maximise the detection probability. The authors in [75] consider three spectrum sensing techniques of primary transmitter detection: Matched filter detection, Energy detection, and Cyclostationary fea-

ture detection. In this paper, these techniques has been compared and analyzed in terms of various sensing parameters. Numerical result shows that cyclostationary detection technique outperforms other two at low signal to noise ratio (SNR) but at the cost of implemetation complexity and long observation time.

2.3 Literature Reveiw on SDR implementation and Dynamic Waveform Design framework

Fifth-generation (5G) communication systems are likely to be based on software-defined radio (SDR) based cognitive radio networks. The high-speed universal access with multiple capabilities is the proposed capabilities likely to be provided in next generation networks. The generalized framework for implementing SDR based CR with flexibility for waveform generation and dynamic access is investigated in [76]. The authors have proposed a unified framework for generating and implementing SDR based dynamic waveform. This generalized framework for CR waveform generation is called spectrally modulated, spectrally encoded (SMSE) framework because coding and modulation both are implemented in frequency domain. Simulation results show the practical suitablility of modeling and analytic expression in CR based scenario.

However, this SMSE framework is extended in [77] where the authors provide an extension to the decision process implementing general soft decision SMSE (SDSMSE) to exploit the advantages of both underlay and overlay CR paradigm. To implement the waveform in flexible and dynamic wireless environment, the framework is shown to improve the spectrum efficiency and maximize the channel capacity for SU. The probability of error taking the different test cases is derived in AWGN channel and is shown to be suitable for CR based applications. The underlay, overlay and hybrid techniques enable the SU to co-exist with PU. The implementation of SMSE cognitive centric overlay waveform on SDR platform is demonstrated in [78]. Multi-carrier transmission waveforms over non-contiguous frequency bands for the cognitive radio is generated through SMSE framework. The spectrum sensing enables to sense only

those sub-carriers which are not occupied by primary users and are available to the secondary user. The non-contiguous OFDM transmission using SMSE is implemented and CR is demonstrated to adjust its parameters such as bandwidth, number of subcarriers etc using this analytic framework. The real time video transmission by SUs and without interference to PUs is demostrated by the authors. When the PU arrives, those sub-carriers are sensed using simple energy detector and they are turned off and CR switches to other sub-carriers which are vacant.

The above SMSE work is further extended in the recent paper [79] where the authors demonstrate the implementation of hybrid underlay/overlay SDR based Cognitive Radio Network. A CR waveform is generated from SD-SMSE framework software defined radio (SDR). The SDR platform implements hybrid underlay/overlay waveform using USRP N210. Different modulation schemes have been used to implement SDR based adaptive rate transmission. The interference limit has been studied practically. Both unused and under-used segments have been exploited. Higher constellation modulation are able to tolerate less interference. To stitch the multiple non-contiguous spectrum sub-bands, waveform generator uses its dynamic capability through SMSE soft decision. The implementation details are also provided in the paper. However, it is shown that if SU is interfering with PU then PU can disrupt the SU transmission by transmitting at much higher power than that of interference limit. This platform provides a test-bed for CR.

Alazemi et al. [80] addressed the problem of flexible spectrum access with software defined radios (SDR). Spectrum fragmentation and interference may become a problem because of the flexibility offered by these radios. The problem of spectrum allocation and schenduling is very critical because of the ability of SDR to configure transmissions anywhere in the available spectrum holes or frequency bands. The authors considered the feasibility of the scheduling and routing in such a scenario under interference constraint and showed that it is not feasible to obtain the optimal solution to this problem. The exceptional

case is there for very small networks. The authors proposed a simulated annealing method as a potential solution to the problem of link scheduling and spectrum allocation. The simulation results show that the interference handling and flexible spectrum assignment capability of the network improves and becomes better with the proposed approach.

The authors in [81] demostrated a novel, fully networked middleware for centrally controlling distributed radio link setups of SDRs and reconfigurable legacy devices. The main motivation of the work originates from the fact that cognitive radio concepts such as the cognitive radio manager or the cognitive engine requires regular experimental verification and testing in complex, real-time and signal processing focused SDR frameworks, e.g. directly in FPGAs or in a software like GNU Radio. The authors show the capabilities of ULLA-X, and present by means of examples its adaptation capabilities for custom radio implementations and its programming concept for different SDR platforms. As an intermediate layer, ULLA-X allows technology-agnostic device parameter monitoring and reconfiguration based on an easy-to learn programming language. Through its functionality, ULLA-X mitigates the complexities arising from using different radio platforms and makes various configuration APIs readily accessible to standard research tools. An efficient spectrum monitoring algorithm is presented in [82]. In the proposed algorithm, the arrival of primary users can be detected during the secondary user transmissions. The proposed technique detects the variations in the signal strength over the reserved OFDM sub-carriers. By doing so, primary user reappearance is detected very quickly and it also reduces the number of times spectrum sensing is to be performed. The proposed algorithm is immune to fading channels in the case of both multiple antenna systems and single antenna systems. It is shown by simulations and by mathematical analysis that the proposed method is twice as complex as traditional energy detector. The impairments in OFDM CR waveform such as inter-carrier interference, narrow band interference and power leakage are also analyzed in this paper.

2.4 Literature Reveiw on Spectrum sensing in Multiple Antenna Scenario

The spectrum sensing in multiple antenna scenario is studied in [83] where the authors study the energy detection in a multiple antenna scenario. The secondary transmitter is assumed to have multiple antennas and hence it receives multiple copies of the primary user signal. The different versions of this PU signal is combined using maximal ratio combining and is given to the traditional energy detector. The performance in terms of probability of detection is analyzed for a fixed false alarm probability and given signal-to-noise ratio. The closed-form expressions for the detection probability and false alarm probability is also derived for rayleigh fading channel. It is shown that the upper bound on the performance is achieved with energy detection based on maximal ratio combining because it employs the channel state information along with the coherent combining. S. H. Hwang et al. [84] presented a new technique to sense the spectrum band. In the proposed technique, the channel that has been considered is Suzuki channel and a number of antennas have been employed. The paper exploits the energy detection which is very simple to implement. To check the performance of the technique two scenarios has been considered. The parameter that has been taken into consideration is a threshold. If the primary user has to be present, then the threshold must be less than the received value of the energy. If this is more than the outcome, then primary user will be absent. Simulation results recommend that by exploiting the proposed scheme, the detection performance can be increased with the help of multiple antennas. Complementary receiver operating curves (ROC) has been exploited to analyze the performance of the proposed technique.

By using improved energy detector instead of traditional/conventional energy detector, the detection performance can be enhanced in case of multiple antenna CR and is studied in [85]. The proposed new energy detector employs the p^{th} power of the absolute samples of primary users (PUs) signals instead of traditionally used sum-squared values. Using an improved energy detector

a cognitive radio (CR) network based on multiple antennas with multiple hopping is studied. The authors derive the analytical expressions for probability of detection and for the probability of false alarm. The work is also extended to cooperative diversity and performance of proposed energy detector is analyzed using multihop cooperative diversity. An efficient spectrum sensing algorithm is introduced which reduces the sensing time and overall diversity branches needed to obtain the optimum performance. Analytically, closed form expressions for obtaining the optimum number of cooperative diversity branches is also derived and it is shown that total error rate can be minimized and quick sensing can be performed by using optimal number of diversity branches.

The PU signal and noise can be taken as independent in multiple antenna cognitive radios and spectrum sensing can be performed using Generalized Likelihood ratio (GLR) detectors which is discussed in [86]. But the main problem of GLR is that it should have all the information about primary user signal characteristics, CSI and noise variance etc. In practical scenarios, all the parameters may not be known and one or more parameters has to be estimated which makes the detectors blind. So, the authors in this paper derive the detection probablility and probability of false alarm for modified GLR analytically. The PU signal and the noise is assumed to be complex zero-mean Gaussian. The proposed GLR detector becomes sub-optimal and robust. The performance of the proposed detector is compared with the traditionally available energy detector and it is also proved that the proposed detector has a low computational complexity.

The authors in [87] study GLRT based spectrum sensing techniques from a different perspective of single carrier frequency division multiple access (SC-FDMA) cognitive radio networks. Considering multiple-input multiple-output (MIMO) CR, Since the optimal performance of GLRT is obtained when the system parameters are known. The authors here study the sub-optimal performance considering unkown noise variance. The analytical expressions for detection probability and probability of false alarm are derived. Closed form

expressions are derived to quantify the computational complexity. A new approach based on multi variate analysis of power spectral density (PSD) of the multiple antenna spectrum sensing in cognitive radios has been proposed in [88]. The authors proposed approach is based on GLRT and flat-fading channels for the received multi antenna signal. The previous work assume the noise variance to be same at different antennas, the authors in this paper consider different noise variances at different antennas. The analytical performance analysis without the knowledge of the exact values of noise variances is implemented and validated using various examples through simulation. This work is extended in [89] where the authors investigated a spectrum sensing method in frequency domain by taking the DFT of the recieved multi antenna signal. The channel is assumed to be flat-faded with noise uncertainty. This proposed method also permits the different noise variances. By neglecting the spatial structure of the primary user's received signals at different antennas and without the knowledge of the values of the noise variances, a different problem of spectrum sensing based on the generalized likelihood ratio test (GLRT) is proposed. The performance analysis is carried out by taking different simulation examples of the proposed approach and comparison is drawn with energy detector and already studied GLRT approaches.

The spectrum sensing of orthogonal space-time block coded signals is discussed in [90] where the authors study the traditional energy detector based on space time block codes (STBC). Two test metrics based on higher order moments are proposed. The detection accuracy is improved by 18% and false alarm probability improves by 1% using proposed first test metric. The second test metric improves the performance in terms of sensitivity to noise uncertainty. It is shown that for an unertainty level of 1 to 2 dB, almost 80% performance enhancement is achieved when compared to the traditional energy detector.

Based on cyclostationary property of the signals, a different spectrum sensing method for receivers with multiple antennas is analyzed in [91].The cyclic covariance matrix is taken as a decision metric to determine the absence or

presence of the primary users. Taking spatially correlated and uncorrelated noise, two test cases are analyzed and spectrum sensing parameters namely, detection probability and false-alarm probability are derived for each of the case considering Rayleigh fading channels. The authors proved that with the proposed method, the noise estimation is not required when cyclic correlation significance test is used and threshold value of the proposed sensing becomes independent of noise variance and number of samples. Through simulations it is shown that the proposed method achieves higher detection probability and robustness in AWGN channel as well as in quasi-static rayleigh faded channels when compared with other existing cyclostationary based spectrum sensing algorithms. In [92], the authors consider the SU power transmit limit to regulate the maximum tolerable interference for PU. Erogodic capacity of SU is derived taking the imperfect CSI into account. The loss in the erogodic capacity due to interference is computed in terms of CDF. A closed form expression for bit error rate is also given analytically and validated through simulations.

Q. Huang in [93] proposed a sensing technique using F-test for multiple antenna cognitive radio systems. The main drawback of this approach is that the prior knowledge about channel state information (CSI) is required. The proposed method is based on the statistical properties of F-distribution and easy to implement. The detection probability and threshold required for hypothesis testing is derived analytically. The authors also investigate the effect of imperfect channel knowledge on the proposed spectrum sensing detector. The proposed F-test based detector is shown to achieve better performance when compared with other popular detectors.

2.5 Literature review on Spectrum Sensing in RF Energy Harvested Relay based Cognitive Radios

To increase the spatial distance of communication and to combat multi-path fading, relay is a powerful tool. In [94], a cognitive relay network with the maximum transmit power limit in a spectrum sharing scenario is considered.

The CR model is analyzed over Rayleigh fading channels and the outage probability expression is derived. It is shown that interference power limit and maximum transmit power constraint can cause the saturation in the outage of SU. The analytical results are validated through simulations. This work is extended in [38] and the total interference from SU transmitter to PU receiver and from PU transmitter to SU receiver is considered in the analysis of two-way cognitive relay networks. From the two available traditional access methods namely, Time-division broadcasting (TDBC) and Multiple access Broadcasting (MABC); TDBC relaying is used with decode and forward protocol. The system performance in terms of relay position relative to the PT and PR is analyzed. The outage probability for SU over rayeigh fading channels for oppurtunistic relay selection is analyzed and validated using Monte Carlo simulations. The mutual interference effect between PU and SU based on the asymptotic diversity order is also analyzed. It is proved that proper placement of relays has a significant impact on the practical performance of the CR relay based system. The authors in [95] analyze the path loss effects while considering the interferences from primary transmitter to secondary receiver and secondary transmitter to primary receiver with multiple antenna terminals and cognitive relay employing amplify and forward technique. The analytical expressions for end-to-end outage probabilities have been derived.

The first analysis to prove the simultaneous transmission of energy and information is studied in [43]. It is shown that there is always a trade-off between reliable information transmission and energy transmission over a noisy channel. The trade-off is defined in terms of coding theorem and a capacity-energy function. The capacity-energy functions are defined and computed for various fading channels.

A. Sultan in [96] considered a CR system model in which SU is capable of harveting RF energy. A finite capacity battery is also considered for analysis. The primary user operates in a time-slotted fashion. The SU senses the spectrum to detect the PU activity depending upon the amount of residual energy

available with the SU. The spectrum sensing is performed at the beginning of each time slot with a goal to maximize the system throughput. The fluctuation in the throughout is investigated by considering different system parameters and optimal sensing decision is based on Markov chain model.

Cognitive Radio with RF energy harvesting capability but without considering the battery or any storage device is considered in [40]. It is assumed that SU can harvest energy from ambient source or environment. Due to limitation of RF-EH hardware, it is assumed that SU can only operate in a time-slotted manner and can perform either spectrum sensing or energy harvesting or data transmission at a time. The trade-off in terms of harvesting-sensing-throughput is analyzed while considering the interference constraints of PU. A multi-slot spectrum sensing is considered which is shown to converge to a single-slot spectrum sensing. Sensing duration, save-ratio and sensing threshold is optimized jointly. Decision fusion and data fusion are generally used and both of which converge while achieving the maximum SU throughput. Simulation Results validate the analytical derivation considering a pre-defined limit of detection probablilty. It is shown that the proposed single-slot spectrum sensing outperforms the existing strategies.

A cognitive radio (CR) network with multiple secondary users (SUs), each of which is equipped with an energy harvesting capability is considered in [39]. The opportunistic use of the idle spectrum, which is not used by primary users (PUs), through a mechanism of two-step opportunistic spectrum access for the SUs, consisting of random channel sensing followed by random channel access is considered. The joint impact of sensing probability, access probability and energy queue capacity on the maximum achievable throughput in a multiuser CR network incorporating energy harvesting is investigated. For two extreme cases, those where the energy queue capacity is either infinite or extremely small, it is shown that the maximum achievable throughput is not affected by the channel access probability if the channel sensing probability is chosen appropriately and the optimal sensing probability is derived as a function of network

parameters such as the energy arrival rate, channel availability probability, and number of contending SUs. The authors in [97] investigate the major trade-offs relating to the energy efficiency in cognitive radio networks. The five main trade-offs (primary user interference, fairness, QoS, network architecture and security) are covered. The reason for considering these parameters is that all the components related to CR network design, implementation and network's operability are affected by variations in these factors. The relationship between these trade-offs is investigated. While satisfying the different constraints in CR, the optimal energy efficiency is also studied.

An energy-harvesting cognitive radio system where the secondary transmitter harvests energy is considered in [98]. The operation of the system is defined by collision constraint and an energy causality constraint. Whereas the former ensures the protection of PU system, the latter ensures the lower consumption of energy than harvested. The sensing duration defining the energy equilibrium regions and maximizing secondary throughput are defined. The optimal pairing of threshold and sensing duration is determined while maximizing the detection probability and minimizing the collision probability. This is because shorter sensing duration increases the false alarm and hence the collision probability. To conserve the energy while satisfying the energy and collision constraints, both sensing threshold and duration need to be optimized jointly for maximizing the secondary system throughput. The work is extended in [51] where the authors consider heterogeneous CR sensor networks(HCRSNs). The data transmit buffers are battery powered devices whereas spectrum sensing equipment is energy harvesting enabled. Two separate scheduling algorithm operate for spectrum sensing and data transmission monitoring. Cooperative Spectrum Sensing is used to sense the the licensed spectrum of PUs. The spectrum sensing problem is formulated as nonlinear programming problem with cross entropy based resource allocation algorithm for available channels whereas data monitoring algorithm is proposed as a joint power and time resource allocation optimization algorithm to save energy and to transmit the data over the

sensed vacant channels. The simulation results show that the reliability of energy harvesting based spectrum sensing can be maintained along with reduced energy consumption of the data sensors. The algorithm for resource allocation of data sensors allocates power, available time and sensed channels in such a way that minimizes the energy consumption of data sensors and PU are also protected from unnecessary interference. The proposed resource-allocation algorithms for the HCRSN are more efficient and optimal as demonstrated in the simulations.

Considering multiple primary user (PU) transceivers instead of multiple SUs for an underlay cognitive relay network a new wireless energy harvesting protocol is proposed in [41]. It is proposed that secondary nodes harvest RF energy from the primary network (PN) while sharing the spectrum in an underlay fashion. To evaluate the impact of different system parameters on the proposed network model, the authors derive the closed expression for outage probability analysis of relay based secondary network (SN) subject to three important power constraints: 1) the maximum transmit power at the secondary source (SS) and at the secondary relay (SR); 2) the peak interference tolerance power permitted at each PU receiver; and 3) the interference power from each PU transmitter to the Secondary relay (SR) and to the secondary destination/receiver (SD). To obtain practical design insights into the impact of different parameters on successful data transmission of the SN, the authors derive throughput expressions for both the delay-sensitive and the delay-tolerant transmission modes. Asymptotic closed-form expressions for the outage probability and the delay-sensitive throughput and an asymptotic analytical expression for the delay-tolerant throughput as the number of PU transceivers goes to infinity is also derived. The results show that the outage probability improves when PU transmitters are located near SS and sufficiently far from SR and SD. It is shown that when the number of PU transmitters is large, the detrimental effect of interference from PU transmitters outweighs the benefits of energy harvested from the PU transmitters.

The authors in [99] consider the interweave cognitive radio system and study the sensing-throughput trade-off. Specifically, the problem is formulated to maximize the throughput of the secondary network while optimizing the sensing duration and satisfying the primary user's interference constraints. The secondary user sense the radio spectrum and occupy the spectrum hole for communication. When the primary user arrives or becomes active, it has to vacant the channel within certain period of time. Energy detection is used as a spectrum sensing technique and it is proved that there is exactly one optimal sensing duration which maximizes the secondary network throughput. The sensing-throughput trade-off problem is redefined and cooperative spectrum sensing is also investigated considering the multiple secondary users using the proposed technique.

From deployment centric veiwpoint, a novel approach that incorporates channel estimation in the CR system model and investigates the impact of imperfect channel knowledge on the performance of the Interweave CR System is proposed in [100]. More particularly, the fluctuations induced in the probability of detection due to variations in the channel or imperfect CSI affect the detectors performance at the secondary transmitter. This can cause the large interference at the primary receivers. Therefore, outage constraints on the detection probability are employed in order to analyze the performance of the Interweave system. In the context of sensing-throughput tradeoff, it is demostrated that with an proper choice of the channel estimation time as determined by the proposed methodology, the throughput performance of the proposed IW-CR system can be significantly increased and degradation in the performance due to imperfect CSI and channel variations can be effectively controlled. The problem of optimal spectrum sensing duration over rayleigh fading channels under the condition of imperfect spectrum sensing is investigated in [48]. The authors argue that spectrum sensing is not required to be performed at the beginning of each time slot because most of the time the primary user's absence may last for several time slots. Considering the rayleigh fading channels, a hidden

Markov chain model is used to describe the imperfect spectrum sensing process. The balance between the different parameters such as the average energy consumption for spectrum sensing, the average interference to the PU and the average throughput of the SU is used to obtain the optimal sensing interval. In order to achieve the higher secondary user (SU) throughput, a hybrid interweave/underlay mode is proposed. An optimization problem is proposed to balance the above said parameters and energy consumption during spectrum sensing. The next sensing time-slot and optimal sensing duration is determined by solving this optimzation problem. The closed form expressions are derived to analyze the average throughput of the SU and the average interference to the PU. Simulation results validate the analytical framework and prove that by adjusting the weight coefficients to create the balance between different parameters, the proposed algorithm can satisfy different requirements of the SU. The authors in [18] study a hybrid interweave/underlay CR system that integrates amplify-and-forward relaying. In this type of hybrid spectrum access system, the secondary users can switch between interweave and underlay spectrum sharing scheme based on the spectrum sensing outcome and the primary users state. A continuous-time Markov chain model is proposed to analyze this type of hybrid cognitive radio spectrum access system also called as cognitive cooperative radio network (CCRN). Considering Nakagami-m fading channel which is different from the previously studied work, the closed form expressions for symbol error rate (SER) and outage probability are derived. The markov chain model is used to characterize the steady-state probabilities of spectrum access for the proposed hybrid model. The comparison betweem Underlay, Interweave and Hybrid model is drawn in terms of symbol error rate (SER), outage probability and outage capacity to show the performance improvement of the proposed network. The network parameters such as the primary arrival rate, the distances from the ST to PR, the interference power threshold of the primary receiver in underlay mode and the average transmit SNR of the secondary network in interweave mode are also investigated and the numerical

results show that the proposed hybrid approach outperforms the conventional underlay spectrum access.

The authors discuss performance tradeoffs related to the energy efficiency, providing insightful results on the complex relationship between different system parameters of cognitive radio networks in [101]. A cooperative CR is analyzed where different SUs having different priorities to use the network resources are parameterized. However, using different spectrum sharing schemes namely underlay, overlay and interweave non-cooperative model is also analyzed. Traditional tradeoffs between sensing accuracy and energy efficiency and between energy efficiency and secondary throughput is also discussed. As a case of overlay CR, a low-priority secondary user can relay data packets for the high-priority SUs using cooperative model is also proposed. With self-interference cancellation, both in the case of half-duplex and full-duplex relays, the energy-throughput tradeoff is analyzed. In a recent paper [47], the authors consider Joint optimization of sensing time and transmission power for a cognitive radio (CR) system. To maximize the energy efficiency, a design problem is formulated with primary user interference constraints as a function of two variables. Comparison of proposed algorithm is provided and evaluated with the existing techniques. The effect of fluctuations in the transmission power on energy efficiency and sensing time is analyzed with an iterative algorithm with low computational complexity proposed. Simulation results have been validated and the effect of varying the power on false alarm probability and detection probablity analyzed. The authors show that at the optimal energy efficiency operating point, the spectrum efficiency condition cannot be met. The authors suggest two solutions to solve this issue. Simulation results have shown that the proposed algorithm outperforms the existing works in terms of maximum energy efficiency, computational complexity and convergence rate.

An energy harvester which extracts energy from the RF signal of a primary user transmitter is considered in [42]. It is assumed that the proposed CR has no any other power source. The cognitive radio first harvests energy from PT and

then transmits within the same time slot. In every time slot, CR first harvest energy for a fixed fraction of the time frame and then transmits data using this harvested energy for the rest of the fraction of the time frame. The authors derive closed-form expression for the optimal harvesting ratio in this short paper considering the primary user interference constraints. The intrinsic harvesting-throughput tradeoff is studied and the authors optimize the harvesting ratio of the cognitive radio to maximise its achievable throughput. Simulations results validate the mathematical analysis of the achievable throughput and optimal harvesting ratio.

2.6 Objectives of the thesis

The main objectives of the proposed research work are stated as under:

- To develop an efficient spectrum sensing technique for SDR based CR.
- To implement new modulation formats with different spectrum sensing techniques.
- To evaluate the comparative performance of proposed modulation format with different spectrum sensing.
- To evaluate the performance of spectrum sensing in multiple antenna scenario.

2.7 Research Contributions based on the above Objectives

The main contributions of the work is summarized as follows

- For better consideration of the generalized analytical framework for CR, SMSE has been conjoined with the CSS technique. Cyclostationary technique has the ability to detect even the traces of the signal present in the deepest noise.
- Analytical expression for the parameters of the sensing technique have been derived in terms of SMSE variables.

- A joint SMSE-CSS based test stat has been proposed for determining the channel occupancy/spectrum holes of PU. The proposed test stat helps for the channel assignment (decision) in a better way by generating the large difference in the threshold and measured values even at low SNR regions.

- Receiver Operating Characteristic (ROC) curves using Constant False Alarm Rate (CFAR) model and threshold adaptation based on instantaneous SNR values have been simulated for the proposed joint scheme and compared with the different detectors traditionally available.

- The proposed spectrum sensing technique is evaluated in multiple antenna scenario and detection probability curves have been drawn and comparison with traditional available detector has been plotted.

- The proposed system has been extended from deployment centric veiwpoint and relay based Interweave/Underlay Cognitive Radio Network has been analyzed with energy harvesting capabilitites.

- New Mathematical modelling of relay based Interweave/Underlay Cognitive Radio Network has been presented and mathematical expressions are derived for optimal system performance.

- Based on sensing accuracy, we derive an expression for optimization of charging duration TSR parameter and sensing duration for maximizing throughput of Interweave Cognitive Radio.

- Based on sensing efficiency, throughput and outage probability for underlay CR is analyzed considering the interference temperature constraints and optimal power distribution parameter at secondary user (SU) terminals.

- The optimized values of switching-time ratios have been derived analytically for both Interweave and Underlay CR. The results thus obtained are compared by taking symmetrical and asymmetric channels between

SU terminals. Analytical results are validated through monte-carlo simulations to confirm the accuracy of the derived expressions.

Chapter 3

Performance Analysis of joint SMSE framework and CSS for CR

3.1 Introduction

This chapter focuses on investigating the performance of spectrum sensing with SMSE framework and to study the effect of sensing on dynamic wavefom design parameters. The issue of efficient utilization of radio resources can be implemented unitedly through dynamic waveform design and an efficient spectrum sensing. In particular, we combine the flexibility (dynamic channel allocation and dynamic waveform design) provided by SMSE framework and sensitivity (ability to deal with the weak signals) provided by Cyclostationary Spectrum Sensing (CSS) to improve the accuracy of final decision for spectrum occupancy. The proposed system design works without having the knowledge of PU waveform still achieving the higher detection probability at low SNR. The analytical expressions have been derived for the proposed combined SMSE-CSS technique and simulated.

3.2 System Model for Interweave CR

We consider a simple CR scenario with Primary User (PU) consisting of a Primary transmitter (PT) communicating with a Primary receiver (PR) and a secondary user (SU) consisting of a Secondary transmitter (ST) communicating with one Secondary receiver (SR) as shown in figure 3.1. The Secondary

transmitter (ST) performs the spectrum sensing periodically over the sensing channel h_{sp} and decides whether the PU is present or absent. SU only communicates if the PU is absent and channel is vacant else it senses the another channel. This is the case of Interweave CR. It is assumed that PT can operate on any waveform design including OFDM or MC-CDMA which is unknown to SU. It is further assumed that both PU and SU network follow the time-slotted synchronous communication.

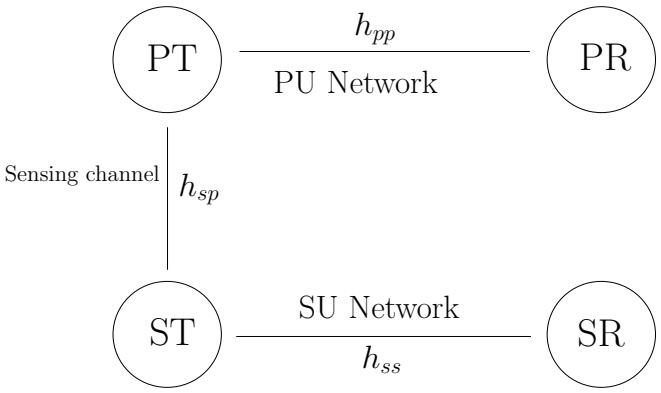

Figure 3.1: System Model (Interweave CR)

The ST can sense unknown PU waveform using its dynamic arrangements through proposed SMSE-CSS technique either one channel at a time or by scanning entire spectrum window. The main advantage of using this dynamic arrangement is that ST need not to have any prior information about PU waveform design and still achieving the high sensing accuracy at low SNR.

Figure 3.2 illustrates the unified transceiver implemented at ST representing cognitive system engine with the proposed joint SMSE-CSS. In this system, PU is sensed and the spectrum decision is taken based on joint proposed SMSE-CSS test metric. With this decision of unoccupied/occupied spectrum, a database is maintained which is upgraded dynamically and is transparent to the user. From implementation point of view, the more elaborated arrangement of sensing and decision blocks at ST transceiver using SDR is shown in figure 3.3. The spectrum of PU is scanned and N channels are filtered using SDR filter banks. This layer of programmable intelligence provided by SDR also adds flexibility

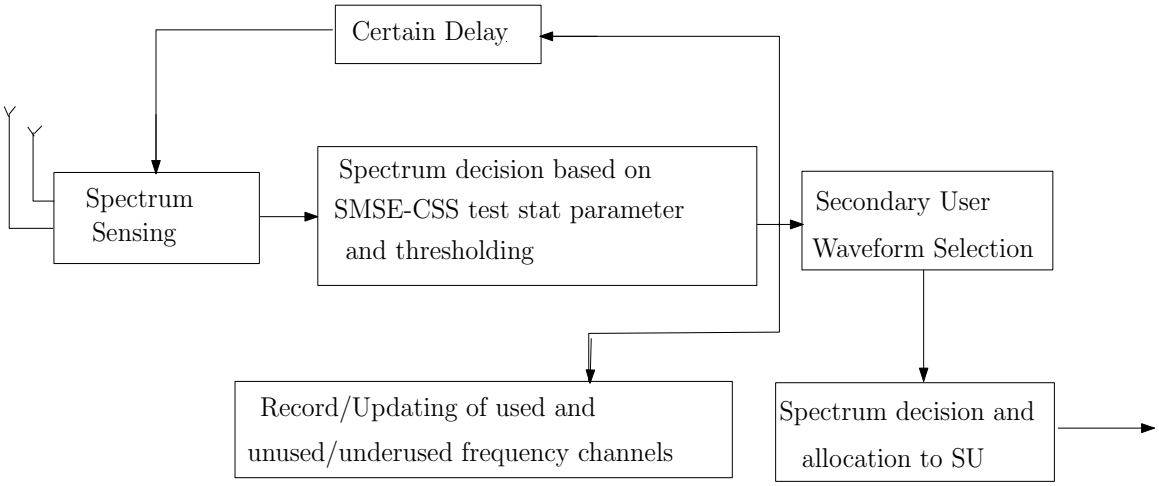

Figure 3.2: Unified Secondary Transciever (Interweave CR)

to the wireless hardware resources to operate dynamically in different frequency bands [102][103]. Each channel is down-converted and joint SMSE-CSS along with the proposed decision test statistics is used to determine the occupancy of N^{th} channel. From this information, bandwidth available for secondary user or being used by PU can be determined which can be further used for spectrum access authorization [29]. Thus, final channel selection for the communica-

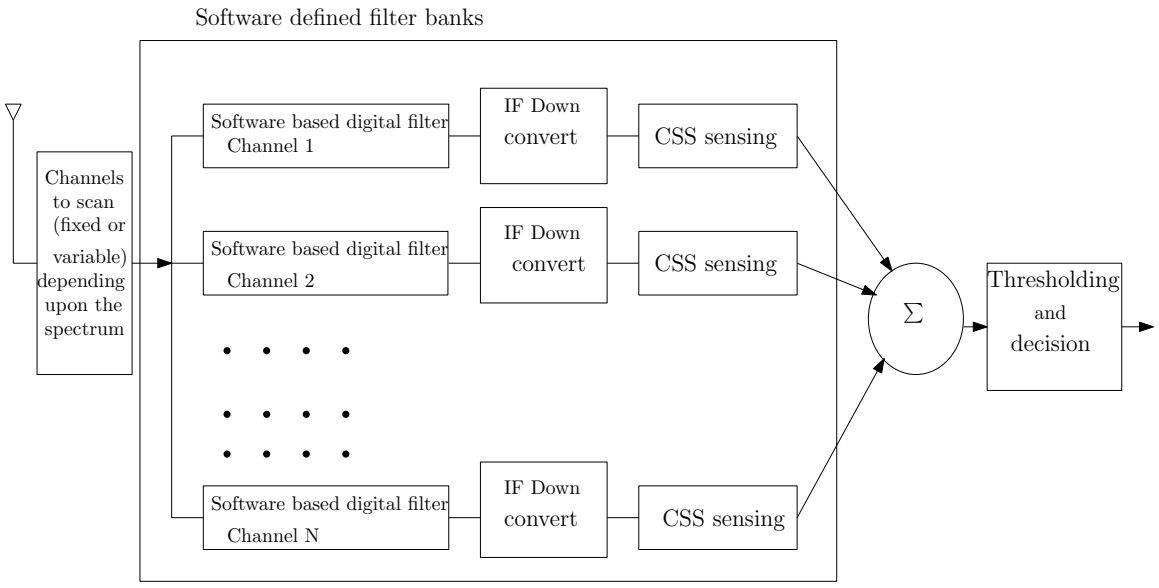

Figure 3.3: Implementation of SDR based CR sensing system

tion between ST-SR is based on the occupancy stats of the PU determined by thresholding and decision block in figure 3.3. The proposed joint SMSE-CSS framework and hypothesis based decision metric test statistics is discussed next.

3.3 Cyclostationary based SMSE framework

In general, signals are classified as SMSE if both the data modulation (spectrally modulated) and the encoding (spectrally encoded) are applied on a component-by-component basis in the frequency domain [76]. Any signal that conforms to the multi-carrier based waveforms can be expressed in terms of its amplitude, phase and frequency characteristics. These three chararterictics help in SMSE waveform design through six design variables. These are: data modulation (d), coding (c), windowing (w), orthogonality (o) and two CR based frequency allocation variables- available frequency band/component variable (a) and used frequency band/component variable (u) [77]. The first three variables account for both amplitude and phase variations where as fourth variable induces phase only variations used for ensuring orthogonality between symbol streams to facilitate multiple access.

The m^{th} frequency component of the k^{th} waveform symbol is given as [77]

$$S_m[k] = a_m u_m c_m d_{m,k} w_m . e^{j(\theta_{d_{m,k}} + \theta_{c_m} + \theta_{w_m} + \theta_{o_{m,k}})} \ , \tag{3.1}$$

where,

$m = 0, 1, 2, \cdots N_f - 1$,

N_f = frequency components available for waveform design,

c_m & d_m = coding and data modulation variables that determine amplitude and/or phase variations,

w_m = windowing operation.

Frequency selection in spectrum involves two variables; $a_m = [a_1, a_2, \cdots a_{N_f-1}] \forall a_i \in \{0, 1\}$ represents the i^{th} available frequency component/band and $u_m = [u_1, u_2, \cdots u_{N_f-1}] \, \forall \, u_i \in \{0, 1\}$ accounts for the i^{th} used band or frequency component. $\theta_{d_{m,k}}$, θ_{c_m}, θ_{w_m}, $\theta_{o_{m,k}}$ represent the respective phases induced during data modulation, coding,

windowing and orthogonality. The discrete time domain SMSE waveform can be expressed by taking IDFT of equation (3.1) as

$$s_k[n] = \frac{1}{N_f}\Re\sum_{m=0}^{N_f-1} a_m u_m c_m d_{m,k} w_m . e^{j(2\pi f_m t_n + \theta_{d_{m,k}} + \theta_{c_m} + \theta_{w_m} + \theta_{o_{m,k}})} \ , \tag{3.2}$$

where $t_k \leq t_n < t_k + T$ and $f_m = f_c + m.\nabla f$, T = symbol duration, $\nabla f = 1/T$ is the frequency resolution, f_c is the carrier frequency of the first sub-band. The linear auto-correlation of equation (3.2) is given as

$$R_x(\tau_0) = E\{s_k[n].s_k^*[n+\tau_0]\} \ , \tag{3.3}$$

where

$$s_k[n].s_k^*[n+\tau_0] = \frac{1}{N_f}\sum_{m=0}^{N_f-1} |A_{m,k}|.|A_{m,k}|.\cos(2\pi f_m t_n + \phi_{m,k}).\cos(2\pi f_m t_{n+\tau_0} + \tau_0 + \phi_{m,k}) \ . \tag{3.4}$$

In equation (3.4), $A_{m,k} = a_m.u_m.c_m.d_{m,k}.w_m$ and $\phi_{m,k} = \theta_{d_{m,k}} + \theta_{c_m} + \theta_{w_m} + \theta_{o_{m,k}}$.

3.3.1 Analytical expression for CSS in terms of SMSE based framework

To detect the built-in periodicity in the modulated signal, CSS defines two functions: *Cyclic Auto-correlation Function (CAF)* and *Spectral Correlation Density Function (SCD)*. The built-in periodicity in the signal is examined using CAF at a cyclic frequency α_0 which is defined for a signal x as [104][63]

$$R_x^{\alpha_0}(\tau_0) = \lim_{N\to\infty}\frac{1}{N}\sum_{n=0}^{N-1} R_x(\tau_0).e^{-j(2\pi\alpha_0 n)} \ , \tag{3.5}$$

where $R_x(\tau_0)$ represents the linear correlation defined by equation (3.3). Considering orthogonal behavior of the IDFT and using the trigonometric identity [105] as $\cos(\theta) + \cos(\theta+\alpha_0)\cos(\theta+2\alpha_0)\ldots\cos(\theta+n\alpha_0) = \frac{\sin(\frac{(n+1)\alpha_0}{2}).\cos(\theta+n\frac{\alpha_0}{2})}{\sin(\frac{\alpha_0}{2})}$, we get

$$\begin{aligned} R_x^{\alpha_0}(\tau_0) &= \lim_{N\to\infty}\frac{1}{N}\frac{1}{2N_f}\sum_{n=0}^{N-1}\sum_{m=0}^{N_f-1}|A_{m,k}|^2 \\ &\quad \times\Re\left[exp\left(-2\pi m\tau_0 + \frac{4\pi mnt_n}{T} + 2\phi_{m,k}\right)\right]e^{-j2\pi\alpha_0 n} \end{aligned} \tag{3.6}$$

Let us define Cyclic Frequency Analysis Parameters as: Cyclic time window $N_0 = \frac{f_s}{\alpha_0}$; Normalized frequency resolution $\frac{1}{N_p} = \frac{f}{f_s}$. From equations (3.4),(3.5) and (3.6), the CAF can be rewritten as

$$\begin{aligned} R_x^{\alpha_0}(\tau_0) &= \lim_{N\to\infty} \frac{1}{N}\frac{1}{2N_f}\sum_{n=0}^{N-1}\sum_{m=0}^{N_f-1} |A_{m,k}|^2 \\ &\quad \times \cos\left[-2\pi m\tau_0 + \frac{4\pi mn}{N_p} + 2\phi_{m,k}\right] e^{-j2\pi\alpha_0 n} \ . \end{aligned} \tag{3.7}$$

Equation (3.7) represents the cyclic analysis of SMSE signal equivalent to searching for a cyclic frequency at a particular time lag in the cyclic auto-correlation function of the PU signal. Due to noise and inherent properties of some signals, the periodicity features are embedded in frequency domain which may not be easily seen in time frames [66]. Hence, the parameter SCD, which is the Fourier transform of the CAF shows the peaks, when the cyclic frequency becomes equal to the fundamental frequencies of the signal under consideration.

$$S_x^{\alpha_0}(f) = \sum_{\tau_0=-\infty}^{+\infty} R_x^{\alpha_0}(\tau_0) e^{-j(2\pi f\tau_0)} \ . \tag{3.8}$$

From equations (3.7) and (3.8), we get

$$S_x^{\alpha_0}(f) = \sum_{\tau_0=-\infty}^{+\infty} \lim_{N\to\infty} \frac{1}{N}\frac{1}{2N_f}\sum_{n=0}^{N-1}\sum_{m=0}^{N_f-1} |A_{m,k}|^2 \times \cos\left[-2\pi m\tau_0 + \frac{4\pi mn}{N_p} + 2\phi_{m,k}\right] e^{-j2\pi(\alpha_0 n + f\tau_0)} \tag{3.9}$$

The peaks of SCD are found by taking partial differential of SCD w.r.t α_0 as $\frac{\partial S_x^{\alpha_0}(f)}{\partial \alpha_0} = 0$. To find the presence of PU signal, the peaks of SCD are determined at cyclic frequency as:

$$Cyclic\ frequency, \quad \alpha_0 = \frac{\phi_{m,k}}{\pi mn}\frac{1}{T_0} \tag{3.10}$$

The above expression determines the values of cyclic frequency for any arbitrary generated waveform, for m^{th} frequency index, k^{th} Symbol, n^{th} sample and $\phi_{m,k}$ depend upon the data modulation and coding being used. So, by expressing cyclic frequency in terms of SMSE variables, multi-cycle test for determining the cyclic frequencies of the PU signal and detecting its presence, both can be

implemented in a simpler way. In other words, *we have combined the flexibility provided by SMSE waveform design and accuracy provided by CSS*. Finally from equations (3.9) and (3.10), generalized SCD can be represented as:

$$S_x^{\alpha_0}(f) = \begin{cases} \sum_{m=0}^{N_f-1} \frac{1}{2N_f} Q\left(f - \frac{\alpha_0}{2} + \frac{\phi_{m,k}}{2\pi mn}\frac{1}{T_0}\right) & at \quad \alpha_0 = \frac{\phi_{m,k}}{\pi mn}\frac{1}{T_0} \\ 0 & otherwise \end{cases} \tag{3.11}$$

where $Q(f)$ is the Fourier Transform of the pulse shaping function $q(t)$ and T_0 is the time-period which is inverse of the frequency resolution. The presence of any arbitrary PU waveform at the any cyclic frequencies can be determined from equation (3.11). This dynamic and unified expression allows considerable flexibility to detect the scenario dependent unknown waveform and robustness against noise uncertainty and interference. This combined arrangement makes the system dynamic in the following way.

This SMSE-CSS has the ability to detect any PU waveform dynamically without having any prior knowledge. Secondly, SDR implementation make the system dynamic in the sense that any part of the spectrum can be scanned either by sweeping the entire band or by frequency hopping (operation in different frequency bands) and finally, dynamic accessing the spectrum (contiguous or non-contiguous) by STs also makes the system dynamic. The binary hypothesis based on decision metric and joint SMSE-CSS framework is discussed next.

3.3.2 Proposed Test Statistics based decisioning through Binary Hypothesis

The spectrum sensor is essentially a binary switch hypothesis-testing problem. Let the following hypothesis be defined for the spectrum switch.

H0: the licensed user (PU) is absent;

H1: the licensed user (PU) is present.

Mathematically, the following hypothesis illustrates the presence ($H1$) and ab-

sence ($H0$) of the PU signal

$$y[n] = \begin{cases} \eta & : H0 \\ |h_{sp}|^2 x[n] + \eta & : H1 \end{cases} \tag{3.12}$$

where $x[n]$ is PT signal, h_{sp} is the sensing channel gain; η is the AWGN noise and $y[n]$ is the signal received by ST. H0 and H1 represent the sensing states of the spectrum switch which determine absence and presence of the PU. In other words, H0 is the null Hypothesis which tells that the spectrum channel under consideration is vacant and H1 is the alternative hypothesis representing the occupied channel. The decision rule for the test metric $\wedge$ given by

$$\wedge \quad \begin{matrix} \geq H1 \\ < H0 \end{matrix} \quad \lambda \quad (Threshold\ Value)\ . \tag{3.13}$$

The process of selecting the threshold value λ is based on the constant false alarm rate (CFAR) model. The threshold may be determined using CFAR model as

$$\lambda = \sqrt{\frac{2\sigma^2 \ln(\frac{1}{P_{fa}})}{2N+1}}\ ,$$

where σ^2 is noise variance, N is the degrees of freedom which can be determined by the number of symbols being used by the design waveform, coding, frequency bands. P_{fa} is the false alarm probability given by the conditional probability $Pr(H1|H0)$. Normally, the spectrum sensors are designed to operate within prescribed minimum error level. The proposed test metric ($\wedge$) is determined from SCD of generalized SMSE design waveform derived in the section 3.3.1 and is obtained by averaging the differential variance along the frequency resolution axis of the SCD as follows:

$$\wedge = \frac{1}{N} \sum_{\alpha_0=-N}^{N} \{\widehat{S(\alpha_0)} - \overline{S(\alpha_0)}\}^2\ , \tag{3.14}$$

where $\widehat{S(\alpha_0)}$ is the differential of the band averaged SCD for the computed cyclic frequencies and $\overline{S(\alpha_0)}$ is the differential of the SCD averaged over the whole spectrum frequency band in concern. This test stat value varies well below the

selected threshold λ if the PU signal is absent and quite above the threshold if the PU signal is present dichotomizing the occupied spectrum band and the noise. The uniqueness of the proposed test stat can be ascertained from the fact that the gap between proposed test stat and threshold value picked to achieve a pre-specified P_{fa} is large and can be easily used to differentiate between noise and the PU signal even in the worst noise conditions.

3.4 Results and Discussion

In this section, the performance of SMSE-CSS demonstrated by analytical expressions in the section 3.3 is validated via computer simulations. The results are presented in three different subsections. In the section 3.4.1, spectrum scenario is created where PUs are randomly occupying the channels. The Primary signal is generated using the two test cases. The results of spectrum sensing are demonstrated using SCD for OFDM and MC-CDMA signals via SMSE-CSS. In particular, normalized alpha-profiles for SMSE design variables are presented with the specifications of DVB-T signal channels from IEEE 802.22 standard [52]. In the second sub-section, the channel occupancy/spectrum holes are detected using the decision metric proposed in the section 3.3.2, identifying the channels available for SU communication. In the third sub-section, comparison for different detection schemes is plotted with the proposed scheme in terms of ROC curves.

3.4.1 Simulation details of Spectrum Scenario and SMSE-CSS sensing of PU

To analyze the spectrum holes and channel occupancy by PU, spectrum scenario is created by choosing 500 MHz-560 MHz band (IEEE 802.22 standard)[11][52] with PU spectrum window defined by 10 channels, each of 6 MHz Bandwidth. PU waveform is generated to randomly occupy the channels. The PU waveform can be OFDM, MC-CDMA etc but SU has no any information about its characteristics. The system represented in figure 3.3 is implemented here and

the spectrum is sensed using proposed SMSE-CSS technique. The channels are filtered using software defined filter banks. Each channel is down-converted and joint SMSE-CSS decision test stat (discussed in the section 3.3.2 and defined by equations 3.13 and 3.14) is used to determine the occupancy/spectrum holes of the channel. The results are presented by taking two PU waveform scenarios- OFDM and MC-CDMA. Both cases are derived from SMSE framework.

Case 1: Assuming OFDM based PU waveform

PU waveform generation: The OFDM is generated in 2K mode with number of subcarriers as 1705; the elementary period taken is 0.109 μsec. The signal is spread in 6MHz bandwidth.

Sensing by ST: The OFDM transmission analytic expression [12] has been derived from the SMSE framework by setting variables $u_i = a_i$, $w_i = 1$ and $_{w_i} = 0 \forall i$ in equation (3.2).

$$s_k[n] = \frac{1}{N_f} \Re\{ \sum_{m=0}^{N_f-1} (\alpha'_{m,k} + \beta'_{m,k}).e^{j(2\pi f_m t_n)} \} \ . \tag{3.15}$$

For QPSK modulation, $\alpha'_{m,k}, \beta'_{m,k} \in \pm 1$; for 16-QAM modulation, $\alpha'_{m,k}, \beta'_{m,k} \in \pm 1, \pm 3$. The PU signal is sensed. Figure 3.4a shows normalized alpha profile averaged over the entire frequency window which shows the presence of OFDM based PU signal.

Case 2: Assuming MC-CDMA based PU waveform:

PU-Waveform generation: Walsh-Hadamard codes are used for spreading purposes for MC-CDMA. We apply spreading codes in frequency domain to map the different chip of the spreading sequence to individual subcarrier and signal is spread in 6 MHz bandwidth.

Sensing by ST: We derive MC-CDMA analytical expression the SMSE framework by putting $u_i = a_i$; $w_i = 1$ and $_{w_i} = 0$; $_{o_i} = 0 \forall i$. Spectral spreading can be accomplished applying random phases 0 or π. So, SMSE expression for

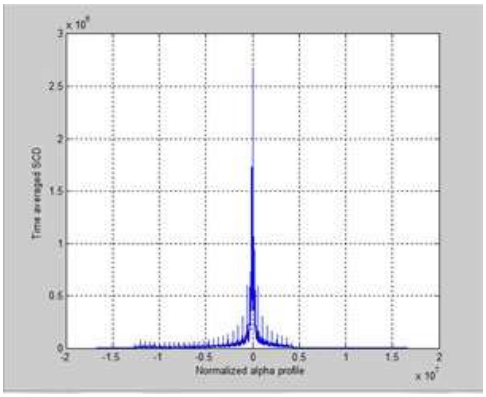

(a) Time averaged SCD with normalized alpha for SMSE-OFDM with CSS

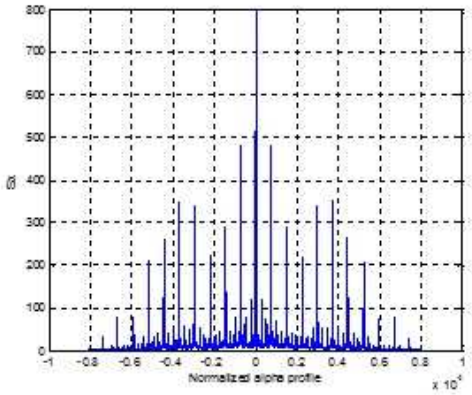

(b) SCD for OFDM and MC-CDMA of PU signals sensed by SU signals

Figure 3.4: SCD profiles with different modulations through SMSE

MC-CDMA derived from equation (3.2) becomes

$$s_k[n] = \frac{1}{N_f} \Re \sum_{m=0}^{N_f-1} (\alpha'_m + \beta'_m).e^{j}(2\pi f_m t_n + \theta_{c_m}) \ . \tag{3.16}$$

In the given results, the peaks become the function of chip rate used, resulting in impulses at the specified cyclic frequencies. Figure 3.4b indicates the normalized alpha profile averaged for SCD of MC-CDMA over the frequency resolution window which shows the presence of MC-CDMA based PU signal.

3.4.2 Detection of Spectrum holes

Figure 3.5a presents the analysis of 10-channel spectrum sensing from 500 MHz−560 MHz. Spectrum occupancy/decision is plotted Vs Number of Channels-Bandwidth product and Bandwidth. Spectrum decision is based on the test statistics described in the section 3.3.2. It is shown that channel number 1, 3, 4, 9 and 10 are vacant whereas channel number 2, 5, 6, 7, 8 are occupied.

Figure 3.5b clearly shows the un-occupied and occupied spectrum channels. The vacant channels show the presence of spectrum hole which can be utilized by the secondary users, thereby improving the spectrum utilization. This record of the spectrum holes is dynamically updated in the database by scanning the different parts of spectrum to be used dynamically.

Table 3.1: Simulation parameters set-up for CR sensing

Parameters	
Frequency Band taken for CR sensing	500 - 560 MHz
No of CR channels	10
Bandwidth/channel	6 MHz
OFDM Encoding/Decoding	Convolution/Veterbi
Modulation	16-QAM
No. of subcarriers in OFDM	1705
Each OFDM subcarrier Bandwidth	3 KHz
OFDM subcarrier sampling frequency	16KHz
Frequency resolution	256 Hz
Cyclic frequency resolution	32 Hz
Spreading codes for MC-CDMA	Walsh Hadamard

3.4.3 Comparison of different detectors in ROC terms

The comparative performance of the proposed spectrum sensing is investigated in this section. ROC (P_{fa} Vs P_d) or equivalently, complementary ROC (Probability of a missed detection, $[P_{md} = 1 - P_d]$ Vs P_{fa}) is the standard way of quantifying the sensing performance and for the verification of detection algorithms [55]. The main aim of the spectrum sensing is to achieve the correct detection at all the times which is not practically achievable because of the statistical nature of the channel. The missed detection occurs when the unoccupied spectrum is detected as busy and may lead to the wasted opportunity. The false alarm occurs when the busy channel is detected as un-occupied that may cause interference and collisions to PU. The probability of false alarm is given by $P_{fa} = Pr(\wedge > \lambda|H0)$ and the probability of correct detection is given by $Pd = Pr(\wedge > \lambda|H1)$. The proposed joint scheme is compared with traditionally available energy detection, matched filtering detection and F- test based [93] detection techniques. P_{fa} is specified at 10% as recommended in IEEE 802.22. The different results of interest are illustrated.

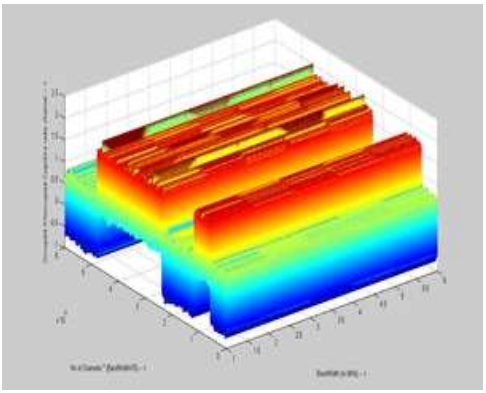

(a) 3D-representation of spectrum scanning and channel occupancy after decision for 10 channels

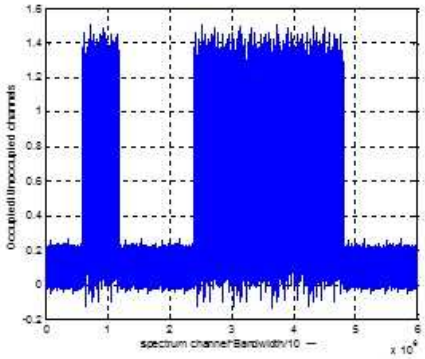

(b) Scanned spectrum and channel occupancy after decision for 10 channels (500-560 MHz spectrum with 6 MHz BW per channel)

Figure 3.5: Spectrum Decision and occupancy statistics of PU

Figure 3.6 shows that better detection probability achieved with the proposed SMSE-CSS technique. It is shown that at low SNR (below 5 dB) with

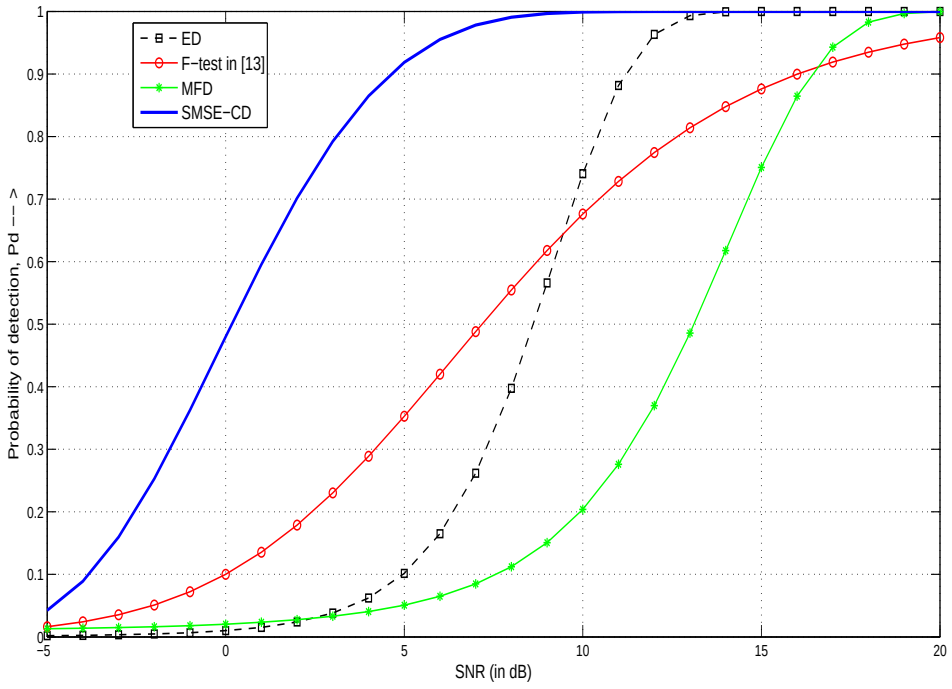

Figure 3.6: P_d Vs SNR for N=4

degrees of freedom N = 4, SMSE-CSS method has higher probability of detection, for instance, at 0 dB SNR, Pd is almost 38% higher than F-test method, about 45% better than MFD and more than 46% as compared to ED. This is due to the fact the CSS is robust to noise uncertainty and SMSE provides flexibility. Figure 3.7 illustrates complementary ROC curve (SNR =0dB) that confirms the higher performance sensitivity for SMSE-CSS. Figure 3.8 plots P_{fa} Vs adaptive threshold with SNR as a parameter. It is shown that if decision threshold is kept constant, then false alarm probability increases as the SNR goes down which is obvious.

However, to support larger number of connected devices in the future IoTs, it is likely to add more degrees of freedom represented in more operating frequency bands. By increasing the degrees of freedom to 8, the comparison of detection probability of different detectors is tabulated in Table 3.2. The performance of energy detection and matched filtering detection methods improves slightly, whereas the performance of both SMSE-CSS and F-test based method

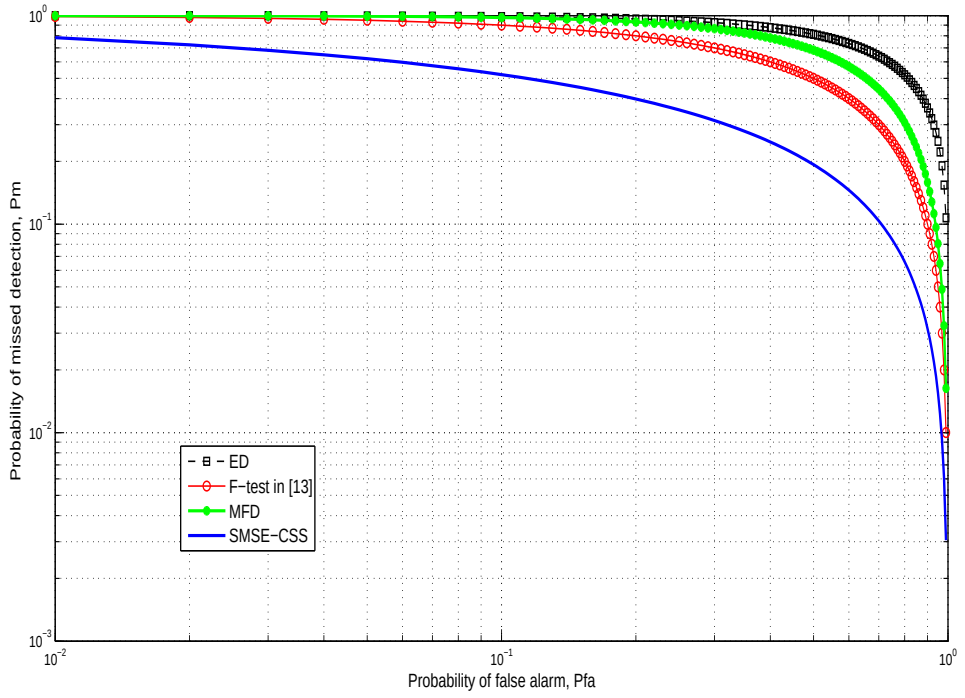

Figure 3.7: Complementary ROC curves (P_m Vs P_{fa}) for N=4 at SNR = 0 dB

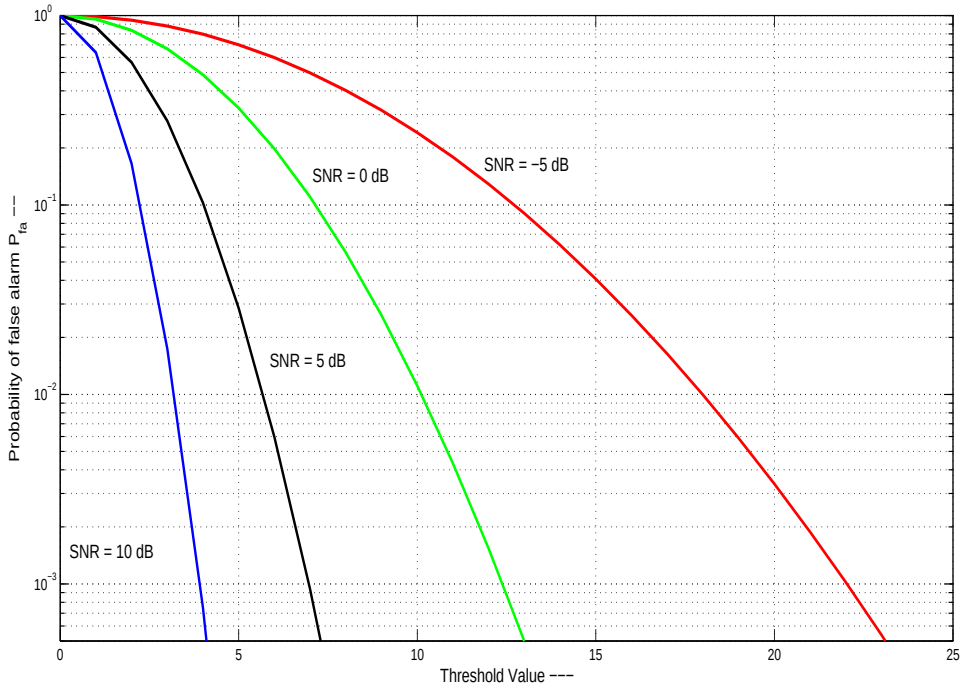

Figure 3.8: P_{fa} Vs Adaptive Threshold with SNR as a parameter for N=4

Table 3.2: Comparison of P_d for different detectors and different degrees of freedom and SNR values

Detectors	Detection Probability (P_d) for different degrees of freedom and SNR at P_{fa} =0.1			
	SNR = 0 dB		SNR = 5 dB	
	N=4	N=8	N=4	N=8
Energy Detection	0.01	0.024	0.1	0.18
Matched filtering Detection	0.02	0.08	0.05	0.13
F-test based Detection [93]	0.1	0.17	0.35	0.54
Joint SMSE-CSS	0.482	0.534	0.92	0.94

improves but still SMSE-CSS outperforms F-test based method.

3.5 Conclusion

The most important resource in wireless communications is the frequency spectrum. The flexibility provided by SMSE framework has been combined with the spectrum sensing method in this chapter. The SMSE framework along with the CSS technique provides a better methodology providing more flexibility and sensitivity for detection of spectrum holes. The proposed test metric uniquely defines the channel occupancy deciding the spectrum holes clearly and increasing the sensing accuracy. SMSE-CSS works well in the low SNR environment and has been proved in ROC graphs.

Chapter 4

Performance Analysis of Spectrum sensing in Multiple Antenna Scenario

4.1 Introduction

In this chapter, the performance of spectrum sensing in multi-antenna scenario has been studied. The SU transmitter is considered to have multi-antennas and proposed Spectally Modulated Spectrally Encoded - Cyclostationary Spectrum Sensing (SMSE-CSS) technique has been applied. The performance has been compared with different detectors traditionally available in multi-antenna scenario. The limitations of the system model considered and investigated is presented. Based on the observations and limitations of the system model discussed in the section 4.3, we modify the system model to consider the relay based CR communication to increase the spatial distance of SU communication. However, to take the full advantage of CR paradigms, hybrid interweave/underlay CR has been taken. From deployment centric view-point, the power limitations and interference constraints has to be considered for SU terminals and cognitive relay. So, we take green-energy into consideration from application point of view for the relay. The relay is considered to employs Amplify and Forward (AF) technique along with Time Switching Relaying protocol (TSR) for energy harvesting. We analyze the underlay CR system with interference constraint and without considering spectrum sensing. However, the complete hybrid Interweave/Underlay CR system considering sensing accuracy and effi-

ciency is analyzed with sensing duration parameter optimization and optimal TSR charging ratio parameter in the next chapter.

4.2 Implementation of Spectrum sensing in multi-antenna scenario

To evaluate the performance of spectrum sensing in multi antenna scenario, we assume that ST is equipped with the M-antennas as shown in figure 4.1.

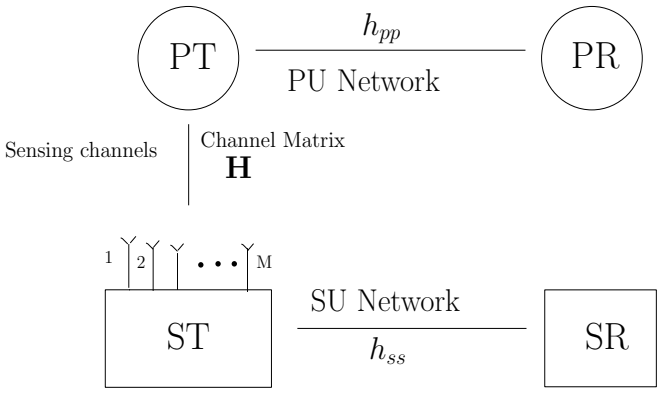

Figure 4.1: System Model (Interweave CR)

The binary hypothesis testing problem is reformulated for multiple antenna scenario as

$$Y[n] = \begin{cases} \eta[n] & : H0 \\ \mathbf{H}x_i[n] + \eta[n] & : H1 \end{cases} \tag{4.1}$$

where $x_i[n]$ is PU signal propagating through h_i fading channel for i^{th} antenna represented by channel matrix $\mathbf{H}$. noise $\eta[n]$ is a stationary-complex, zero mean and white noise with covariance matrix represented by

$$E\{\eta[n] * \eta^H[n - \tau_0]\} = \delta(\tau_0) diag\{\sigma_1^2, \sigma_2^2, \sigma_3^2, ...\sigma_M^2\}$$

We assume uncorrelated noise at each antenna with different variance across antennas. Under Hypothesis $H1$, M * 1 vector $\mathbf{H}$ represents the channel gain and is constant during the sensing duration. $Y[n]$ is M * L matrix that represents the signal received by ST and L represents the number of samples at the antennas. We further assume that PU signal carrier is modulated by independent data streams which is a valid assumption for an OFDM signal. The

decision rule can be rewritten as

$$T_{opt} = \|\mathbf{H}^H Y\|^2 \quad \begin{matrix} \geq H1 \\ < H0 \end{matrix} \quad \lambda \quad .$$

We use maximum ratio combiner (MRC), which gives the weights to the observations at the different antennas according to their channel gains. The observed vector at each antenna is Guassian Random Variable with zero mean and has χ^2 distribution. The weighted summation of χ^2 distributed random variables are generated while using MRC. There is no exact form for this distribution but can be approximated by gamma distribution [106], the PDF of which is given as

$$f_{\chi^2}(x : k, p) = x^{k-1} \frac{e^{\frac{-x}{p}}}{p^k \Gamma(k)} \ .$$

Under the hypothesis $H0$, the test statistics can be approximated as

$$T(\mathbf{Y}) \sim \mathcal{CN}\left(0, \sum_{1}^{M} \frac{2\|h_i' y_i\|^2}{\sigma_i^2}\right) \ . \tag{4.2}$$

whereas for hypothesis $H1$ the test statistics can be approximated by

$$T(\mathbf{Y}) \sim \mathcal{CN}\left(\frac{1}{M}\sum_{i=1}^{M} R_{x_i}^{\alpha_0}(\tau_0), \sum_{1}^{M} \frac{2\|h_i' y_i\|^2}{\sigma_i^2}\right) \ . \tag{4.3}$$

4.2.1 Performance of Spectrum Sensing in Multi-antenna scenario

The two key parameters used to evaluate the performance of spectrum sensing are detection probability (the probability of accurately detecting the $H1$, the presence of PU) and false alarm probability (the probability of mistakenly detecting as PU). For SMSE-CSS described in the previous section, the threshold used to achieve the desired P_{fa} is defined as

$$\int_{\lambda}^{\infty} f_{\chi^2}(x)dx = P_{fa}$$

The detection probability is found as

$$P_d = Pr(T > \lambda | H1) = 1 - F_{T|H1}(\lambda)$$

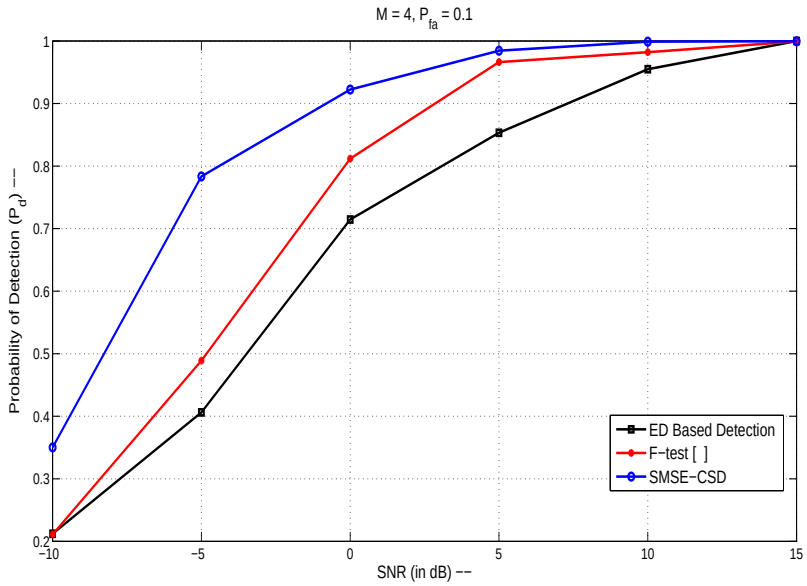

Figure 4.2: Probability of detection Vs SNR (in dB) at M = 4

$F_{T|H1}(\lambda)$ is the CDF of test statistics under $H1$. However, the most popular Generalized likelihood ratio (GLR) criteria fails in low SNR region when H1 is very close to H0, which is of significant interest in spectrum sensing. The figure 4.2 compares the detection probability of SMSE-CSS with the other traditionally available detectors for number of antennas, M = 4 and the false alarm probability, $P_{fa} = 0.1$.

The plots shows approx 30% improvement in detection probability when compared with F-test [93] and traditional energy detector. By increasing the number of antennas, the detection probability improves as expected shown in figure 4.3. However, the improvement in detection probability is less when number of antennas is increased from 6 to 8.

4.3 Some Observations/Limitations of the CR model investigated

- The spatial distance of communication is a limiting factor for CR system under study. However, to increase the spatial distance of communication, we are extending our system model to investigate relay based CR communication system.

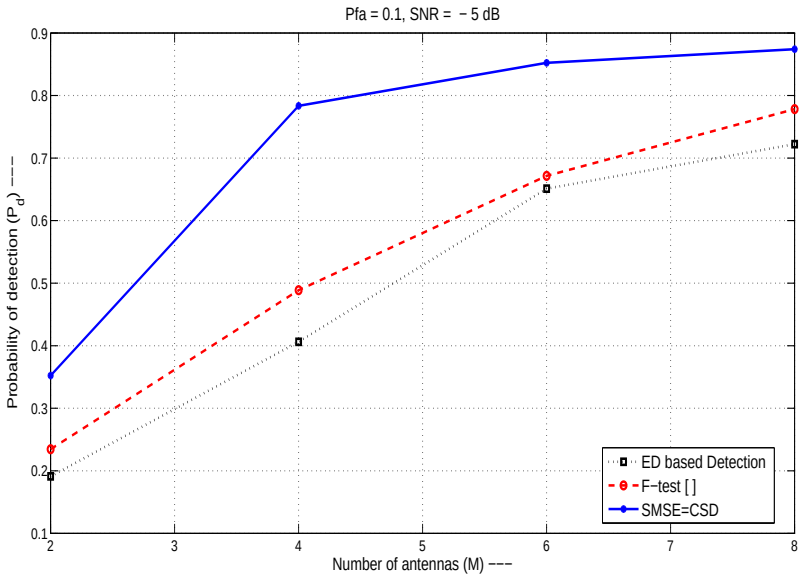

Figure 4.3: Probability of detection Vs Number of antennas (M) at SNR = -5 dB

- The effect of only Interweave CR has been considered in the work uptill now. The Underlay CR and hybrid of Underlay and Interweave CR can be studied to increase the system performance which is also discussed in the next section.

- The interference constraints in Underlay CR need to be incorporated and power allocation plays an important role during underlay CR operation.

- The practical scenario of deployment of the system model battery-operated devices needs to be considered or some-other source of power/energy needs to be considered. There has been a tremendous interest in green energy harveting now a days among the research community in the recent past. So, based on the above obserations we have modified our system model and investigated the optimal performance of the hybrid interweave/underlay CR system considering the system performance parameters in terms of throughput and outage capacity, throughput and erogodic sum-rate. The Analytical derivations have been derived for underlay CR without considering sensing in the section 4.4.

4.4 System model for EH Relay based CR

We consider a cognitive radio network in which two SU terminals T_a and T_b communicate with each other through Energy harvesting enabled two-way cognitive relay as shown in figure 4.4. There are two types of relay networks in practice, One Way Relay Network (OWRN) and Two Way Relay Network (TWRN). In OWRN, the data flow is unidirectional i.e., source sends the information to the relay and then relay sends it to the destination. In TWRN, the two source nodes simultaneously send information to each other[107]. We consider two-way cognitive relay in our system model. We assume that both T_a and T_b terminals have fixed power supplies whereas relay T_r employing Amplify-and-Forward (AF) scheme has no fixed power supply and needs to harvest energy from the received signal. We consider Time-switching relaying protocol (TSR) for energy harvesting and information transmission. Spectrum sharing is assumed only in underlay manner here such that there is no sensing required and SU co-exists with the PU. However, this system model and work done here acts as a base work for hybrid Interweave/Underlay CR system to be discussed in the next chapter.

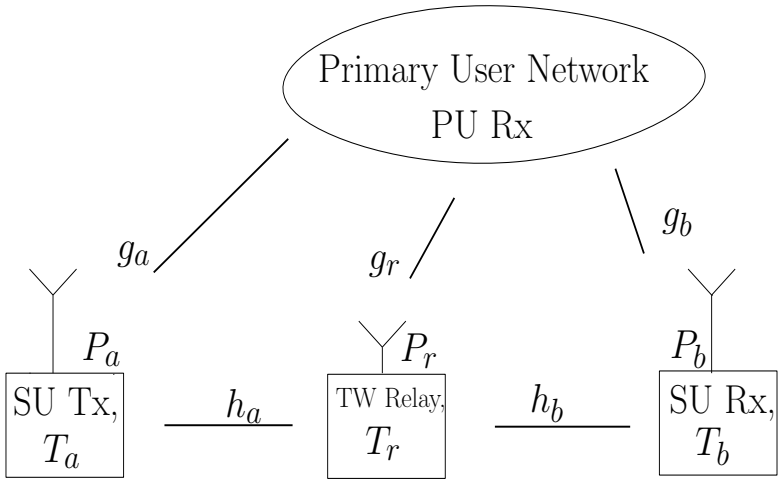

Figure 4.4: System Model

SU network operates in underlay mode with power constraints and maximum tolerable Interference limit value, I_p is transmitted by PU to SU terminal T_a through some pilot channel.

The CR communication takes place in two phases as shown in figure 4.5. In the first phase, both terminals T_a and T_b transmit their data simultaneously to the relay T_r. The signal received at the relay T_r is represented as [108]

$$y_r = \sqrt{P_a} h_a x_a + \sqrt{P_b} h_b x_b + n_r \ , \tag{4.4}$$

where x_a and x_b are unit energy transmit symbols from terminals T_a, T_b, P_a and P_b represent the power of the SU termiinals T_a and T_b ; h_a, h_b are the channel coefficients between $T_a \rightarrow T_r$ and $T_b \rightarrow T_r$. This received signal y_r is used for wireless energy harvesting at relay and information processing. In the second phase, relay transmits the signal to both the terminals using harvested energy in the first phase. The power allocation strategy applied considering interference limits is given as

$$P_a = (1-\alpha)\frac{I_p}{|g_a|^2}; \quad P_b = \alpha \frac{I_p}{|g_b|^2} \quad and \quad P_r = \frac{I_p}{|g_r|^2} \ , \tag{4.5}$$

such that maximum tolerable interference limit $I_p = P_a |h_a|^2 + P_b |h_b|^2$ and α is Interference Power Distribution Parameter (IPDP).

The equation (4.5) is justified on the following grounds. *Firstly,* the SU terminals T_a and T_b transmit simultaneously because it is a two-way relay transmission with power P_a and P_b. Hence, the total interference power constraint I_p is transmitted by PU to both SU terminal. This total power has to be distributed to SU terminals in such a way that when both SU terminals transmit the total power constraint does not exceed I_p at the PU receiver. *Secondly,* taking into account the statistical nature of the channel, effective power becomes $\frac{I_p}{|g_i|^2}$ where $i \ \epsilon \ \{a, b\}$. Therefore power distribution parameter α is taken to account the channel variations and resulting effective power constraint is defined by equation (4.5).

We assume that Channel state information (CSI) between $T_a \rightarrow R$ and $T_b \rightarrow R$ is known at both terminals by employing pilot based channel estimation.

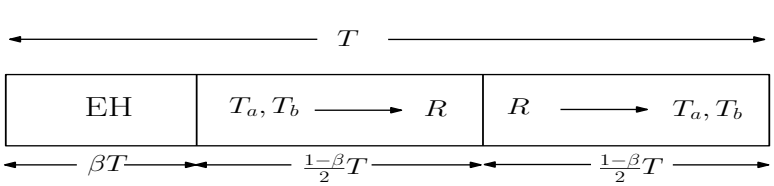

Figure 4.5: Frame structure for EH relay based Underlay CR

Considering AF relay, the end-to-end SNRs at the SU terminals T_a and T_b are given as[108]

$$\gamma_a = \frac{P_r P_b}{N_0}\left[\frac{|h_a|^2 |h_b|^2}{(P_r + P_a)|h_a|^2 + P_b |h_b|^2]}\right] ,$$
$$\gamma_b = \frac{P_r P_a}{N_0}\left[\frac{|h_a|^2 |h_b|^2}{(P_r + P_b)|h_b|^2 + P_a |h_a|^2]}\right] . \tag{4.6}$$

As shown in figure 4.5, the RF energy is harvested in the fraction βT of the time frame and information processing and transmission takes place in $\frac{(1-\beta)T}{2}$. Assuming charging by both the terminals, energy harvested at the relay in fraction βT is given by

$$E_H = \zeta[P_a |h_a|^2 + P_b |h_b|^2]\beta T . \tag{4.7}$$

where ζ is the efficiency of the energy harvesting circuit The harvested power is available at relay for disposal as

$$P_r = \frac{E_H}{\frac{(1-\beta)T}{2}} = \frac{2\zeta\beta}{1-\beta}\left[P_a |h_a|^2 + P_b |h_b|^2\right] . \tag{4.8}$$

4.5 Outage Probablility of Simple Underlay CR under RF Energy Harvesting

By definition, the outage probability is the probability that the instantaneous end-to-end SNRs at SU terminals falls below a predefined threshold, γ_{th} [49] Putting the value of P_r, power available at the relay after harvesting RF energy at the relay from equation (4.8) into (4.6) and simplifying, we get SNR at SU

terminals T_a as

$$\gamma_a = \frac{2\zeta[P_a |h_a|^2 + P_b |h_b|^2]\beta P_b}{N_0} \left\{ \frac{|h_a|^2 |h_b|^2}{[2\zeta\beta[P_a |h_a|^2 + P_b |h_b|^2] + (1-\beta)P_a] |h_a|^2 + P_b |h_b|^2 (1-\beta)} \right\}. \quad (4.$$

Simplifying by factorizing the denominator, we get the end-to-end SNRs for both SU terminals T_a and T_b under RF energy harvesting are given by

$$\gamma_a = \frac{2\zeta\beta P_b |h_a|^2 |h_b|^2}{N_0[(1-\beta) + 2\zeta\beta |h_a|^2]}$$
$$\gamma_b = \frac{2\zeta\beta P_a |h_a|^2 |h_b|^2}{N_0[(1-\beta) + 2\zeta\beta |h_b|^2]} \quad (4.10)$$

The outage probability at SU terminal T_a is given by

$$[P_{out}]_A = Pr(\gamma_a < \gamma_{th}). \quad (4.11)$$

Let us define $a_1 = \zeta\beta; x = |h_a|^2; y = |h_b|^2; z = |g_a|^2; u = |g_b|^2; b = 1-\beta$ such that above SNRs can be rewritten as

$$\gamma_a = \frac{2a_1 P_b xy}{N_0[b + 2a_1 x}$$
$$\gamma_b = \frac{2a_1 P_a xy}{N_0[(b + 2a_1 y} \quad (4.12)$$

Solving the above probability equation (4.11)by using equation (4.12), we get

$$[P_{out}]_A = Pr\left[\frac{2a_1 P_b xy}{N_0[b + 2a_1 x]} < \gamma_{th}\right]. \quad (4.13)$$

Putting interference constraint for P_b from equation (4.5), we get

$$[P_{out}]_A = Pr\left[\frac{2a_1 \alpha I_p xy}{N_0 z[b + 2a_1 x]} < \gamma_{th}\right]$$
$$[P_{out}]_A = Pr\left[\frac{y}{z} < \frac{\gamma_{th} N_0[b + 2a_1 x]}{2a_1 \alpha I_p x}\right] \quad (4.14)$$

Solving the above equation as

$$[P_{out}]_A = \int_0^\infty F_{\frac{y}{z}}\left[\frac{\gamma_{th} N_0(b + 2a_1 x)}{2a_1 I_p \alpha x}\right] f_x(x)dx \quad (4.15)$$

We take wireless channels h_a, h_b, g_a, g_b and g_r as rayleigh faded and it is a well-known that the square of rayleigh random variable is an exponential

random variable. So, distribution of x, y random variables can be represented as an exponential distribution. Since x and y are exponential random variables, therefore $f_x(X) = \frac{1}{\lambda_x} e^{\frac{-x}{\lambda_x}}, \quad f_y(Y) = \frac{1}{\lambda_y} e^{\frac{-y}{\lambda_y}}, \quad F_{\frac{y}{z}}(X) = \frac{X}{X + \frac{\lambda_y}{\lambda_z}}$

$$[P_{out}]_A = \int_0^\infty \frac{\left[\frac{\gamma_{th} N_0 (b+2a_1 x)}{2a_1 I_p \alpha x}\right]}{\frac{\lambda_y}{\lambda_z} + \left[\frac{\gamma_{th} N_0 (b+2a_1 x)}{2a_1 I_p \alpha x}\right]} \frac{1}{\lambda_x} e^{\frac{-x}{\lambda_x}} dx \tag{4.16}$$

Solving the above integral by partial fraction and applying simple mathematical operations, we get

$$\begin{aligned} [P_{out}]_A &= \frac{1}{\lambda_x} \int_0^\infty \frac{\gamma_{th} N_0 a_1 \lambda_z}{a_1 I_p \alpha \lambda_y + \gamma_{th} N_0 a_1 \lambda_z} e^{\frac{-x}{\lambda_x}} dx - \frac{\gamma_{th} N_0 b \lambda_z (-2 I_p \alpha \lambda_y)}{(2a_1 I_p \alpha \lambda_y + 2\gamma_{th} N_0 a_1 \lambda_z)\lambda_x} \\ &\quad \int_0^\infty \frac{1}{\gamma_{th} N_0 a_1 \lambda_z + (2a_1 I_p \alpha \lambda_y + 2\gamma_{th} N_0 a_1 \lambda_z) x} e^{\frac{-x}{\lambda_x}} dx \end{aligned} \tag{4.17}$$

$$\begin{aligned} [P_{out}]_A &= \frac{\gamma_{th} N_0 \lambda_z}{I_p \alpha \lambda_y + \lambda_z \gamma_{th} N_0} + \frac{\gamma_{th} N_0 \lambda_z (1-\beta)(2 I_p \alpha \lambda_y)}{(2 I_p \alpha \lambda_y + 2\lambda_z \gamma_{th} N_0))^2 \zeta \beta \lambda_x}. \\ &\quad exp\left\{\frac{\gamma_{th} N_0 \lambda_z (1-\beta)}{(2 I_p \alpha \lambda_y + 2\lambda_z \gamma_{th} N_0)\zeta \beta \lambda_x}\right\} . Ei\left\{\frac{\gamma_{th} N_0 \lambda_z (1-\beta)}{(2 I_p \alpha \lambda_y + 2\lambda_z \gamma_{th} N_0)\zeta \beta \lambda_x}\right\} \end{aligned} \tag{4.18}$$

Similarly, the outage probability at SU terminal T_b is given by

$$\begin{aligned} [P_{out}]_B &= \frac{\gamma_{th} N_0 \lambda_u}{I_p (1-\alpha) \lambda_x + \lambda_u \gamma_{th} N_0} + \frac{\gamma_{th} N_0 \lambda_u (1-\beta)(2 I_p (1-\alpha) \lambda_x)}{(2 I_p (1-\alpha) \lambda_x + 2\lambda_u \gamma_{th} N_0)^2 \zeta \beta \lambda_y}. \\ &\quad exp\left\{\frac{\gamma_{th} N_0 \lambda_u (1-\beta)}{(2 I_p (1-\alpha) \lambda_x + 2\lambda_u \gamma_{th} N_0)\zeta \beta \lambda_y}\right\} . Ei\left\{\frac{\gamma_{th} N_0 \lambda_u (1-\beta)}{(2 I_p (1-\alpha) \lambda_x + 2\lambda_u \gamma_{th} N_0)\zeta \beta \lambda_y}\right\} \end{aligned} \tag{4.19}$$

$Ei(x)$ represents the exponential integral. The figure 4.6 shows the plot of the above derivation and valiates the simulation with analytical for outage probabilities of SU terminals T_a and T_b. It is observed that both outages are symmetrical and intersect at $\alpha = 0.5$.

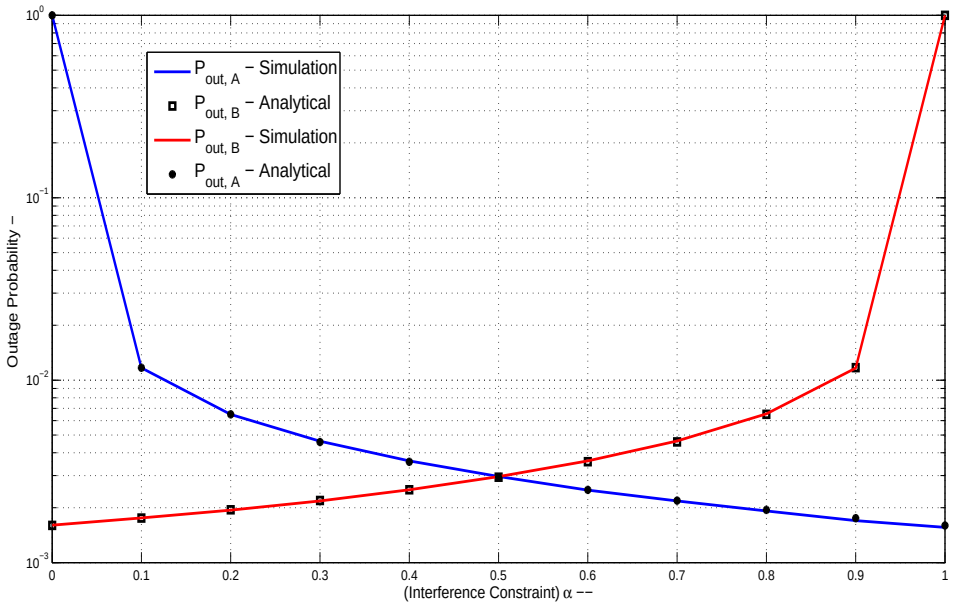

Figure 4.6: $P_{out}A$ and $P_{out}B$ Vs α (Inteference constraint factor)

4.6 Throughput Analysis of Simple Underlay CR with RF Energy Harvesting

For fixed rate transmission systems, that is, delay sensitive system, the throughput is defined as

$$T = (1-\beta)\frac{R}{2}(1-P_{out,A}) + (1-\beta)\frac{R}{2}(1-P_{out,B}) \tag{4.20}$$

where R is fixed tansmission rate. High SNR approximations are used in the literature to simplify the multiplication of exponential with incomplete gamma function or exponential integral type equations [109][110][111]. Using high SNR approximation of the exponential integral as $Ei(x) = -0.5677 - \ln(x)$, we re-write the outage probabilities from equations (4.18) and (4.19) as

$$\begin{aligned}[P_{out}]_A \simeq\ & \frac{\gamma_{th}N_0\lambda_z}{I_p\alpha\lambda_y + \lambda_z\gamma_{th}N_0} + \frac{\gamma_{th}N_0\lambda_z(1-\beta)(2I_p\alpha\lambda_y)}{(2I_p\alpha\lambda_y + 2\lambda_z\gamma_{th}N_0))^2\zeta\beta\lambda_x} \\ & \left(-0.5677 - \ln\left(\frac{\gamma_{th}N_0\lambda_z(1-\beta)}{(2I_p\alpha\lambda_y + 2\lambda_z\gamma_{th}N_0)\zeta\beta\lambda_x}\right)\right)\end{aligned} \tag{4.21}$$

and

$$[P_{out}]_B \simeq \frac{\gamma_{th}N_0\lambda_u}{I_p(1-\alpha)\lambda_x + \lambda_u\gamma_{th}N_0} + \frac{\gamma_{th}N_0\lambda_u(1-\beta)(2I_p(1-\alpha)\lambda_x)}{(2I_p(1-\alpha)\lambda_x + 2\lambda_u\gamma_{th}N_0))^2\zeta\beta\lambda_y} \left(-0.5677 - \ln\left(\frac{\gamma_{th}N_0\lambda_u(1-\beta)}{(2I_p(1-\alpha)\lambda_x + 2\lambda_u\gamma_{th}N_0)\zeta\beta\lambda_y}\right)\right) \quad (4.22)$$

The throughput variation taking symmetrical and asymmetrical channels and with different values of TSR parameter β are shown in figure 4.7 and 4.8.

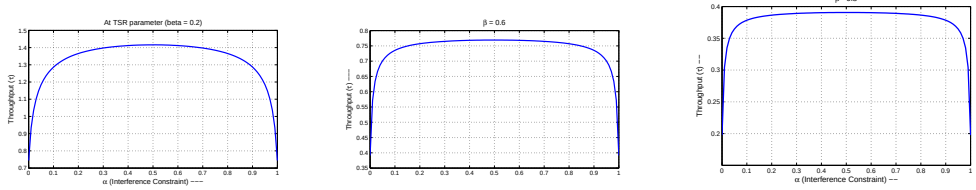

(a) TSR parameter β = 0.2 (b) $\beta = 0.6$ (c) $\beta = 0.8$

Figure 4.7: Variation of Interference Power distribution factor α Vs Throughput at different β assuming symmetric channels

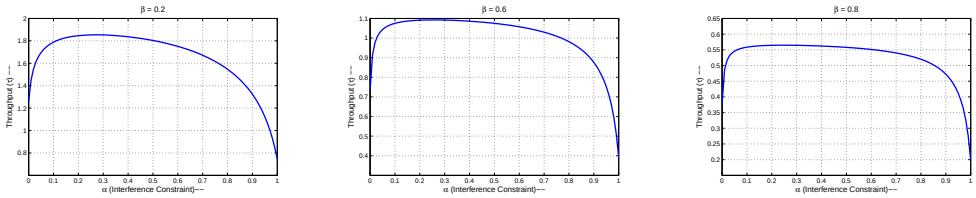

(a) TSR parameter β = 0.2 (b) $\beta = 0.6$ (c) $\beta = 0.8$

Figure 4.8: Variation of Interference Power distribution factor α Vs Throughput at different β assuming Asymmetric channels

Hence, from the figure 4.7 and 4.8, we analyze in all the cases that at maximum system throughput, the variations in α are not large and so, α can be taken independent of β. The figure 4.9 shows the 3D plot of SU Throughput w.r.t. α and β parameters.

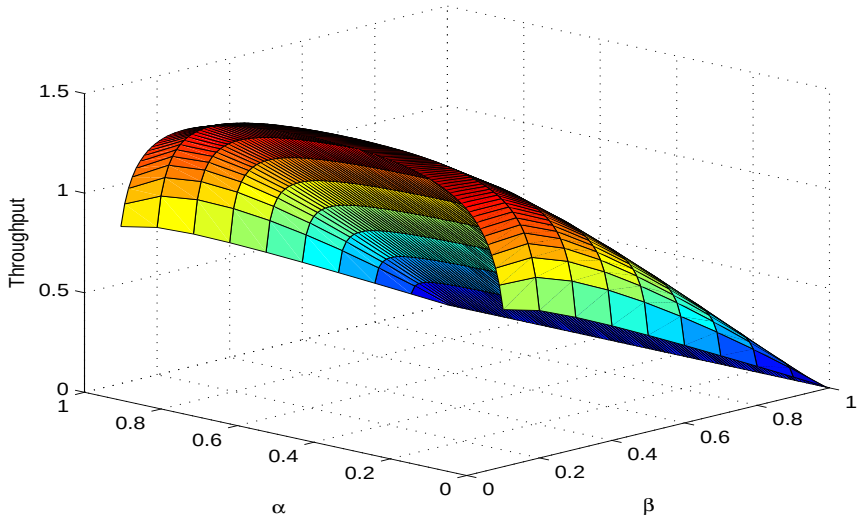

Figure 4.9: Throughput Vs $\alpha and \beta$

4.7 Conclusion

In this chapter, we evaluated the performance of spectrum sensing in a multiple antenna scenario. We analyzed the detection probability in multi antenna scenario by varying the number of antennas. It is observed that detection probability gets saturated and the increment in probability of detection is low when we increase the number of antennas from 6 to 8. Further it is observed that to improve the SU transmission, the energy and spatial distance constraints needs to be considered. Therefore, we modified the system model and analyzed the relay based underlay CR communication. The two-way cognitive relay employed TSR protocol for energy harvesting. We undertook the simple underlay CR without spectrum sensing and considering only interference constraints. An analytical expression for outage probability and throughput has been derived. In the results, throughput variation for different values of TSR parameter β and interference constraint α has been plotted for symmetrical and asymmetrical channels. Analytical derivation is validated by computer simulations.

Chapter 5

Performance Optimization of Energy Harvesting based Interweave/Underlay CR Network

5.1 Introduction

In this chapter, new hybrid Interweave/Underlay relay CR network has been investigated. The relay employs Amplify and forward (AF) technique along with Time-switching relaying protocol (TSR) for energy harvesting. Based on sensing accuracy, we derive an expression for optimization of charging duration TSR parameter and sensing duration for maximizing throughput of interweave Cognitive Radio (CR). Based on sensing efficiency, throughput and outage probability for underlay CR is analyzed considering the interference temperature constraints and optimal power distribution parameter at secondary user (SU) terminals. Variations in the sum-rate and detection probability are considered in terms of CDF of the terminal Signal to Noise Ratios (SNRs). We prove that erogodic sum-rate is maximized in underlay CR case, when interference power distribution parameter is half across the SU terminals. The optimized values of switching-time ratios have been derived analytically for both Interweave and Underlay CR. The results thus obtained are compared by taking symmetrical and asymmetric channels between SU terminals.

5.2 Proposed System model for EH based Hybrid CR

We consider a cognitive radio network in which two SU terminals T_a and T_b communicate with each other through Energy harvesting enabled two-way cognitive relay as shown in figure 5.1. We assume that both T_a and T_b terminals have fixed power supplies whereas relay T_r employing Amplify-and-Forward (AF) scheme has no fixed power supply and needs to harvest energy from the received signal. We consider Time-switching relaying protocol (TSR) for energy harvesting and information transmission. Spectrum sharing may be employed between PU and SU in an interweave or underlay manner. Spectrum sensing is performed at secondary transceiver (ST) terminal T_a. All channels of the network are assumed to be reciprocal and experience quasi-static block Rayleigh fading, whose coefficients remain constant over the communication Time frame [110][112].

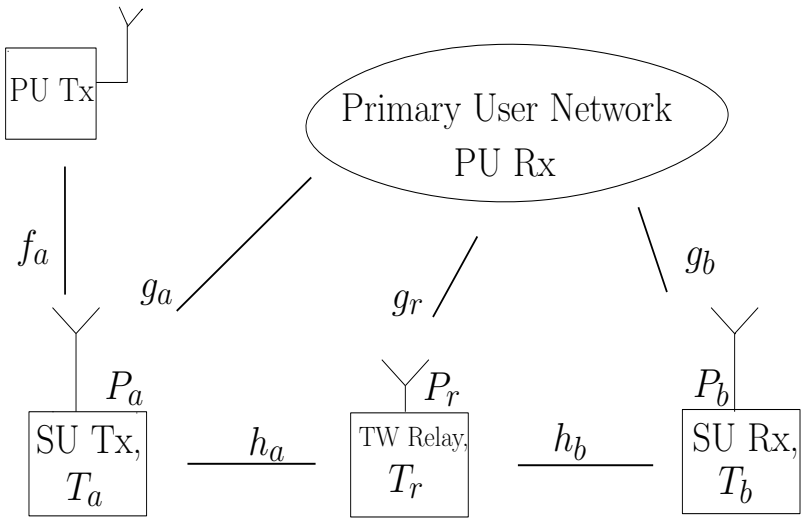

Figure 5.1: System Model

The following hypothesis illustrates the presence ($H1$) and absence ($H0$) of the PU signal

$$Y_{T_a} = \begin{cases} \delta & : H0 \\ \|f_a\|^2 P_{PT} + \delta & : H1 \end{cases} \tag{5.1}$$

where f_a represents the power gain of the sensing channel between SU Tx and PU Tx and δ is the AWGN noise at ST. PU signal, P_{PT} may be considered as an OFDM signal employing Phase shift keying modulation (PSK) or QAM and AWGN noise as complex gaussian with mean 0 and variance σ^2 [51]. Sensing-based spectrum sharing is considered in this research work [58]. According to this the secondary users use spectrum sensing to determine the status (active/idle) of a frequency band (as in interweave CR) and choose their transmit power based on the decision of spectrum sensing, that is, they use higher transmit power if the frequency band is idle and lower if it is active, in order to avoid causing harmful interference similar to the overlay CR scheme. Depending upon the outcome of spectrum sensing, if PU signal is absent (that is, PU is not communicating at all) SU network operates in an interweave manner without power constraints with P_a, P_b and P_r representing the maximum transmit powers of the secondary terminals T_a, T_b and relay T_r respectively. Where as if PU signal is present, SU network operates in underlay mode with power constraints and maximum tolerable Interference limit value, I_p is transmitted by PU to SU terminal T_a through some pilot channel.

The CR communication takes place in two phases. In the first phase, both terminals T_a and T_b transmit their data simultaneously to the relay T_r. The signal received at the relay T_r is represented as [108]

$$y_r = \sqrt{P_a} h_a x_a + \sqrt{P_b} h_b x_b + n_r \tag{5.2}$$

where x_a and x_b are unit energy transmit symbols from terminals T_a, T_b and h_a, h_b are the channel coefficients between $T_a \rightarrow T_r$ and $T_b \rightarrow T_r$. This received signal y_r is used for wireless energy harvesting at relay and information processing. In the second phase, relay transmits the signal to both the terminals using harvested energy in the first phase. Under Hypothesis :H0, that is, when the channel is idle, the CR system operates without power constraints (interweave) whereas in underlay case (Hypothesis: H1) the power constraints are applied to SU Terminals T_a and T_b and relay T_r and power allocation strategy applied considering interference limits is given as by equations (4.5) such that maxi-

mum tolerable interference limit $I_p = P_a |h_a|^2 + P_b |h_b|^2$ and α is Interference Power Distribution Parameter (IPDP).

We have considered only protection of PU Rx in the system model because interference from PU Tx to SU Rx only results in lowering of throughout [113]. Terminal T_a can employ conventional energy based detection or cyclostationary feature detection for spectrum sensing. Sensing accuracy can be determined in terms of probability of false alarm, P_{fa} and Probability of detection, P_d whereas sensing efficiency can be accessed by throughput of the sensed opportunities [111]. Assuming the second-order cyclostationary-sensing, the PDF of hypothesis H_0 and H_1 approach circularly symmetric-complex gaussian distribution with the probability of false alarm P_{fa} given by [114]

$$P_{fa} = \exp\left\{\frac{-(2\tau f_s + 1)\lambda^2}{2\delta^4}\right\} \tag{5.3}$$

and probability of detection P_d for second-order cyclostationary detection is given as [114]

$$P_d = Q\left(\frac{\sqrt{2P_{PT}}\,\|f_a\|}{\delta}, \lambda\sqrt{\frac{2\tau f_s + 1}{2\bar{\gamma} + 1}}\frac{1}{\delta^2}\right) \tag{5.4}$$

where λ is the detection threshold, δ^2 = variance of the AWGN Noise, $\gamma = \frac{P_{PT}\|f_a\|^2}{\delta^2}$; τ is the sensing time and f_s is the sampling frequency. Considering AF relay, the end-to-end SNRs at the SU terminals T_a and T_b are given as in equation (4.6). As shown in figure 5.2, the RF energy is harvested in the fraction βT of the time frame and information processing and transmission takes place in $(1 - \tau - \beta)T$. Assuming charging by both the terminals, energy harvested at the relay in fraction βT is given by

$$E_H = \zeta[P_a |h_a|^2 + P_b |h_b|^2]\beta T \tag{5.5}$$

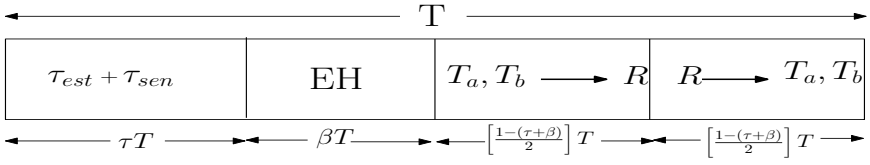

Figure 5.2: Sensing-EH frame structure

where ζ is the efficiency of the energy harvesting circuit.This harvested energy is used to relay the information to both SU terminals under strict power constraints (Hypothesis: H1) as

$$P_r = min\left\{P_r^H, \frac{I_p}{|g_r|^2}\right\} \tag{5.6}$$

where P_r^H, disposal power available at the relay (Hypothesis: H0) is given as

$$P_r^H = \frac{E_H}{\frac{[1-(\tau+\beta)]T}{2}} = \frac{2\zeta\beta}{1-(\tau+\beta)}\left[P_a\left|h_a\right|^2 + P_b\left|h_b\right|^2\right] \tag{5.7}$$

We here assume that harvested energy is small enough and does not exceed interference limits of PU receiver such that $P_r = min\left\{P_r^H, \frac{I_p}{|g_r|^2}\right\} \simeq P_r^H$ most of the time. From equations (4.6) and (5.7), SNRs at SU terminals T_a and T_b are given as

$$\begin{aligned}\gamma_a &= \frac{2\zeta\beta P_b[P_a\left|h_a\right|^2 + P_b\left|h_b\right|^2]}{N_0} \\ &\left[\frac{\left|h_a\right|^2\left|h_b\right|^2}{[2\zeta\beta[P_a\left|h_a\right|^2 + P_b\left|h_b\right|^2] + (1-\tau-\beta)P_a]\left|h_a\right|^2 + P_b\left|h_b\right|^2(1-\tau-\beta)}\right]\end{aligned} \tag{5.8}$$

Simplifying by factorizing the denominator, we get

$$\gamma_a = \frac{2\zeta[P_a\left|h_a\right|^2 + P_b\left|h_b\right|^2]\beta P_b[\left|h_a\right|^2\left|h_b\right|^2]}{N_0[(1-\tau-\beta) + 2\zeta\beta\left|h_a\right|^2][P_a\left|h_a\right|^2 + P_b\left|h_b\right|^2]}$$

Hence, the end-to-end SNRs for both SU terminals T_a and T_b are given by

$$\begin{aligned}\gamma_a &= \frac{2\zeta\beta P_b\left|h_a\right|^2\left|h_b\right|^2}{N_0[(1-\tau-\beta) + 2\zeta\beta\left|h_a\right|^2]} \\ \gamma_b &= \frac{2\zeta\beta P_a\left|h_a\right|^2\left|h_b\right|^2}{N_0[(1-\tau-\beta) + 2\zeta\beta\left|h_b\right|^2]}\end{aligned} \tag{5.9}$$

In particular, CR successfully detects the spectrum hole with probability of $P(H_0)(1-P_{fa})$ and starts transmission (Interweave case) or detects the presence of PU with probability $(1-P(H_0))P_d$ -Underlay case.

5.3 Performance Analysis of Interweave CR

5.3.1 Throughout-Analysis

The throughput-sensing trade-off for Interweave CR is defined as [98]

$$R_s(IW) \simeq [\left(\frac{1-(\tau+\beta)}{2}\right)(1-P_{fa})P(H_0)]C_0 \tag{5.10}$$

where $P(H_0)$ represents the primary user activity, the probability of occurrence of hypothesis H_0 and ergodic-rate C_0 given by $C_0 = E[\ln(1+\gamma_a)+\ln(1+\gamma_b)]$. The achievable throughput of SU is higher, if P_{fa} is lower as there are more chances of channel reuse [101]. The throughput-sensing optimization problem for sensing duration τ and TSR switching parameter β is defined as

$$\widehat{R_s(IW)} = \min_{\tau}\left[\max_{\beta}\left(\frac{1-(\tau+\beta)}{2}\right)(1-P_{fa})P(H_0).E[\ln(1+\gamma_a)+\ln(1+\gamma_b)]\right] \tag{5.11}$$

We assume that sensing is performed periodically after fixed time slots and SU terminal, T_a can sense the primary signal accurately with $P_d \simeq 1$. Also, the probability of accessing the occupied channel is taken smaller than 0.1, in practice [50]. So, the approximation errors are rather smaller. To look into the insights, we try to optimize τ and β through high SNR approximations because in interweave case, the CR network may work in high SNR regions and we can approximate

$$\ln(1+\gamma_a) \simeq \ln(\gamma_a); \quad and \quad \ln(1+\gamma_b) \simeq \ln(\gamma_b) \tag{5.12}$$

5.3.2 Time-switching ratio β Optimization

To maximize the throughput and to find the optimized value of switching time duration β , we differentiate equation (5.11) w.r.t. β as

$$\frac{\partial R_s(IW)}{\partial\beta} = \left(\frac{1-\tau-\beta}{2}\right)\frac{\partial}{\partial\beta}[E[\ln(1+\gamma_a)]+E[\ln(1+\gamma_b)]]-\frac{1}{2}[E[\ln(1+\gamma_a)]+E[\ln(1+\gamma_b)]] = 0 \tag{5.13}$$

Applying the high SNR approximations, we get

$$\frac{\partial R_s(IW)}{\partial\beta} = \left(\frac{1-\tau-\beta}{2}\right)\frac{\partial}{\partial\beta}[E[\ln(\gamma_a)]+E[\ln(\gamma_b)]]-\frac{1}{2}[E[\ln(\gamma_a)]+E[\ln(\gamma_b)]] = 0 \tag{5.14}$$

Let us consider the channels between the SU terminals as the Rayleigh faded with the probability density function (PDF) as $f_x(X) = \frac{1}{\lambda_x} e^{\frac{-x}{\lambda_x}}$, $f_y(Y) = \frac{1}{\lambda_y} e^{\frac{-y}{\lambda_y}}$ where x and y are random variables taken as $x = |h_a|^2; y = |h_b|^2$. Integrating equation (5.9) to obtain $E[\ln(\gamma_a)]$ as

$$E[\ln(\gamma_a)] = \ln\left[\frac{P_b}{N_0}\right] + \int_0^\infty \ln x f_X(x)dx + \int_0^\infty \ln y f_Y(y)dy - \int_0^\infty \ln\left[\frac{1-\beta}{2\zeta\beta} + x\right] f_X(x)dx$$

We get,

$$\begin{aligned} E[\ln(\gamma_a)] &= \ln\left(\frac{2\zeta\beta P_b}{(1-\tau-\beta)N_0}\right) + 2[EulerGamma] + \ln\lambda_x\lambda_y \\ &\quad - \exp\left\{\frac{1-\tau-\beta}{2\zeta\beta\lambda_x}\right\} Ei\left\{\frac{1-\tau-\beta}{2\zeta\beta\lambda_x}\right\} \\ E[\ln(\gamma_b)] &= \ln\left(\frac{2\zeta\beta P_a}{(1-\tau-\beta)N_0}\right) + 2[EulerGamma] + \ln\lambda_x\lambda_y \\ &\quad - \exp\left\{\frac{1-\tau-\beta}{2\zeta\beta\lambda_y}\right\} Ei\left\{\frac{1-\tau-\beta}{2\zeta\beta\lambda_y}\right\} \end{aligned} \tag{5.15}$$

where $EulerGamma$ is a constant equal to -0.5772. Now, solving equations (5.14) and (5.15), we get

$$\begin{aligned} &\left[\tfrac{(1-\tau)(1-\tau-\beta)}{2\zeta\lambda_x\beta^2} + 1\right] \exp\left\{\tfrac{1-(\tau+\beta)}{2\zeta\beta\lambda_x}\right\} Ei\left\{\tfrac{1-(\tau+\beta)}{2\zeta\beta\lambda_x}\right\} + 4(0.5722) + \\ &2\ln\left[\tfrac{1-(\tau+\beta)}{\beta}\right] - \ln\left[\tfrac{4P_aP_b\lambda_x^2\lambda_y^2\zeta^2}{N_0^2}\right] + \left[\tfrac{(1-\tau)(1-\tau-\beta)}{2\zeta\lambda_y\beta^2} + 1\right] \exp\left\{\tfrac{1-(\tau+\beta)}{2\zeta\beta\lambda_y}\right\} Ei\left\{\tfrac{1-(\tau+\beta)}{2\zeta\beta\lambda_y}\right\} = 0 \end{aligned} \tag{5.16}$$

To get the closed form expression, we need to apply the approximation of exponential integral considering fixed τ. Using the approximation $Ei(x) = e^{-x}\ln(1+\frac{1}{x})$ and[115] rational approximation for $ln(1+x) = \frac{2x}{2+x}$ for $x\varepsilon\{0,\infty\}$, solving for β we get

$$\begin{aligned} &\left[\frac{2\zeta\beta\lambda_x}{(1-\tau)+\beta(\zeta\lambda_x-1)}\right]\left[\frac{2\zeta\lambda_x\beta^2 - \beta(1-\tau) + (1-2\tau+\tau^2)}{2\zeta\beta^2\lambda_x}\right] + 6.2888 - \frac{8\beta}{1-\tau} \\ &\qquad - \ln\left[\frac{4P_aP_b\lambda_x^2\lambda_y^2\zeta^2}{N_0^2}\right] + \\ &\left[\frac{2\zeta\beta\lambda_y}{(1-\tau)+\beta(\zeta\lambda_y-1)}\right]\left[\frac{2\zeta\lambda_y\beta^2 - \beta(1-\tau) + (1-2\tau+\tau^2)}{2\zeta\beta^2\lambda_y}\right] = 0 \end{aligned}$$

$$8\beta^4\left[\frac{(\zeta\lambda_x-1)(\zeta\lambda_y-1)}{1-\tau}\right]-\beta^3\left[4\zeta^2\lambda_x\lambda_y+10\zeta(\lambda_x+\lambda_y)+(\zeta\lambda_x-1)(\zeta\lambda_y-1)C-16\right]+$$
$$\beta^2(1-\tau)\left[\zeta(\lambda_x+\lambda_y)-[\zeta(\lambda_x+\lambda_y)-2]C-6\right]-\beta(1-\tau)^2\left[4-\zeta(\lambda_x+\lambda_y)+C\right]-$$
$$(2\tau^3-6\tau^2+6\tau-2)=0 \tag{5.17}$$

where the value of Constant $C=\ln\left[\frac{P_aP_b\lambda_x^2\lambda_y^2\zeta^2}{N_0^2}\right]-4.2888$. Since the value of switching-time ratio β is between 0 to 1, so we neglect the higher powers in the above equation to get the optimum value β^*_{opt}. The error induced by neglecting the higher order terms is rather small because in interweave case, the SUs terminals access the channel with full power. The optimized value of TSR switching-time ratio β^*_{opt} is given as

$$\beta^*_{opt} = \frac{(1-\tau)(4-\zeta(\lambda_x+\lambda_y)+C)}{2(\zeta(\lambda_x+\lambda_y)(1-C)+2C-6)}- \sqrt{\frac{(1-\tau)^2(4-\zeta(\lambda_x+\lambda_y)+C)^2}{4(\zeta(\lambda_x+\lambda_y)(1-C)+2C-6)}-\frac{6\tau^2-6\tau+2}{(1-\tau)(\zeta(\lambda_x+\lambda_y)(1-C)+2C-6)}} \tag{5.18}$$

The performance analysis of this optimized time-switching ratio β^*_{opt} and the error induced is due to approximation is tabulated in table 5.2 and discussed in the results section.

5.3.3 Optimizing the Sensing-duration parameter τ

Since decreasing the sensing duration results in un-reliable spectrum sensing. So, to maximize the throughput, the optimal value of τ is subject to the constraints as

$$\begin{aligned}\max_{s}\ R\ (IW) \quad s.t. \quad P_d &\geq \widehat{P_d}\\ P_{fa} &\leq \widehat{P_{fa}}\\ 0<\tau&<(1-\beta)\end{aligned} \tag{5.19}$$

where $\widehat{P_d}$ is the lower bound on detection probability and $\widehat{P_{fa}}$ represents the upper bound of false alarm probability. The optimum value of τ is found by differentiating the equation (5.11) w.r.t. τ as

$$\frac{\partial R_s(IW)}{\partial \tau} = \left(\frac{1-\tau-\beta}{2}\right)(1-P_{fa})\frac{\partial}{\partial \tau}[E[\ln(\gamma_a)]+E[\ln(\gamma_b)]] - \frac{1}{2}(1-P_{fa})[E[\ln(\gamma_a)]+ E[\ln(\gamma_b)]] + \left(\frac{1-\tau-\beta}{2}\right)[E[\ln(\gamma_a)]+E[\ln(\gamma_b)]]\left[-\frac{\partial P_{fa}}{\partial \tau}\right] = 0 \quad (5.20)$$

The values of $\frac{\partial}{\partial \tau}[E[\ln(\gamma_a)]$ and $\frac{\partial}{\partial \tau}[E[\ln(\gamma_b)]$ are found by differentiating the eq. (5.15). Constant terms after differentiation become zero. The differential is put in the eq. (5.20). After simple mathematical adjustments we get

$$\left(\frac{1-(\tau+\beta)}{2}\right)(1-P_{fa})\left(\frac{1}{2\zeta\beta\lambda_x}\exp\left\{\frac{1-(\tau+\beta)}{2\zeta\beta\lambda_x}\right\}Ei\left\{\frac{1-(\tau+\beta)}{2\zeta\beta\lambda_x}\right\}+ \frac{1}{2\zeta\beta\lambda_y}\exp\left\{\frac{1-(\tau+\beta)}{2\zeta\beta\lambda_y}\right\}Ei\left\{\frac{1-(\tau+\beta)}{2\zeta\beta\lambda_y}\right\}\right)+\left[\frac{1-(\tau+\beta)}{2}(P_{fa}*A_0)-\frac{(1-P_{fa})}{2}\right] \left(-2\ln[1-(\tau+\beta)]-4(0.5722)+\ln\left[\frac{4P_aP_b\lambda_x^2\lambda_y^2\zeta^2\beta^2}{N_0^2}\right] - \exp\left\{\frac{1-(\tau+\beta)}{2\zeta\beta\lambda_x}\right\}Ei\left\{\frac{1-(\tau+\beta)}{2\zeta\beta\lambda_x}\right\}-\exp\left\{\frac{1-(\tau+\beta)}{2\zeta\beta\lambda_y}\right\}Ei\left\{\frac{1-(\tau+\beta)}{2\zeta\beta\lambda_y}\right\}\right)=0 \quad (5.21)$$

For closed form expression using the approximation $Ei(x) = e^{-x}\ln(1+\frac{1}{x})$ and[115] rational approximation for $ln(1+x) = \frac{2x}{2+x}$ for $x\varepsilon\{0,\infty\}$ and upper bound of P_{fa}, we get

$$\frac{1+\beta(2\zeta\lambda_x-1)-\tau}{1+\beta(\zeta\lambda_x-1)-\tau}+\frac{1+\beta(2\zeta\lambda_y-1)-\tau}{1+\beta(\zeta\lambda_y-1)-\tau}-\frac{4(\beta+\tau)}{2-(\tau+\beta)}=\ln\left[\frac{P_aP_b\lambda_x^2\lambda_y^2\zeta^2\beta^2}{N_0^2}\right]-0.2888 \quad (5.22)$$

$$\tau^3(C-6)+\tau^2[\zeta\beta(\lambda_x+\lambda_y)(7-C)+3\beta(C-6)-4(C-4)]+\tau[\beta^2(\zeta^2\lambda_x\lambda_y(C-8)+ 2\zeta(\lambda_x+\lambda_y)(7-C)+3C-18)+\beta(\zeta(\lambda_x+\lambda_y)(3C-13)+32-8C)+5C-14]+ [\beta^3(\zeta^2\lambda_x\lambda_y(C-8)+\zeta(\lambda_x+\lambda_y)(7-C)+C-6)+\beta^2(2\zeta^2\lambda_x\lambda_y(4-C)+ \zeta(\lambda_x+\lambda_y)(3C-13)+16-4C)-\beta(2\zeta(\lambda_x+\lambda_y)C-6\zeta\lambda_y+5C+14) +(6\zeta^2\lambda_x\lambda_y+4-2C)]=0 \quad (5.23)$$

Table 5.1: Iterative Algorithm for finding the optimized value of sensing duration τ^*_{opt} for Interweave CR

Iterative Algorithm for finding τ^*_{opt}
Step1 :
Initialize P_a, P_b, ζ,λ_x, λ_y, N_0, β, τ_{min},τ_{max}, ϵ
k = 2;
Step 2:
$\hat{\tau}_k = \tau_{max}$
$\hat{\tau}_{k-1} = \tau_{min}$
Step 3:
while $((f(\hat{\tau}_k) - f(\hat{\tau}_{k-1})) > \epsilon)$
k = k+1;
Step 4:
Compute $\hat{\tau}_k = \frac{\tau_{min} + \tau_{max}}{2}$
if $(f(\tau_{max}).f(\hat{\tau}_k) > 0)$ **Then**
$\tau_{min} = \hat{\tau}_k$
else
$\tau_{max} = \hat{\tau}_k$
end if
end while
Step 5:
Return τ_k

where the value of the constant $C = \ln\left[\frac{P_a P_b \lambda_x^2 \lambda_y^2 \zeta^2 \beta^2}{N_0^2}\right] - 0.2888 - \widehat{P_{fa}}$ The optimized value of τ^*_{opt} is numerically found from the above by using Iterative bisection method as described in table 5.1.

5.4 Performance Analysis of Hybrid Underlay CR

In underlay case, the SU terminals operate with strict power allocation policy defined by equation (4.5). By considering these constraints, the end-to-end

SNRs are redefined from equation (5.9) as

$$\gamma_a = \frac{2\zeta\beta\alpha I_p \left|h_a\right|^2 \left|h_b\right|^2}{N_0 \left|g_b\right|^2 \left[(1-\tau-\beta)+2\zeta\beta \left|h_a\right|^2\right]}$$
$$\gamma_b = \frac{2\zeta\beta(1-\alpha) I_p \left|h_a\right|^2 \left|h_b\right|^2}{N_0 \left|g_a\right|^2 \left[(1-\tau-\beta)+2\zeta\beta \left|h_b\right|^2\right]} \tag{5.24}$$

5.4.1 Outage Probability Analysis

The outage probability $P_{out,A}$ and $P_{out,B}$ at SU terminal T_a and T_b is mathematically written as

$$P_{out,A} = Pr(\gamma_a < \gamma_{th})$$
$$P_{out,B} = Pr(\gamma_b < \gamma_{th}) \tag{5.25}$$

Using equation (5.24) and (5.25), putting the value of γ_a, we get

$$\begin{aligned} P_{out,A} &= Pr\left[\frac{2\zeta\beta\alpha I_p xy}{N_0 z[1-\tau-\beta+2\zeta\beta x]} < \gamma_{th}\right] \\ &= Pr\left[\frac{y}{z} < \frac{\gamma_{th} N_0[1-\tau-\beta+2\zeta\beta x]}{2\zeta\beta\alpha I_p x}\right] \end{aligned} \tag{5.26}$$

where $x = \left|h_a\right|^2; y = \left|h_b\right|^2; z = \left|g_a\right|^2; u = \left|g_b\right|^2$. Since we are considering rayleigh fading channels and the square of rayleigh random variables is exponential, therefore x and y are exponential random variables with PDFs $f_x(X) = \frac{1}{\lambda_x} e^{\frac{-x}{\lambda_x}}, \quad f_y(Y) = \frac{1}{\lambda_y} e^{\frac{-y}{\lambda_y}}, \quad F_{\frac{y}{z}}(X) = \frac{X}{X+\frac{\lambda_y}{\lambda_z}}$

Solving the above equation as

$$P_{out,A} = \int_0^\infty F_{\frac{y}{z}}\left[\frac{\gamma_{th} N_0(1-\tau-\beta+2\zeta\beta x)}{2\zeta\beta I_p \alpha x}\right] f_x(X) dx$$

$$P_{out,A} = \int_0^\infty \frac{\left[\frac{\gamma_{th} N_0(1-\tau-\beta+2\zeta\beta x)}{2\zeta\beta I_p \alpha x}\right]}{\frac{\lambda_y}{\lambda_z} + \left[\frac{\gamma_{th} N_0(1-\tau-\beta+2\zeta\beta x)}{2\zeta\beta I_p \alpha x}\right]} \frac{1}{\lambda_x} e^{\frac{-x}{\lambda_x}} dx \tag{5.27}$$

$$P_{out,A} = \frac{1}{\lambda_x}\int_0^\infty \frac{\gamma_{th} N_0 \zeta\beta\lambda_z}{\zeta\beta I_p \alpha\lambda_y + \gamma_{th} N_0 \zeta\beta\lambda_z} e^{\frac{-x}{\lambda_x}} dx - \frac{\gamma_{th} N_0(1-\tau\beta)\lambda_z(-2 I_p \alpha\lambda_y)}{(2\zeta\beta I_p \alpha\lambda_y + 2\gamma_{th}\zeta\beta N_0\lambda_z)\lambda_x}\int_0^\infty \frac{1}{\gamma_{th} N_0 \zeta\beta\lambda_z + (2\zeta\beta I_p \alpha\lambda_y + 2\gamma_{th} N_0 \zeta\beta\lambda_z)x} e^{\frac{-x}{\lambda_x}} dx \tag{5.28}$$

The outage probability $P_{out,A}$ at SU terminal T_a is derived as

$$\begin{aligned} P_{out,A} &= \frac{N_0\lambda_z\gamma_{th}}{I_p\alpha\lambda_y + \lambda_z N_0\gamma_{th}} + \frac{\alpha I_p\gamma_{th}N_0\lambda_z\lambda_y(1-\tau-\beta)}{2(I_p\alpha\lambda_y + \lambda_z N_0\gamma_{th})^2\zeta\beta\lambda_x}. \\ & exp\left\{\frac{\gamma_{th}N_0\lambda_z(1-\tau-\beta)}{2(I_p\alpha\lambda_y + \lambda_z N_0\gamma_{th})\zeta\beta\lambda_x}\right\}.Ei\left\{\frac{\gamma_{th}N_0\lambda_z(1-\tau-\beta)}{2(I_p\alpha\lambda_y + 2\lambda_z N_0\gamma_{th})\zeta\beta\lambda_x}\right\} \end{aligned} \tag{5.29}$$

Similarly, outage probability at SU terminal T_b can be expressed as

$$\begin{aligned} P_{out,B} &= \frac{N_0\lambda_u\gamma_{th}}{I_p(1-\alpha)\lambda_x + \lambda_u N_0\gamma_{th}} + \frac{I_p(1-\alpha)\gamma_{th}N_0\lambda_u\lambda_x(1-\tau-\beta)}{2(I_p(1-\alpha)\lambda_x + \lambda_u N_0\gamma_{th})^2\zeta\beta\lambda_y}. \\ & exp\left\{\frac{\gamma_{th}N_0\lambda_u(1-\tau-\beta)}{(2I_p(1-\alpha)\lambda_x + 2\lambda_u N_0\gamma_{th})\zeta\beta\lambda_y}\right\}.Ei\left\{\frac{\gamma_{th}N_0\lambda_u(1-\tau-\beta)}{2(I_p(1-\alpha)\lambda_x + \lambda_u N_0\gamma_{th})\zeta\beta\lambda_y}\right\} \end{aligned} \tag{5.30}$$

The analytical and simulation results for outage probability are plotted in figure 5.6 and discussed in the result section.

5.4.2 Erogodic Sum-Rate Analysis and Optimizing (α)

In Underlay CR, the performance of secondary systems is limited by the interference constraint of the primary users rather than the maximum available power at the secondary nodes. The $\max(P_{max}, \frac{I_p}{|g_i|^2}) = \frac{I_p}{|g_i|^2}$ with very high probability exhibits flooring for reasonable values of $\frac{P_{max}}{N_0}$. Secondary nodes are most likely to operate in this outage floor region where outage is the lowest. Therefore, optimizing the interference power distribution parameter α is justified and inherently, the variations in the channel estimation translate to the variations in parameters namely detection probability and sum-rate[100]. The corresponding ergodic sum-rate for the system under consideration is given by

$$C_1 = E[\ln(1+\gamma_a)] + E[\ln(1+\gamma_b)] \tag{5.31}$$

The optimization problem for maximizing ergodic sum-rate with Interference power distribution parameter, α is expressed as

$$\begin{aligned} \widehat{C_1} = C_{max} &= \underset{\alpha}{opt}\{E[\ln(1+\gamma_a)] + E[\ln(1+\gamma_b)]\} \\ &= \frac{\partial E[\ln(1+\gamma_a)]}{\partial\alpha} + \frac{\partial E[\ln(1+\gamma_b)}{\partial\alpha} = 0 \end{aligned} \tag{5.32}$$

It is evident from equations (5.32) and (5.24) that only numerator term involves α and $(1-\alpha)$ and concavity of ergodic sum-rate can be readily established. The optimized value of IPDP α that maximizes sum-rate is found to be $\frac{1}{2}$ independent of other system parameters, which implies that the sum-rate is always maximum when the interference power distribution is half among the SU terminals T_a and T_b.

5.4.3 Throughput Analysis

Throughput is much smaller in underlay case as compared to the idle channel/interweave case. So, the approximation error is small when P_d is normally taken > 0.9. The variations in the channel translate to the variations in the performance parameters P_d and C_1. We study these variations by characterizing their Cumulative Distribution Functions (CDF) as F_{C_1} and F_{P_d}. Subject to average detection constraint on detection probability P_d and power constraints on SU terminals, the throughput is expressed as

$$R_s(UL) \simeq \left[\left(\frac{1-(\tau+\beta)}{2} \right) (1 - P(H_0))P_d \right] C_1 \tag{5.33}$$

The optimization problem to maximize the throughput for CR system under consideration is defined as

$$\widehat{R_s(UL)} \simeq \min_{\tau} \left[\max_{\beta} \left(\frac{1-(\tau+\beta)}{2} \right) E_{P_d}[P_d](1 - P(H_0))E_{\widehat{C_1}}[\widehat{C_1}] \right] \tag{5.34}$$

The detection probability constraint is considered by defining the CDF of P_d as F_{P_d} and is derived as

$$\begin{aligned} Pr\{P_d > x\} &= 1 - F_{P_d}(x) \\ &= 1 - Pr\{P_d < x\} \\ &= 1 - Pr\left\{ \frac{\sqrt{2P_{PT}}g_a}{\delta} < Q^{-1}\left[x, \lambda\sqrt{\frac{2N+1}{2P_{PT}\lambda_u + 1}}\frac{1}{\delta^2} \right] \right\} \end{aligned} \tag{5.35}$$

where Q^{-1} is the inverse of generalized Marcum-Q function [116]. The value of the inverse is found by defining the lower and upper bound given as $lu =$

$-a-\sqrt{-2\ln(Z)}$ and $ub = a+\sqrt{-2\ln(Z)}$ where $Z = Q_m(a,b)$ [116, Eq. 4.56] The CDF of capacity C_1 is derived by first considering CDF for γ_a and γ_b as

$$F_{\gamma_a}(x) = Pr\{\gamma_a < x\}$$
$$F_{\gamma_b}(x) = Pr\{\gamma_b < x\} \tag{5.36}$$

which is nothing but outage probabilities $P_{out,A}$ and $P_{out,B}$ (replacing γ_{th} by x). The PDF of γ_a and γ_b can be found by integrating the CDF as $f_{\gamma_a}(x) = \frac{dF_{\gamma_a}(x)}{dx}$ and $f_{\gamma_b}(x) = \frac{dF_{\gamma_b}(x)}{dx}$

$$f_{\gamma_a}(x) = \frac{\alpha I_p N_0 \lambda_x \lambda_z}{(I_p\alpha\lambda_x + N_0\lambda_z x)^2} + \frac{2I_p\alpha\lambda_y(1-\tau-\beta)N_0\lambda_z[(2I_p\alpha\lambda_y)^2\zeta\beta\lambda_x + 2I_p\alpha\lambda_y(1-\tau-\beta)N_0\lambda_z x - 4(N_0\lambda_z)^2\zeta\beta\lambda_x x^2]}{(2I_p\alpha\lambda_y + 2\lambda_z N_0 x)^4(\zeta\beta\lambda_x)^2} \exp\left\{\frac{xN_0\lambda_z(1-\tau-\beta)}{(2I_p\alpha\lambda_y + 2\lambda_z N_0 x)\zeta\beta\lambda_x}\right\}.Ei\left\{\frac{xN_0\lambda_z(1-\tau-\beta)}{(2I_p\alpha\lambda_y + 2\lambda_z N_0 x)\zeta\beta\lambda_x}\right\} - \frac{(1-\tau-\beta)N_0\lambda_z(I_p\alpha\lambda_y)^2}{2(I_p\alpha\lambda_y + \lambda_z N_0 x)^3\zeta\beta\lambda_x}$$

$$f_{\gamma_b}(x) = \frac{(1-\alpha)I_p N_0 \lambda_y \lambda_u}{(I_p(1-\alpha)\lambda_y + N_0\lambda_u x)^2} + \frac{2I_p(1-\alpha)\lambda_x(1-\tau-\beta)N_0\lambda_u[(2I_p(1-\alpha)\lambda_x)^2\zeta\beta\lambda_y}{(2I_p(1-\alpha)\lambda_x + 2N_0\lambda_u x)^4(\zeta\beta\lambda_y)^2} + \frac{2I_p(1-\alpha)\lambda_x(1-\tau-\beta)N_0\lambda_u x - 4(N_0\lambda_u)^2\zeta\beta\lambda_y x^2]}{(2I_p(1-\alpha)\lambda_x + 2N_0\lambda_u x)^4(\zeta\beta\lambda_y)^2} \exp\left\{\frac{xN_0\lambda_u(1-\tau-\beta)}{(2I_p(1-\alpha)\lambda_x + 2\lambda_u N_0 x)\zeta\beta\lambda_y}\right\}.$$
$$Ei\left\{\frac{xN_0\lambda_u(1-\tau-\beta)}{(2I_p(1-\alpha)\lambda_x + 2\lambda_u N_0 x)\zeta\beta\lambda_y}\right\} - \frac{(1-\tau-\beta)N_0\lambda_u(I_p(1-\alpha)\lambda_x)^2}{2(I_p(1-\alpha)\lambda_x + \lambda_u N_0 x)^3\zeta\beta\lambda_y} \tag{5.37}$$

The CDF of capacity C_1 is given by

$$F_{C_1}[x] = Pr\{\ln(1+\gamma_a) + \ln(1+\gamma_b) < x\} \tag{5.38}$$

and evaluated as

$$F_{C_1}(z) = \int_0^\infty f_{\gamma_a}(x) f_{\gamma_b}\left(\frac{z}{x}\right)\frac{1}{x}dx \tag{5.39}$$

Hence, by considering variations in terms of CDF of capacity and detection probability in the underlay CR, the optimized value of parameters can be found and throughput can be calculated from equation (5.34). Solving by substitution of variables as $\frac{1-\tau-\beta}{\beta} = \frac{1}{z}$; *or* $\beta = \frac{(1-\tau)z}{1+z}$, the optimized value of switching

time ratio in case of underlay is found to be

$$\beta_{opt} = (1-\tau)\left[1+\sqrt{\frac{\frac{4(\zeta\lambda_x\lambda_y)^2 I_p\alpha(1-\alpha)}{\gamma_{th}N_0[(1-\alpha)\lambda_z+\alpha\lambda_u]} - \left(2-\frac{\gamma_{th}N_0[(1-\alpha)\lambda_z+\alpha\lambda_u]}{I_p\alpha(1-\alpha)}\right)\zeta\lambda_x\lambda_y}{\left(\frac{\lambda_z\lambda_u\gamma_{th}N_0}{(1-\alpha)\lambda_z+\alpha\lambda_u}\right)\left(2-\frac{\gamma_{th}N_0[(1-\alpha)\lambda_z+\alpha\lambda_u]}{I_p\alpha(1-\alpha)}\right)+\zeta\lambda_x\lambda_y}}\right]^{-1} \quad (5.40)$$

The following section evaluates these equations numerically and by simulations to validate the analytical expressions.

5.5 Results and Discussions

The accuracy of derived expressions are validated through numerical evaluation and monte-carlo simulations in this section. The performance analysis of Interweave CR is discussed followed by Underlay CR. The results are compared by considering the symmetrical and asymmetric channels between SU terminals.To introduce asymmetry we take distance metric between SU terminals $d_{h_b} = 3d_{h_a}$ and the path loss exponent of 3. The energy harvesting efficiency $\zeta = 0.6$, the distance between PR network and SU is also taken as three times the distance between $T_a \rightarrow T_r$ and $T_r \rightarrow T_b$. The probability of false alarm, $P_{fa} = 0.1$ and probability of detection is taken as $P_d = 0.9$ where ever required and the PU activities represented by $P(H_0)$ and $P(H_1)$ is taken as 0.5. We assume that equal power is allocated to the SU terminals in interweave CR case as both SU terminals can operate without power constraints.

Figure 5.3 shows the analytical-exact and approximate values of optimum time-switching ratio β for different SU power for interweave CR. The plot justifies the fact that when SU Tx power is high as is normally in interweave case, the charging is fast and the optimal switching-time is less. The approximation error is more at lower power levels and is tabulated in Table 5.2.

Figure 5.4 plots the Throughput Vs SU Power allocation ($P_a = P_b$) and the compares throughput with optimized time-switching ratio considering symmetrical and asymmetric channel cases. This plot also shows the performance for optimized and fixed time-switching ratios. The throughput decreases when we

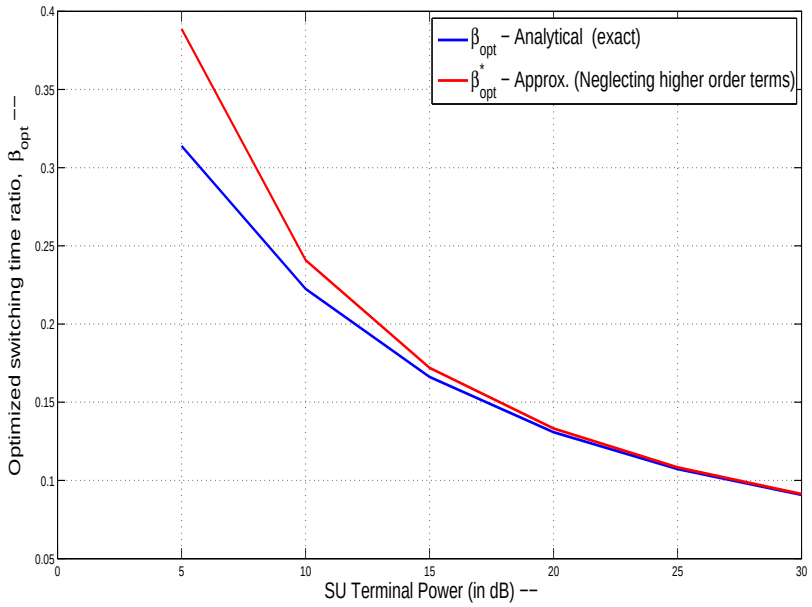

Figure 5.3: SU terminal Power (in dB) Vs optimized switching-time ratio β_{opt}, for fixed sensing duration τ

Table 5.2: Approximation Error in neglecting the higher order terms for switching-time ratio β^*_{opt} (Interweave CR)

SU Power (in dB)	β_{opt}**- Exact**	β^*_{opt} **- Approx (neglecting higher order terms)**
30 dB	0.09077	0.09129
25 dB	0.10729	0.10836
20 dB	0.13080	0.13319
15 dB	0.16615	0.17197
10 dB	0.22248	0.24088
5 dB	0.31393	0.38881

introduce asymmetry and the optimized switching time ratio and fixed time ratio are tight bound. This is because in case of asymmetry the channel SNR and throughput becomes more dependent on distance factor. In figure 5.5 for SU terminal Powers fixed, throughput is plotted with optimized transmission

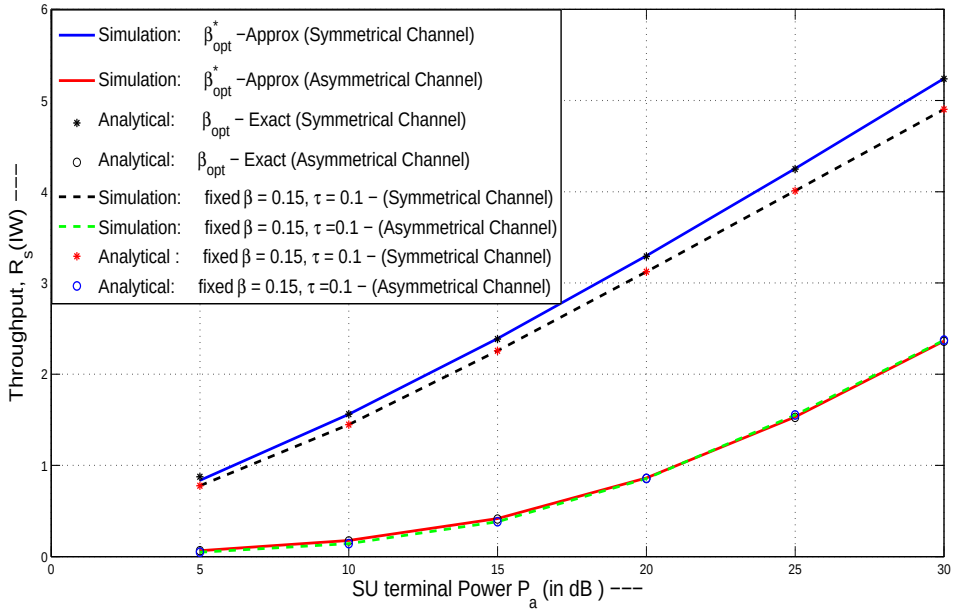

Figure 5.4: Throughput Vs SU Power (Assuming P_a= P_b) for Symmetrical and Asymmetrical case with optimized switching ratio β^*_{opt}

Table 5.3: Throughput in Interweave CR (with Symmetric and Asymmetric channels) with fixed sensing duration $\tau = 0.1$

SU Power (in dB)	**Throughput in Interweave CR**			
	Symmetric channel		**Asymmetric channel**	
	β^*_{opt}	$\beta = 0.15(fixed)$	β^*_{opt}	$\beta = 0.15(fixed)$
30 dB	5.2	4.92	2.43	2.41
20 dB	3.42	3.18	0.87	0.867
10 dB	1.6	1.52	0.28	0.28

time frame for symmetrical and asymmetric channels. We observe that the throughput decreases by 50% in case of asymmetric channel. As we are considering EH by both SU terminals, asymmetry increases the time relay takes to harvest optimal RF energy else we need to increase the SU terminal powers. As we increase the sensing duration and switching-time, the accuracy of the sensing and relay power increase but this increase in the accuracy and power

results in shorting of the transmission time. Moreover, there is no transmission during the sensing duration. So, with the proposed optimization, suitable transmission time is obtained and trade-off between throughput, switching and sensing is obtained for proper utilization of the resources in Interweave CR.

Now, we discuss the performance of Underlay CR system where the SU terminals power is limited by Interference constraint and Interference power distribution (IPDP) parameter α. The IDPD (α) determines the power allocated to SU terminals and is defined by equation (4.5), which clearly influences the system throughput and sum-rate. The Figure 5.6 plots the terminal outages with IPDP α. For symmetrical SU channel, both terminal outages are symmetrical and have identical dependence on interference-temperature whereas the channel asymmetry induces the deviation and some non-linearity in that terminal outage. The non-linearity is in the direction of asymmetry and increase as the SU terminal moves away from relay. However, optimal value of IDPD, α where the ergodic sum-rate shows maximum is always $\frac{1}{2}$ and is proved analytically. The variation in ergodic sum-rate with interference-limit $\frac{I_p}{N_0}$ is shown in figure

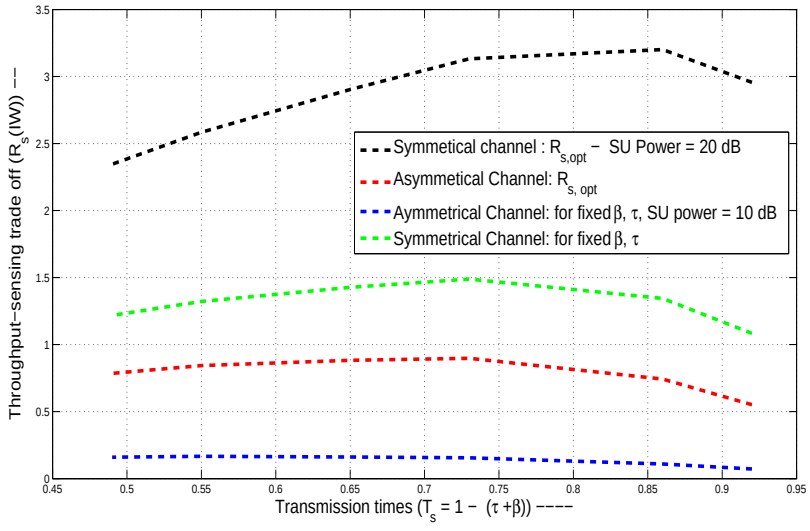

Figure 5.5: Throughput Vs Transmission time (1 - $\tau - \beta$), for Symmetrical and Asymmetrical channel cases

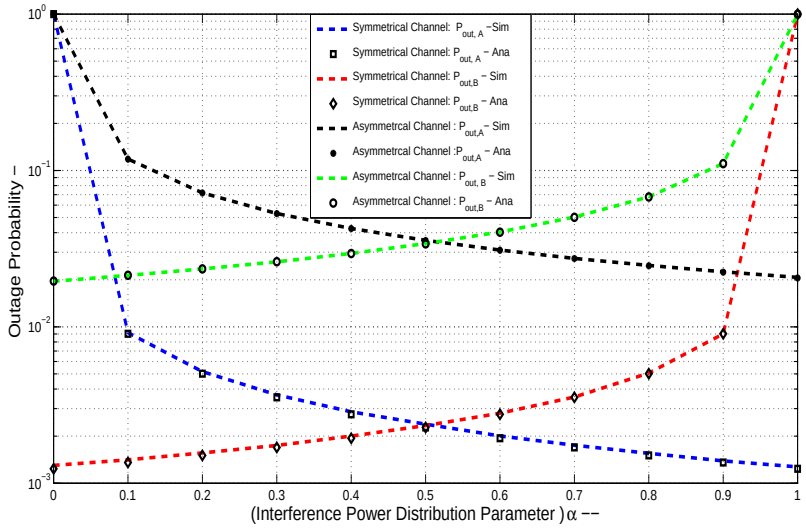

Figure 5.6: Outage Probability at SU terminal A and B Vs Interference Power distribution parameter α

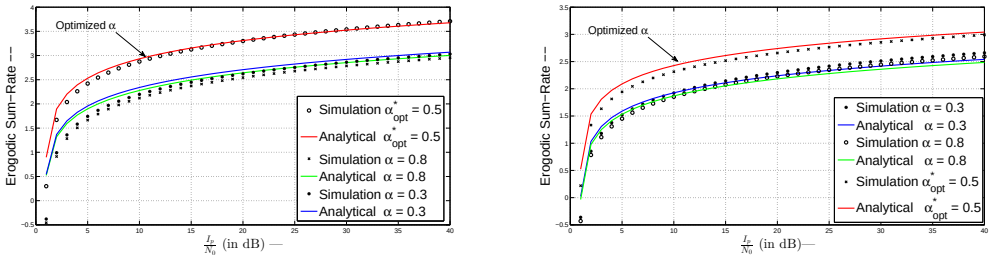

(a) Ergodic-Sum Rate Vs $\frac{I_p}{N_0}$, the interference limit for $\tau = 0$

(b) [Ergodic-Sum Rate Vs $\frac{I_p}{N_0}$, the interference limit for $\tau = 0.15$

Figure 5.7: Variation of Erogodic Sum-Rate Vs Interference Power distribution factor α at Constant τ

5.7. In other words, we analyze that in underlay CR, when the interference limits applies to the SU terminals, the sum-rate is maximized when there is equal interference power distribution among the SU terminals. This is independent of the other parameters β and τ. The variations of the terminal SNR γ_a in terms of CDF Vs capacity for different values of Interference temperature limit, I_p is shown in figure 5.8. As the I_p values increases, the CDF becomes more loose bound with linearity and inclines towards exponential. We analyze

that at higher side values of interference tolerance, the increase in the capacity is exponential. This can happen when SU network is moving away from PU receiver. But the reasonable values of I_p as 10 dB is normally taken in underlay case. Finally, figure 5.10 plots the throughout Vs SU terminal power allocation P_a and IPDP α, taking symmetric channel and asymmetric channels. We infer that in underlay case, the throughput decrease not only depends upon asymmetry of the SU channel but also on the power allocation policy. The more SU power allocation means the PU is able to tolerate high interference temperature and the optimal and fixed time-switching values overlap for higher values at optimized values of α and β.

5.6 Conclusion

From deployment point of view, an Interweave/Underlay cognitive radio with two-way energy harvesting relay using TSR protocol is proposed. We derived the optimized values of TSR time-switching ratio parameter and sensing duration for Interweave CR; Interference-power distribution and time-switching ratio for Underlay CR. The expressions for throughput, terminal outages and

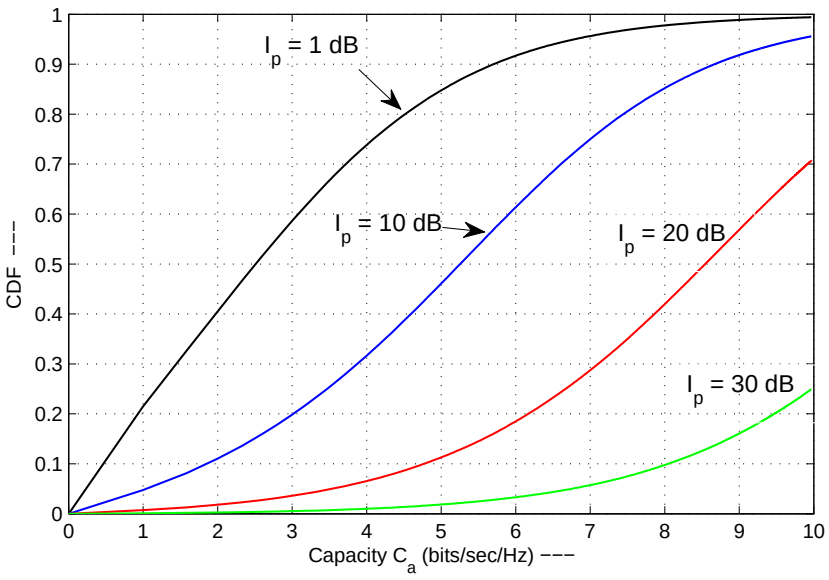

Figure 5.8: CDF of γ_a for different values of I_p, the interference limit

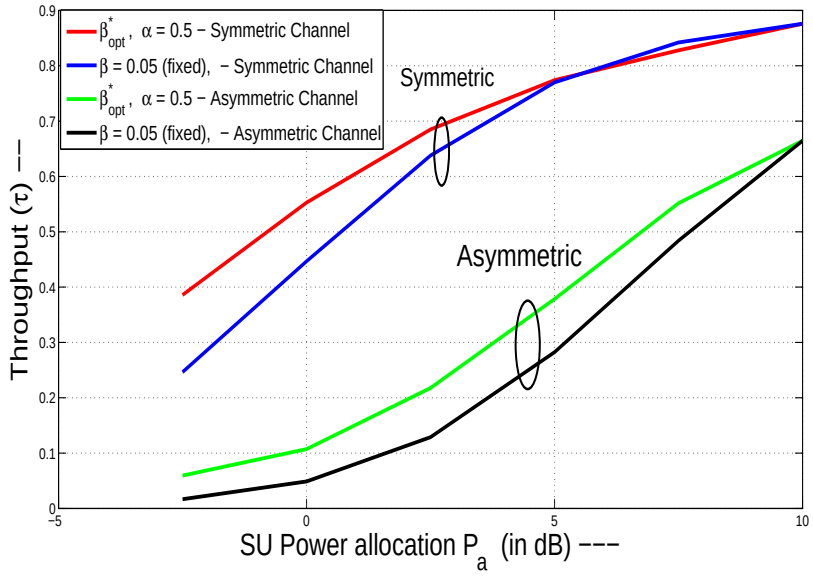

Figure 5.9: Variation of Throughput Vs SU Power allocation P_a

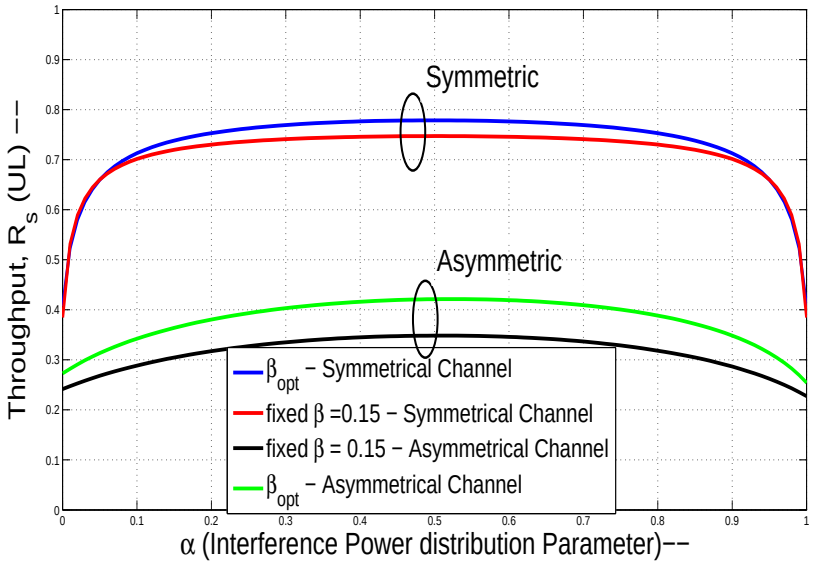

Figure 5.10: Throughput Vs Interference Power distribution factor α for symmetric and asymmetric channels cases at $\frac{I_p}{N_0} = 10dB$

sum-rate for an underlay CR are also derived. We proved that the different parameters can be chosen to obtain the optimized system performance in both underlay and Interweave cases. Analytical and computer simulations show that the proposed optimization results in better trade-off between the system

Table 5.4: Throughput in Underlay CR (with Symmetric and Asymmetric channels)

SNR Values	**Throughput in Underlay CR**			
	Symmetric channel		**Asymmetric channel**	
	β^*_{opt}	$\beta = 0.05(fixed)$	β^*_{opt}	$\beta = 0.05(fixed)$
0 dB	0.55	0.438	0.11	0.047
5 dB	0.76	0.752	0.38	0.29
10 dB	0.883	0.883	0.57	0.572

throughput and time-switching when compared with the fixed parameters considering both symmetrical and asymmetric SU channels. For future work, the system performance considering hybrid Interweave, overlay and underlay CR considering battery buffer constraints and different energy harvesting models can be of interest.

Chapter 6

Conclusion and Future Scope

6.1 Conclusion

The most important resource in wireless communications is the frequency spectrum. Cognitive Radio proposes an efficient spectrum utilization by sensing, sharing and dynamic access capability. This thesis focusses on study and analysis of the different spectrum sensing issues such as sensitivity and flexibility etc. In this work, we conjointed the SMSE framework (for providing flexibility by Dynamic waveform design) with CSS technique (for providing sensitivity). The proposed system design works without having the knowledge of PU waveform still achieving the higher detection probability at low SNR and hence improves the overall decision accuracy of the system for detection of spectrum holes. The proposed test metric uniquely defines the channel occupancy deciding the spectrum holes clearly and increasing the sensing accuracy. SMSE-CSS works well in the low SNR environment and has been proved in ROC plots. The further investigations on channel occupancy taking into account the channel coefficients and noise uncertainty can be of interest. The system model is extended by taking the mulitple antennas at SU transmitter. The proposed technique is implemented in multiple antenna scenario with maximal ratio combining. But this system has low spatial distance of communication. Hence, cognitive relay based communication with RF energy harvesting capabilities has been proposed from practical deployment veiw-point. We investigated the performance of an Interweave/Underlay cognitive radio with two-way energy harvesting relay us-

ing TSR protocol. We derived the optimized values of TSR time-switching ratio parameter and sensing duration for Interweave CR; Interference-power distribution and time-switching ratio for Underlay CR. The expressions for throughput, terminal outages and sum-rate for an underlay CR are also derived. We proved that the different parameters can be chosen to obtain the optimized system performance in both underlay and Interweave cases. Analytical and computer simulations show that the proposed optimization leads to the better trade-off between the system throughput and time-switching when compared with the fixed parameters considering both symmetrical and asymmetric SU channels. For future work in this direction, the system performance considering hybrid Interweave, overlay and underlay CR considering battery buffer constraints and different energy harvesting models can be of interest.

6.2 Future Scope

In context to SMSE framework, the further investigations on channel occupancy taking into account the channel coefficients and noise uncertainty can be of interest. It would be more interesting to consider Single-Carrier FDMA (also known as DFT-precoded OFDMA) used by the LTE uplink waveform for PU sensing. A cyclic-prefixed single carrier modulation with frequency-domain equalization and Filter Bank multicarrier (FBMC) type waveforms would provide an extension to the existing work done in this thesis.

However, the RF energy harvesting has a much wider scope and the work can be extended considering battery buffer constraints taking the different energy harvesting models. The Overlay CR along with hybrid (Interweave and Underlay) CR is yet another area to be explored. The investigations into multi-user scenario for CR and PU both can bring new insights into the system performance.

6.3 List of SCI Publications

- Supreet Singh, Surbhi Sharma, "A joint SMSE waveform design and blind cyclostationary based sensing for cognitive radios", in Iranian Journal of Science and Technology-Transactions of Electrical Engineering (Springer), Vol 41, Issue 2, pp 93-101, July 2017.

- Supreet Singh and Surbhi Sharma, Performance Optimisation of RF Energy Harvesting Relay based Interweave/Underlay Cognitive Radio Network International Journal of Electronics, Taylor and Francis, Vol 104, Issue 9, pp-1546-1561, Sept 2017.

- Supreet Singh, Surbhi Sharma, Performance analysis of spectrum sensing techniques over TWDP fading channels for CR based IoTs, In AEU - International Journal of Electronics and Communications, Vol 80, Oct 2017, page 210-217, ISSN 1434-8411, https://doi.org/10.1016/j.aeue.2017.08.001

Bibliography

[1] T. Yucek and H. Arslan, "A survey of spectrum sensing algorithms for cognitive radio applications," *IEEE Communications Surveys Tutorials*, vol. 11, pp. 116–130, First 2009.

[2] E. Grayver, *Implementing Software Defined Radio*, vol. 18. Springer, 2013.

[3] C. Kabiri, "On the performance of underlay cognitive radio networks with interference constraints and relaying," *Ph.D dissertation*, 2015.

[4] J. Mitola, "Cognitive radio—an integrated agent architecture for software defined radio,," *Ph.D dissertation*, 2000.

[5] F. C. Commission, "Spectrum policy task force report, et docket no. 02-135,," 2002.

[6] S. Haykin, "Cognitive radio: brain-empowered wireless communications," *IEEE Journal on Selected Areas in Communications*, vol. 23, pp. 201–220, Feb 2005.

[7] I. F. Akyildiz, W. y. Lee, M. C. Vuran, and S. Mohanty, "A survey on spectrum management in cognitive radio networks," *IEEE Communications Magazine*, vol. 46, pp. 40–48, April 2008.

[8] G. F. Gott, S. K. Chan, C. Pantjiaros, J. Brown, P. J. Laycock, M. Broms, and S. Boberg, "Recent work on the measurement and analysis of spectral occupancy at HF," in *1994 Sixth International Conference on HF Radio Systems and Techniques*, pp. 144–149, Jul 1994.

[9] M. Matinmikko, M. Mustonen, M. Hyhty, T. Rauma, H. Sarvanko, and A. Mmmel, "Distributed and directional spectrum occupancy measurements in the 2.4 GHz ISM band," in *2010 7th International Symposium on Wireless Communication Systems*, pp. 676–980, Sept 2010.

[10] R. Aguilar-Gonzalez, M. Cardenas-Juarez, U. Pineda-Rico, and E. Stevens-Navarro, "Spectrum occupancy measurements below 1 GHz in the city of San Luis Potosi, Mexico," in *2013 IEEE 78th Vehicular Technology Conference (VTC Fall)*, pp. 1–5, Sept 2013.

[11] A. Goldsmith, S. A. Jafar, I. Maric, and S. Srinivasa, "Breaking spectrum gridlock with cognitive radios: An information theoretic perspective," *Proceedings of the IEEE*, vol. 97, pp. 894–914, May 2009.

[12] V. Chakravarthy, X. Li, R. Zhou, Z. Wu, and M. Temple, "Novel overlay/underlay cognitive radio waveforms using SD-SMSE framework to enhance spectrum efficiency-Part II: Analysis in fading channels," *IEEE Transactions on Communications*, vol. 58, pp. 1868–1876, June 2010.

[13] R. Vahdani and A. Falahati, "An interference alignment design with higher multiplexing gain by the reduced channel extension," *IEEE Transactions on Vehicular Technology*, vol. PP, no. 99, pp. 1–1, 2015.

[14] G. Ozcan, M. C. Gursoy, N. Tran, and J. Tang, "Energy-efficient power allocation in cognitive radio systems with imperfect spectrum sensing," *IEEE Journal on Selected Areas in Communications*, vol. 34, pp. 3466–3481, Dec 2016.

[15] E. Axell, G. Leus, E. G. Larsson, and H. V. Poor, "Spectrum sensing for cognitive radio : State-of-the-art and recent advances," *IEEE Signal Processing Magazine*, vol. 29, pp. 101–116, May 2012.

[16] H. Sun, W. Y. Chiu, J. Jiang, A. Nallanathan, and H. V. Poor, "Wideband spectrum sensing with sub-nyquist sampling in cognitive radios,"

IEEE Transactions on Signal Processing, vol. 60, pp. 6068–6073, Nov 2012.

[17] F. Khozeimeh and S. Haykin, "Brain-inspired dynamic spectrum management for cognitive radio ad hoc networks," *IEEE Transactions on Wireless Communications*, vol. 11, pp. 3509–3517, October 2012.

[18] T. M. C. Chu, H. Phan, and H. J. Zepernick, "Hybrid interweave-underlay spectrum access for cognitive cooperative radio networks," *IEEE Transactions on Communications*, vol. 62, pp. 2183–2197, July 2014.

[19] A. Ali and W. Hamouda, "Advances on spectrum sensing for cognitive radio networks: Theory and Applications," *IEEE Communications Surveys Tutorials*, vol. PP, no. 99, pp. 1–1, 2017.

[20] A. Kaushik, S. K. Sharma, S. Chatzinotas, B. Ottersten, and F. Jondral, "Performance analysis of hybrid cognitive radio systems with imperfect channel knowledge," in *2016 IEEE International Conference on Communications (ICC)*, pp. 1–7, May 2016.

[21] S. Gmira, A. Kobbane, and E. Sabir, "A new optimal hybrid spectrum access in cognitive radio: Overlay-Underlay mode," in *International Conference on Wireless Networks and Mobile Communications (WINCOM)*, pp. 1–7, Oct 2015.

[22] M. Usman and I. Koo, "Access strategy for hybrid underlay-overlay cognitive radios with energy harvesting," *IEEE Sensors Journal*, vol. 14, pp. 3164–3173, Sept 2014.

[23] E. F. Orumwense, T. J. Afullo, and V. M. Srivastava, "On increasing the energy efficiency of cognitive radio network base stations," in *2017 IEEE 7th Annual Computing and Communication Workshop and Conference (CCWC)*, pp. 1–6, Jan 2017.

[24] R. Tandra and A. Sahai, "SNR walls for signal detection," *IEEE Journal of Selected Topics in Signal Processing*, vol. 2, pp. 4–17, Feb 2008.

[25] H. Urkowitz, "Energy detection of unknown deterministic signals," *Proceedings of the IEEE*, vol. 55, pp. 523–531, April 1967.

[26] V. I. Kostylev, "Energy detection of a signal with random amplitude," in *IEEE International Conference on Communications. Conference Proceedings. ICC 2002 (Cat. No.02CH37333)*, vol. 3, pp. 1606–1610 vol.3, 2002.

[27] F. F. Digham, M.-S. Alouini, and M. K. Simon, "On the energy detection of unknown signals over fading channels," *IEEE transactions on communications*, vol. 55, no. 1, pp. 21–24, 2007.

[28] M. Oner and F. Jondral, "Cyclostationarity-based methods for the extraction of the channel allocation information in a spectrum pooling system," in *Proceedings. 2004 IEEE Radio and Wireless Conference (IEEE Cat. No.04TH8746)*, pp. 279–282, Sept 2004.

[29] D. Cohen, L. Pollak, and Y. C. Eldar, "Carrier frequency and bandwidth estimation of cyclostationary multiband signals," in *2016 IEEE International Conference on Acoustics, Speech and Signal Processing (ICASSP)*, pp. 3716–3720, March 2016.

[30] A. V. Dandawate and G. B. Giannakis, "Statistical tests for presence of cyclostationarity," *IEEE Transactions on Signal Processing*, vol. 42, pp. 2355–2369, Sep 1994.

[31] M. H. Mohamad, H. C. Wen, and M. Ismail, "Matched filter detection technique for GSM band," in *2012 International Symposium on Telecommunication Technologies*, pp. 271–274, Nov 2012.

[32] M. D. S. Mosleh, A. A. Tadaion and M. Aref, "Performance comparison of the Neyman-Pearson fusion rule with counting rules for spectrum sensing in cognitive radio," *Iranian Journal of Science and Technology Transactions of Electrical Engineering*, vol. 36, no. 1, pp. 1–17, 2013.

[33] M. Mueck, S. Filin, H. Harada, G. Dimitrakopoulos, G. Baldini, A. Ahtiainen, J. Gebert, K. Nolte, J. Prez-Romero, O. Sallent, and F. Casadevall, "ETSI reconfigurable radio systems - software defined radio and cognitive radio standards," in *IEEE 20th International Symposium on Personal, Indoor and Mobile Radio Communications*, pp. 1–5, Sept 2009.

[34] "What is software defined radio?." http://www.wirelessinnovation.org/assets/documents/S Accessed: 2013-11-30.

[35] A. P. Vinod, E. M.-K. Lai, and A. Omondi, "Special issue on signal processing for software defined radio handsets," *Journal of Signal Processing Systems*, vol. 62, no. 2, pp. 113–115, 2011.

[36] S. Hara and R. Prasad, "Design and performance of multicarrier CDMA system in frequency-selective rayleigh fading channels," *IEEE Transactions on Vehicular Technology*, vol. 48, pp. 1584–1595, Sep 1999.

[37] E. Axell and E. G. Larsson, "Optimal and sub-optimal spectrum sensing of OFDM signals in known and unknown noise variance," *IEEE Journal on Selected Areas in Communications*, vol. 29, pp. 290–304, February 2011.

[38] X. Zhang, Z. Zhang, J. Xing, R. Yu, P. Zhang, and W. Wang, "Exact outage analysis in cognitive two-way relay networks with opportunistic relay selection under primary user's interference," *IEEE Transactions on Vehicular Technology*, vol. 64, pp. 2502–2511, June 2015.

[39] Y. H. Bae and J. W. Baek, "Achievable throughput analysis of opportunistic spectrum access in cognitive radio networks with energy harvesting," *IEEE Transactions on Communications*, vol. 64, pp. 1399–1410, April 2016.

[40] S. Yin, Z. Qu, and S. Li, "Achievable throughput optimization in energy harvesting cognitive radio systems," *IEEE Journal on Selected Areas in Communications*, vol. 33, pp. 407–422, March 2015.

[41] Y. Liu, S. A. Mousavifar, Y. Deng, C. Leung, and M. Elkashlan, "Wireless energy harvesting in a cognitive relay network," *IEEE Transactions on Wireless Communications*, vol. 15, pp. 2498–2508, April 2016.

[42] M. Zheng, C. Xu, W. Liang, and H. Yu, "Harvesting-throughput tradeoff for RF-powered underlay cognitive radio networks," *Electronics Letters*, vol. 52, no. 10, pp. 881–883, 2016.

[43] L. R. Varshney, "Transporting information and energy simultaneously," in *IEEE International Symposium on Information Theory*, pp. 1612–1616, July 2008.

[44] Y. Liu, L. Wang, M. Elkashlan, T. Q. Duong, and A. Nallanathan, "Two-way relaying networks with wireless power transfer: Policies design and throughput analysis," in *IEEE Global Communications Conference*, pp. 4030–4035, Dec 2014.

[45] E. Salahat, A. Kulaib, N. Ali, and R. Shubair, "Exploring symmetry in wireless propagation channels," in *European Conference on Networks and Communications (EuCNC)*, pp. 1–7, June 2017.

[46] A. A. Nasir, X. Zhou, S. Durrani, and R. A. Kennedy, "Relaying protocols for wireless energy harvesting and information processing," *IEEE Transactions on Wireless Communications*, vol. 12, pp. 3622–3636, July 2013.

[47] F. Awin, E. Abdel-Raheem, and M. Ahmadi, "Joint optimal transmission power and sensing time for energy efficient spectrum sensing in cognitive radio system," *IEEE Sensors Journal*, vol. 17, pp. 369–376, Jan 2017.

[48] B. Liu, Z. Li, J. Si, and F. Zhou, "Optimal sensing interval in cognitive radio networks with imperfect spectrum sensing," *IET Communications*, vol. 10, no. 2, pp. 189–198, 2016.

[49] V. P. Tuan and H. Y. Kong, "Impact of residual transmit RF impairments on energy harvesting relay selection systems," *International Journal of Electronics*, vol. 104, no. 6, pp. 928–941, 2017.

[50] C. Yang, Y. Fu, and J. Yang, "Optimisation of sensing time and transmission time in cognitive radio-based smart grid networks," *International Journal of Electronics*, vol. 103, no. 7, pp. 1098–1111, 2016.

[51] D. Zhang, Z. Chen, J. Ren, N. Zhang, M. Awad, H. Zhou, and X. Shen, "Energy harvesting-aided spectrum sensing and data transmission in heterogeneous cognitive radio sensor network," *IEEE Transactions on Vehicular Technology*, vol. PP, no. 99, pp. 1–1, 2016.

[52] C. R. Stevenson, G. Chouinard, Z. Lei, W. Hu, S. J. Shellhammer, and W. Caldwell, "IEEE 802.22: The first cognitive radio wireless regional area network standard," *IEEE Communications Magazine*, vol. 47, pp. 130–138, January 2009.

[53] L. Lu, X. Zhou, U. Onunkwo, and G. Y. Li, "Ten years of research in spectrum sensing and sharing in cognitive radio," *EURASIP Journal on Wireless Communications and Networking*, vol. 2012, no. 1, p. 28, 2012.

[54] M. S. O. Alink, A. B. J. Kokkeler, E. A. M. Klumperink, G. J. M. Smit, and B. Nauta, "Lowering the SNR wall for energy detection using cross-correlation," *IEEE Transactions on Vehicular Technology*, vol. 60, pp. 3748–3757, Oct 2011.

[55] M. Hamid, N. Bjrsell, and S. B. Slimane, "Energy and eigenvalue based combined fully blind self adapted spectrum sensing algorithm," *IEEE Transactions on Vehicular Technology*, vol. 65, pp. 630–642, Feb 2016.

[56] B. Li, M. Sun, X. Li, A. Nallanathan, and C. Zhao, "Energy detection based spectrum sensing for cognitive radios over time-frequency doubly selective fading channels," *IEEE Transactions on Signal Processing*, vol. 63, pp. 402–417, Jan 2015.

[57] W. L. Chin, J. M. Li, and H. H. Chen, "Low-complexity energy detection for spectrum sensing with random arrivals of primary users," *IEEE Transactions on Vehicular Technology*, vol. 65, pp. 947–952, Feb 2016.

[58] T. Cui, F. Gao, and A. Nallanathan, "Optimization of cooperative spectrum sensing in cognitive radio," *IEEE Transactions on Vehicular Technology*, vol. 60, pp. 1578–1589, May 2011.

[59] W. Zhang, R. K. Mallik, and K. B. Letaief, "Optimization of cooperative spectrum sensing with energy detection in cognitive radio networks," *IEEE Transactions on Wireless Communications*, vol. 8, pp. 5761–5766, December 2009.

[60] H. Sun, A. Nallanathan, S. Cui, and C. X. Wang, "Cooperative wideband spectrum sensing over fading channels," *IEEE Transactions on Vehicular Technology*, vol. 65, pp. 1382–1394, March 2016.

[61] S. Nallagonda, S. Suraparaju, S. D. Roy, and S. Kundu, "Performance of energy detection based spectrum sensing in fading channels," in *2011 2nd International Conference on Computer and Communication Technology (ICCCT-2011)*, pp. 575–580, Sept 2011.

[62] H. Hu, H. Zhang, H. Yu, and Y. Chen, "Spectrum-energy-efficient sensing with novel frame structure in cognitive radio networks," {*AEU*} - *International Journal of Electronics and Communications*, vol. 68, no. 11, pp. 1065 – 1072, 2014.

[63] W. A. Gardner, A. Napolitano, and L. Paura, "Cyclostationarity: Half a century of research," *Signal Processing*, vol. 86, no. 4, pp. 639 – 697, 2006.

[64] W. Lei, X. Jing, Z. Tong, and Y. Xiao, "Digital implementation analysis of cyclostationary algorithms in cognitive radio," in *2011 IEEE International Conference on Signal Processing, Communications and Computing (ICSPCC)*, pp. 1–4, Sept 2011.

[65] S. Haykin, D. J. Thomson, and J. H. Reed, "Spectrum sensing for cognitive radio," *Proceedings of the IEEE*, vol. 97, pp. 849–877, May 2009.

[66] L. Safatly, B. Aziz, A. Nafkha, Y. Louet, Y. Nasser, A. El-Hajj, and K. Y. Kabalan, "Blind spectrum sensing using symmetry property of cyclic autocorrelation function: from theory to practice," *EURASIP Journal on Wireless Communications and Networking*, vol. 2014, no. 1, pp. 1–13, 2014.

[67] T. E. Bogale and L. Vandendorpe, "Multi-cycle cyclostationary based spectrum sensing algorithm for OFDM signals with noise uncertainty in cognitive radio networks," in *MILCOM 2012 - IEEE Military Communications Conference*, pp. 1–6, Oct 2012.

[68] L. Yang, Z. Chen, and F. Yin, "Cyclo-energy detector for spectrum sensing in cognitive radio," {*AEU*} - *International Journal of Electronics and Communications*, vol. 66, no. 1, pp. 89 – 92, 2012.

[69] G. Huang and J. K. Tugnait, "On cyclostationarity based spectrum sensing under uncertain gaussian noise," *Signal Processing, IEEE Transactions on*, vol. 61, no. 8, pp. 2042–2054, 2013.

[70] W. M. Jang, "Blind cyclostationary spectrum sensing in cognitive radios," *IEEE Communications Letters*, vol. 18, pp. 393–396, March 2014.

[71] Y. Zeng and Y. C. Liang, "Robustness of the cyclostationary detection to cyclic frequency mismatch," in *21st Annual IEEE International Symposium on Personal, Indoor and Mobile Radio Communications*, pp. 2704–2709, Sept 2010.

[72] T. Dzenli and O. Akay, "A new spectrum sensing strategy for dynamic primary users in cognitive radio," *IEEE Communications Letters*, vol. 20, pp. 752–755, April 2016.

[73] M. D. Felice, K. R. Chowdhury, A. Kassler, and L. Bononi, "Adaptive sensing scheduling and spectrum selection in cognitive wireless mesh networks," in *Proceedings of 20th International Conference on Computer Communications and Networks (ICCCN)*, pp. 1–6, July 2011.

[74] M. Cardenas-Juarez, M. Ghogho, U. Pineda-Rico, and E. Stevens-Navarro, "Improved semi-blind spectrum sensing for cognitive radio with locally optimum detection," *IET Signal Processing*, vol. 10, no. 5, pp. 524–531, 2016.

[75] A. Bagwari and B. Singh, "Comparative performance evaluation of spectrum sensing techniques for cognitive radio networks," in *2012 Fourth International Conference on Computational Intelligence and Communication Networks*, pp. 98–105, Nov 2012.

[76] M. L. Roberts, M. A. Temple, R. A. Raines, R. F. Mills, and M. E. Oxley, "Communication waveform design using an adaptive Spectrally Modulated, Spectrally Encoded (SMSE) framework," *IEEE Journal of Selected Topics in Signal Processing*, vol. 1, pp. 203–213, June 2007.

[77] V. Chakravarthy, X. Li, Z. Wu, M. A. Temple, F. Garber, R. Kannan, and A. Vasilakos, "Novel overlay/underlay cognitive radio waveforms using {SD-SMSE} framework to enhance spectrum efficiency- Part I: Theoretical framework and analysis in AWGN channel," *IEEE Transactions on Communications*, vol. 57, pp. 3794–3804, December 2009.

[78] R. Zhou, X. Li, V. Chakravarthy, C. Bullmaster, B. Wang, R. Cooper, and Z. Wu, "Software defined radio implementation of SMSE based overlay cognitive radio," in *2010 IEEE Symposium on New Frontiers in Dynamic Spectrum (DySPAN)*, pp. 1–2, April 2010.

[79] P. Rose, R. Zhou, Y. Qu, V. Chakarvarthy, Z. Wu, and Z. Zhang, "Demonstration of hybrid overlay/underlay waveform generator with spectrally compliant cognitive capability via SD-SMSE framework," in

2016 13th IEEE Annual Consumer Communications Networking Conference (CCNC), pp. 258–259, Jan 2016.

[80] M. F. Uddin, H. M. K. AlAzemi, and C. Assi, "Optimal flexible spectrum access in wireless networks with software defined radios," *IEEE Transactions on Wireless Communications*, vol. 10, pp. 314–324, January 2011.

[81] A. Patra, A. Achtzehn, and P. Mhnen, "ULLA-X: A programmatic middleware for generic cognitive radio network control," in *2015 IEEE International Symposium on Dynamic Spectrum Access Networks (DySPAN)*, pp. 265–266, Sept 2015.

[82] A. Ali and W. Hamouda, "Spectrum monitoring using energy ratio algorithm for OFDM-based cognitive radio networks," *IEEE Transactions on Wireless Communications*, vol. 14, pp. 2257–2268, April 2015.

[83] A. Pandharipande and J. P. M. G. Linnartz, "Performance analysis of primary user detection in a multiple antenna cognitive radio," in *2007 IEEE International Conference on Communications*, pp. 6482–6486, June 2007.

[84] S. H. Hwang, J. H. Baek, and O. A. Dobre, "Spectrum sensing using multiple antenna-aided energy detectors for cognitive radio," in *2009 Canadian Conference on Electrical and Computer Engineering*, pp. 209–212, May 2009.

[85] A. Singh, M. R. Bhatnagar, and R. K. Mallik, "Performance of an improved energy detector in multihop cognitive radio networks," *IEEE Transactions on Vehicular Technology*, vol. 65, pp. 732–743, Feb 2016.

[86] A. Taherpour, M. Nasiri-Kenari, and S. Gazor, "Multiple antenna spectrum sensing in cognitive radios," *IEEE Transactions on Wireless Communications*, vol. 9, pp. 814–823, February 2010.

[87] A. Kumar, S. Dwivedi, and A. K. Jagannatham, "GLRT based spectrum sensing for MIMO SC-FDMA cognitive radio networks," *IEEE Wireless Communications Letters*, vol. 4, pp. 593–596, Dec 2015.

[88] J. K. Tugnait, "Multiple antenna spectrum sensing for cognitive radios in unknown noise," in *2011 IEEE 12th International Workshop on Signal Processing Advances in Wireless Communications*, pp. 431–435, June 2011.

[89] J. K. Tugnait, "On multiple antenna spectrum sensing under noise variance uncertainty and flat fading," *IEEE Transactions on Signal Processing*, vol. 60, pp. 1823–1832, April 2012.

[90] A. B. H. Hmida, S. Cherif, and H. Besbes, "Spectrum sensing based on STBC higher order statistics for cognitive radio systems," in *Third International Conference on Communications and Networking*, pp. 1–5, March 2012.

[91] P. Urriza, E. Rebeiz, and D. Cabric, "Multiple antenna cyclostationary spectrum sensing based on the cyclic correlation significance test," *IEEE Journal on Selected Areas in Communications*, vol. 31, pp. 2185–2195, November 2013.

[92] H. A. Suraweera, P. J. Smith, and M. Shafi, "Capacity limits and performance analysis of cognitive radio with imperfect channel knowledge," *IEEE Transactions on Vehicular Technology*, vol. 59, pp. 1811–1822, May 2010.

[93] Q. Huang and P. J. Chung, "An F-test based approach for spectrum sensing in cognitive radio," *IEEE Transactions on Wireless Communications*, vol. 12, pp. 4072–4079, August 2013.

[94] Z. Yan, X. Zhang, and W. Wang, "Exact outage performance of cognitive relay networks with maximum transmit power limits," *IEEE Communications Letters*, vol. 15, pp. 1317–1319, December 2011.

[95] Y. Cao and C. Tellambura, "Outage analysis of ZFB-MRT/MRC underlay two-way relay systems," *IEEE Communications Letters*, vol. 19, pp. 1049–1052, June 2015.

[96] A. Sultan, "Sensing and transmit energy optimization for an energy harvesting cognitive radio," *IEEE Wireless Communications Letters*, vol. 1, pp. 500–503, October 2012.

[97] E. F. Orumwense, T. J. Afullo, and V. M. Srivastava, "Main trade-offs for energy efficiency in cognitive radio networks," in *2016 IST-Africa Week Conference*, pp. 1–8, May 2016.

[98] W. Chung, S. Park, S. Lim, and D. Hong, "Spectrum sensing optimization for energy-harvesting cognitive radio systems," *IEEE Transactions on Wireless Communications*, vol. 13, pp. 2601–2613, May 2014.

[99] Y. C. Liang, Y. Zeng, E. C. Y. Peh, and A. T. Hoang, "Sensing-throughput tradeoff for cognitive radio networks," *IEEE Transactions on Wireless Communications*, vol. 7, pp. 1326–1337, April 2008.

[100] A. Kaushik, S. K. Sharma, S. Chatzinotas, B. Ottersten, and F. K. Jondral, "Sensing-throughput tradeoff for interweave cognitive radio system: A deployment-centric viewpoint," *IEEE Transactions on Wireless Communications*, vol. 15, pp. 3690–3702, May 2016.

[101] M. Costa and A. Ephremides, "Energy efficiency versus performance in cognitive wireless networks," *IEEE Journal on Selected Areas in Communications*, vol. 34, pp. 1336–1347, May 2016.

[102] Bunty and S. Sengar, "A filter bank implementation and performance analysis of MC-DS-CDMA," *International Journal of Recent Trends in Engineering and Technology*, vol. 4, pp. 76–80, Nov 2010.

[103] P. Atungire, T. F. Rahman, F. Granelli, and C. Sacchi, "Open-field emulation of cooperative relaying in LTE-A downlink using the GNU radio platform," *IEEE Network*, vol. 28, pp. 20–26, September 2014.

[104] R. Chopra, D. Ghosh, and D. K. Mehra, "FRESH filter-based spectrum sensing in the presence of cyclic frequency offset," *IEEE Wireless Communications Letters*, vol. 5, pp. 124–127, April 2016.

[105] G. P. Tolstov, *Fourier series*. Courier Corporation, 2012.

[106] A. Tabesh, A. Taherpour, and Z. Pourgharehkhan, "Multiple antenna spectrum sensing using statistical A-Priori information in cognitive radios," *IET Signal Processing*, vol. 7, pp. 59–70, February 2013.

[107] V. N. S. P.G.S. Velmurugan and S. J. Thiruvengadam, "Joint channel and power allocation for cognitive radio systems with physical layer network coding," *Iranian Journal of Science and Technology-Transactions of Electrical Engineering*, vol. 37, no. 2, pp. 147–159, 2013.

[108] P. K. Upadhyay and S. Prakriya, "Performance of analog network coding with asymmetric traffic requirements," *IEEE Communications Letters*, vol. 15, pp. 647–649, June 2011.

[109] Z. Yang, Z. Ding, P. Fan, and G. K. Karagiannidis, "Outage performance of cognitive relay networks with wireless information and power transfer," *IEEE Transactions on Vehicular Technology*, vol. 65, pp. 3828–3833, May 2016.

[110] S. Luo, R. Zhang, and T. J. Lim, "Optimal save-then-transmit protocol for energy harvesting wireless transmitters," *IEEE Transactions on Wireless Communications*, vol. 12, pp. 1196–1207, March 2013.

[111] R. Yu, Y. Zhang, L. Yi, S. Xie, L. Song, and M. Guizani, "Secondary users cooperation in cognitive radio networks: balancing sensing accuracy and efficiency," *IEEE Wireless Communications*, vol. 19, pp. 30–37, April 2012.

[112] D. K. Nguyen, M. Matthaiou, T. Q. Duong, and H. Ochi, "RF energy harvesting two-way cognitive DF relaying with transceiver impairments,"

in *2015 IEEE International Conference on Communication Workshop (ICCW)*, pp. 1970–1975, June 2015.

[113] M. Elkashlan, L. Wang, T. Q. Duong, G. K. Karagiannidis, and A. Nallanathan, "On the security of cognitive radio networks," *IEEE Transactions on Vehicular Technology*, vol. 64, pp. 3790–3795, Aug 2015.

[114] W.-j. Yue, B.-y. Zheng, and Q.-m. Meng, "Cyclostationary property based spectrum sensing algorithms for primary detection in cognitive radio systems," *Journal of Shanghai Jiaotong University (Science)*, vol. 14, no. 6, pp. 676–680, 2009.

[115] F. Topsok, "Some bounds for the logarithmic function," *Inequality theory and applications*, vol. 4, p. 137, 2006.

[116] M. K. Simon and M. S. Alouini, *Digital communication over fading channels*, vol. 95. John Wiley & Sons, 2005.